

# Modelling changing travel behaviour in response to road capacity reductions

The impact of reallocating road space in urban areas on car use

Sander van Heyningen

Delft University of Technology

# Modelling changing travel behaviour in response to road capacity reductions

The impact of reallocating road space in urban areas on car use

by

Sander van Heyningen

to obtain the degree of Master of Science  
in Civil Engineering - Traffic and Transport Engineering,  
at the Delft University of Technology,  
to be defended publicly on Friday March 7, 2025 at 3:00 PM.

Student number: 4938755  
Project duration: July 15, 2024 – March 7, 2025  
Thesis committee: Dr. M. Snelder, TU Delft, Chair  
Dr. V. L. Knoop, TU Delft, Supervisor  
Ir. R. T. J. van der Kleij, Municipality of Rotterdam

Cover: Coolsingel after redesign (image by author)

# Preface

This thesis marks the end of my studies in Civil Engineering at TU Delft. Seven years ago, I started my bachelor's degree at this university, driven by the desire to contribute to society in a meaningful way. I wasn't exactly sure what that would look like, but I knew I wanted to work on projects that have a direct impact on people's daily lives—whether through safe infrastructure, sustainable cities or efficient transportation systems. Over the years, I explored different fields within civil engineering, but it was in traffic and transportation that I found my true passion. What fascinates me most is the combination of technical aspects and human behaviour. Mobility shapes the way people experience cities, and I developed an interest in how thoughtful design can improve urban life. Throughout my studies, I have not only gained technical skills but also learned to think critically about mobility, urban planning and sustainability. Looking back, I can see how much I have grown, both professionally and personally, through the challenges and opportunities that came my way. This journey has strengthened my ambition to continue working on efficient transportation systems and improving urban liveability in the future.

This thesis is the final project of the Traffic and Transportation track of my master's degree. Throughout my studies, I gained a lot of knowledge about the different aspects in mobility. I chose the topic of disappearing traffic for my thesis because I am motivated to make cities more liveable, and I was genuinely curious about how disappearing traffic works. The process was challenging at times, especially in the beginning when I was unsure whether the model would be feasible to construct. But figuring it out, step by step, made the end result all the more rewarding.

Without the help of my supervisors, this project wouldn't have been possible. I would like to thank my committee for their guidance throughout this process. Maaïke, for being the chair of my committee and for connecting me to the XCARCITY project, of which this thesis is a part. Victor, for his valuable input in shaping this research, and for providing a space where I could share my thoughts and freely discuss ideas. I also want to thank Robbert and Will from the Municipality of Rotterdam for their support during this thesis. They not only guided me but also gave me hands-on experience with real projects and an inside look at working for a municipality.

Besides my supervisors, I am also grateful to my colleagues at the Municipality of Rotterdam, who were always willing to answer my questions and made my time at the office enjoyable. Additionally, I want to thank my university friends for making the thesis room a great place to work, and for providing much-needed relaxation outside of working hours, whether it was grabbing a coffee or having a drink after long day of studying. I genuinely value their support and friendship, which significantly enhanced my experience and made this journey a whole lot more fun.

*Sander van Heyningen  
Delft, March 2025*

# Summary

High car usage in urban areas has negative effects on liveability, such as reduced air quality, increased noise pollution, higher urban heat levels and reduced traffic safety. Additionally, cars occupy significant urban space that could otherwise be allocated to greenery, recreational areas, or alternatively, more space-efficient modes of transport such as walking and cycling. As cities continue to grow and densify, addressing these challenges becomes increasingly important to ensure a healthy and sustainable urban environment.

In response, many cities in the Netherlands aim to transition to a low-car urban environment, where car usage is significantly reduced, though not entirely prohibited. One strategy to achieve this involves reducing road network capacity, which not only limits space for cars but can also reduce overall car usage in the area—a phenomenon referred to in the literature as “disappearing traffic”. However, policymakers often lack robust tools to predict the outcomes of such interventions. This study addresses the following research question: *How can changes in travel behaviour be accurately predicted following road capacity reductions in urban areas and what insights can be drawn from these predictions?*

This research develops a model to estimate changes in travel behaviour and the resulting traffic dynamics following a road capacity reduction, focusing on the evening peak period. The model uses an iterative process to establish a new equilibrium between traffic congestion and car usage. It considers four alternatives: car, public transport, cycling and a “no trip” option, representing changes in destination, departure time or trip frequency. The iterative process consists of three steps. (1) A dynamic traffic simulation is conducted, implementing the road capacity reduction to determine travel times for car trips for a given traffic demand. (2) This is followed by an assessment to evaluate whether traffic congestion has stabilised. (3) Finally, the traffic demand is recalculated based on the updated travel times over the network. If congestion has not stabilised, the cycle repeats until equilibrium is reached, with shifts from car use to alternatives as travel times rise.

The research also included an analysis of the effects on car usage on large-scale roadworks in Rotterdam South (from January 2023 to July 2024) at the Roseknoop intersection. During the phase of highest capacity reduction, involving the closure of a major 2x2 road, evening peak traffic entering the area decreased by 4,400 car trips (15% of total). This indicates that at least 4,400 travellers adapted their behaviour, such as switching modes, altering departure times, changing destination out of the intervention area or reducing trip frequency. Notably, some adaptations persisted after road capacity was restored, suggesting lasting behavioural changes.

The model estimating the effect of road capacity interventions was calibrated using data from a macroscopic traffic model as well as from one of the two roadwork phases in the Roseknoop case study. In the calibration, the model parameters of the utility functions for the alternatives are found by using the Maximum Likelihood Estimation. Validation on the other phase of the Roseknoop roadworks demonstrated that the model outputs aligned more closely with observed traffic conditions than scenarios without demand reduction. Although the model performed well qualitatively, quantitative assessment of its accuracy remains challenging.

The model revealed distinct patterns in travel behaviour changes. Short trips, including those within cities or between nearby cities, predominantly shifted to alternative modes like cycling or public transport when the travel time due to road capacity reductions increased. In contrast, longer trips showed minimal mode shifts, with adaptations such as changing destinations, departure times or trip frequencies (e.g., increased remote working) being more common.

---

To conclude, the developed model demonstrates that recalculating traffic demand based on simulated travel times can provide policymakers with valuable insights into the impacts of road capacity reductions. Both the model and the data analysis suggest that the overall effect on congestion is limited. Although traffic congestion does increase slightly, it is certainly not as severe as it would be if no traffic were to leave at all. This can be attributed to the self-regulating nature of travel behaviour, where individuals adapt their travel patterns in response to reduced road capacity. Notably, some of these adaptations persist even after capacity is restored, suggesting that alternative behaviours—such as switching to public transport or cycling, adjusting schedules or reducing trip frequency—may offer benefits that, for some users, surpass the convenience of driving. While further research is needed to confirm this trend, it underscores the potential for sustainable reductions in traffic demand, contributing to the goals of creating low-car cities.

Furthermore, effective communication plays an important role in mitigating potential initial congestion during road capacity reductions and should be considered in future implementations. While the effect of communication was not explicitly analysed in this study, a lack of communication could result in considerable traffic congestion on the first day of implementation. Providing clear and timely information can help travellers prepare for the changes and adjust their behaviour in advance, leading to a more gradual and manageable transition to the new traffic conditions.

In summary, road capacity reductions, when combined with well-calibrated models and strategic communication, can support the transition to low-car cities with minimal disruptions while encouraging sustainable travel behaviour changes.

# Contents

<b>Preface</b>	<b>i</b>
<b>Summary</b>	<b>ii</b>
<b>1 Introduction</b>	<b>1</b>
1.1 Context . . . . .	1
1.2 Research objectives and scope . . . . .	2
1.3 Research questions . . . . .	3
1.4 Thesis Outline . . . . .	3
<b>2 Literature review</b>	<b>4</b>
2.1 Literature review methodology . . . . .	4
2.2 Disappearing traffic in general . . . . .	4
2.3 Case studies research into disappearing traffic . . . . .	5
2.4 Behavioural adaptation in response to road capacity reductions . . . . .	7
2.5 Insights from capacity expansion: understanding induced demand . . . . .	8
2.5.1 Generated traffic . . . . .	9
2.5.2 Induced demand from economical perspective . . . . .	11
2.5.3 Modelling implementations induced demand . . . . .	11
2.5.4 What can be learned from induced demand? . . . . .	12
2.6 Modelling disappearing traffic . . . . .	12
2.6.1 Increase in travel time over network . . . . .	12
2.6.2 Mobility distribution . . . . .	12
2.7 Conclusions from literature . . . . .	13
<b>3 Methodology</b>	<b>15</b>
3.1 Model iteration process . . . . .	16
3.1.1 Step 1: Traffic simulation . . . . .	16
3.1.2 Step 2: Check for stabilised traffic . . . . .	17
3.1.3 Step 3: Recalculation traffic demand . . . . .	18
3.2 Model calibration . . . . .	19
3.3 Model validation . . . . .	20
<b>4 Model specification</b>	<b>21</b>
4.1 Threshold value for congestion indicator . . . . .	22
4.2 Utility functions . . . . .	22
4.3 Calculation new mobility distribution . . . . .	23
4.4 Optimisation convergence . . . . .	24
4.5 External trips in the RODY model . . . . .	24
4.6 Optional: reducing initial car traffic demand . . . . .	25
4.7 Optional: adjusting the travel time matrix for the alternatives . . . . .	26
<b>5 Case study</b>	<b>27</b>
5.1 Introduction case study . . . . .	27
5.2 Car trips: reduction in traffic volume . . . . .	29
5.3 Car trips: change in trip length distribution . . . . .	33
5.4 Cycling and public transport trips . . . . .	36
<b>6 Model calibration</b>	<b>37</b>
6.1 Step 1: Model with alternatives car, bike and public transport . . . . .	38
6.2 Step 2: discrepancy between model outcome and observed traffic . . . . .	40
6.3 Step 3: Final model including no trip alternative . . . . .	43

6.3.1	Data for calibrating no trip alternative . . . . .	43
6.3.2	Determination of model parameters . . . . .	43
6.4	Results calibrated model . . . . .	46
<b>7</b>	<b>Model validation</b>	<b>49</b>
7.1	Model result Roseknoop roadworks phase 1 . . . . .	49
7.2	Comparison traffic conditions model outcome to observations . . . . .	52
7.3	Conclusion model validation . . . . .	53
<b>8</b>	<b>Conclusion</b>	<b>54</b>
8.1	Findings . . . . .	54
8.2	Model assumptions and limitations . . . . .	57
8.3	Final conclusions . . . . .	58
8.4	Implications for science . . . . .	58
8.5	Implications for practice . . . . .	59
<b>A</b>	<b>Code DiTra model</b>	<b>63</b>
A.1	Main code DiTra model . . . . .	63
A.2	Code functions for DiTra model . . . . .	69
<b>B</b>	<b>Determination threshold KS-value</b>	<b>84</b>
<b>C</b>	<b>Reference locations data analysis</b>	<b>88</b>
<b>D</b>	<b>Mathematical functions change in mobility distribution</b>	<b>90</b>
<b>E</b>	<b>Congestion heat maps of phase 1 (outcome DiTra model)</b>	<b>92</b>



# 1

## Introduction

In many cities nowadays, cars dominate the urban landscape. This car dominance began in the 1960s when auto mobiles became more affordable for the wider public, leading to a substantial increase in car ownership and usage. Over the following decades, this trend continued, resulting in the expansion of the road network and the growing spatial separation between residential and commercial areas [Harms, 2003]. Also in the last decade, from 2010 to 2020, the car use increased in the Netherlands with 9 percent, which is higher than the growth of the population above the age of 18, which was 7 percent [Zijlstra et al., 2022]. Today, 55 percent of the space on Dutch streets is allocated to car traffic and car parking [Liere et al., 2017]. Private cars require significantly more space compared to other transport modalities; a car driving at a speed of 50 km per hour occupies 28 times more space than a moving bicycle, and when parked, it needs 10 times more space than a bicycle [Liere et al., 2017]. Given the ongoing urban growth and increasing population densities, particularly in major cities in the Netherlands [de Jong et al., 2022], this makes it even more important to address the issue of space allocation. By rethinking urban space usage, cities can create more room for sustainable and space-efficient modes of transport, as well as creating more greenery and recreational space in the cities.

Widespread car use also contributes to reduced traffic safety and various environmental challenges. Higher levels of car dependency are linked to increased accident risks, whereas a shift towards cycling has been shown to improve overall road safety when the number of car kilometres in urban areas is reduced [Wegman et al., 2012]. The environmental challenges include air pollution and increased noise and heat levels in urban areas [HealthEffectsInstitute, 2010] [Nieuwenhuijsen et al., 2016]. These issues, along with the extensive use of urban space for cars, have been linked to a decline in urban liveability. In response, many European cities are increasingly reallocating space away from cars and encouraging reductions in car usage. This transition aligns with the broader objective of achieving net zero carbon emissions by 2050, necessitating a move from fossil fuel-powered vehicles to more sustainable modes of transport [Bode et al., 2019].

### 1.1. Context

To enhance urban liveability, many Dutch cities aim to reduce car usage and want a transition to a low-car city [Jorritsma et al., 2023]. The term “low-car city” is not specified very accurately, but it generally refers to cities with policies aimed at reducing car presence without entirely banning cars from urban areas. Low car developments, which are a key feature of low-car cities, typically include residential or mixed-use areas designed to limit car use. These developments often offer limited parking to discourage car ownership and use by residents [Melia et al., 2011].

The Dutch Institute for Mobility Policy (KiM) has outlined various policies to implement low-car cities [Jorritsma et al., 2023]. These policies include adjusting the urban environment, modifying parking regulations and redesigning roads and streets. Specifically, the intervention of closing streets to car traffic and redesign streets can reduce the urban space consumption of the car and can simultaneously mitigate noise and air pollution by decreasing car use. KiM has studied the effects of these policies



on car ownership and usage. However, the impact of closing and redesigning streets on car use remains uncertain. Closing streets can potentially lead to vehicles taking longer detours, but it may also reduce the overall car use. This phenomenon, known as disappearing traffic [Cairns et al., 2002], is a central aspect of this study, as it can significantly impact predictions of car use in response to road capacity reductions. Despite its potential benefits, there is currently insufficient knowledge to accurately incorporate disappearing traffic into traffic models [Vonk et al., 2024]. The term “disappearing traffic” is interpreted differently across studies, depending on the specific elements considered. Some studies focus on the reduction in car trips within a particular area, while others examine the overall reduction in trips across all modes of transport. In this study, both aspects are addressed to provide a comprehensive understanding of the phenomenon.

Current research on disappearing traffic mainly consists of independent case studies, making it difficult to predict its occurrence due to its location-specific nature. Currently, there is not enough knowledge about disappearing traffic to determine in which situations the overall car use decreases and to what extent disappearing traffic occurs. Therefore, a comprehensive study is needed to understand the effects of reducing road capacity on car use and predict the level of disappearing traffic on future road capacity reduction scenarios.

In line with the broader trend towards low-car cities, Rotterdam is making significant efforts to reduce car space and promote alternative modes of transport. These initiatives reflect a growing recognition of the need to rethink urban mobility. Rotterdam is the second-largest city in the Netherlands and is a relatively car-oriented city compared to many other Dutch cities. This focus on cars can be traced back to the post-Second World War reconstruction, when the city was rebuilt with considerable space allocated for cars [Mingardo, 2020]. Over the past decade, however, there has been increasing attention towards reallocating car space to other modes of transport. For instance, in 2021, the Coolsingel in the city centre was renovated, reducing the road from two lanes to one lane in each direction. This transformation created additional space for cyclists and pedestrians [Gemeente Rotterdam, 2024d]. The municipality remains committed to further reducing car space. Upcoming projects include the redevelopment of Hofplein, currently a major roundabout dominated by car traffic, into a pedestrian-friendly area with increased greenery [Gemeente Rotterdam, 2024b]. Additionally, the Traffic Circulation Plan aims to implement smaller infrastructural changes to discourage car use.

To support these initiatives, the municipality seeks to predict the impact of these road interventions. Traditional traffic models, which assume constant traffic demand, often overestimate congestion levels. For example, the redevelopment of the Roseknoop, located in the south of Rotterdam, resulted in less congestion than predicted by existing traffic models. Consequently, the municipality aims to develop a model that can simultaneously predict reductions in car trips and accurately estimate the resulting traffic patterns.

## 1.2. Research objectives and scope

The primary objective of this research is to develop a predictive model that estimates the levels of disappearing traffic based on a given capacity reduction and the current road network usage. This model aims to provide urban planners and policymakers with a tool to better understand and anticipate the impacts of reducing road space allocated to cars. Additionally, the research seeks to identify key variables influencing the changing travel behaviour associated to road capacity reductions and derive insights into the mechanisms underlying this phenomenon. The results obtained from the model will be analysed to assist policymakers in making informed decisions about road space allocation and traffic reduction strategies.

The predictive model is designed to estimate the levels of disappearing traffic during the evening peak as this period represents the highest demand on the traffic network. The model will focus on the three most utilised modes of transport: car, public transport and bicycle. It emphasises the changing modal split resulting from increased car travel times. Additionally, an opt-out alternative, the ‘no trip’ option, is incorporated to account for the aggregated effects of changes in destination, departure time and trip frequency. While the model will be specifically tailored to the city of Rotterdam, the methodology employed is transferable to other European cities.

## 1.3. Research questions

In order to reach the above mentioned objectives, a research question is formed. The central research question for this study is: *How can the change in travel behaviour be accurately predicted following road capacity reductions in urban areas, and what insights can be drawn from these predictions?*.

To address this question comprehensively, several sub-research questions are formed.

1. Under what conditions does disappearing traffic occur, and what are the key drivers behind this phenomenon?
2. What are the essential components of a predictive model for estimating disappearing traffic and how are its components interconnected?
3. What insights do two case studies of road capacity reductions in Rotterdam provide about changing travel patterns?
4. What are the key characteristics of the calibrated predictive model?
5. How does the predictive model perform when applied to a case study in Rotterdam?
6. What insights can be drawn from the model's application for future urban planning and traffic management?

## 1.4. Thesis Outline

The structure of this report is designed to provide a logical flow, beginning with a theoretical foundation and moving toward model development, calibration and practical application. Each chapter contributes to the central question by addressing specific sub-research questions.

Chapter 2 presents a thorough review of the literature on disappearing traffic and changing travel behaviour. The chapter describes case studies about disappearing traffic and also investigates induced demand. Based on findings in literature, the first question is answered; *Under what conditions does disappearing traffic occur, and what are the key drivers behind this phenomenon?*.

In Chapter 3, the theoretical framework and approach for constructing the predictive model are presented. This chapter outlines the various steps involved, providing a conceptual explanation of each step, and establishes the relationships between them. With this information, the following research question is addressed: *What are the essential components of a predictive model for estimating disappearing traffic, and how are these components interconnected?* The components of the model are subsequently defined in a more mathematical context in Chapter 4.

Following, two phases of roadworks in the south of Rotterdam are investigated in Chapter 5. The insights gained from these case studies provide an answer to the question *What insights do two case studies of road capacity reductions in Rotterdam provide about changing travel patterns?*. Besides answering this research question, the case studies also form a base for the calibration and validation of the model.

Based on the outcome on one of the two case studies, Chapter 6 provides the method applied to calibrate the model. The resulting calibrated model answers the question *What are the key characteristics of the calibrated predictive model?*.

The calibrated model is then applied to another case study, which is presented in Chapter 7. This chapter examines the effectiveness of the model in predicting disappearing traffic across case studies in Rotterdam and answers the fifth research question *How does the predictive model perform when applied to a case study in Rotterdam?*.

Finally, Chapter 8 provides the findings to the research questions. It summarizes the insights gained from the model's application and discussing their implications scientific research and practical implications for future traffic management and urban planning.

# 2

## Literature review

This chapter presents the findings of the literature review on changes in travel behaviour resulting from changes in road capacity. The focus of this review is the overall reduction in car trips, commonly referred to as disappearing traffic. The objective of this literature review is to develop an understanding of when and how disappearing traffic occurs. This will contribute to the formulation of the theoretical model by identifying the key variables influencing this phenomenon.

The chapter begins with an outline of the methodology employed in the literature review in Section 2.1. This is followed by a discussion of reports that describe disappearing traffic in general in Section 2.2. Section 2.3 examines key case studies in which road capacity has been reduced. Subsequently, changes in behaviour in response to reductions in road capacity are explored in Section 2.4. The concept of induced demand, which represents the opposite effect of disappearing traffic, is discussed in Section 2.5. The modelling approaches applicable to changing travel behaviour and disappearing traffic are then outlined in Section 2.6. Finally, the chapter concludes with a summary of the key insights from the literature review in Section 2.7.

### 2.1. Literature review methodology

For this research, it is essential to establish a comprehensive understanding of the state of the art on disappearing traffic in order to address the research question: "How can changes in travel behaviour be accurately predicted following road capacity reductions in urban areas during the evening rush hour, and what insights can be drawn from these predictions?". Relevant literature on disappearing traffic has been identified using Google Scholar, Scopus, and TRID.

The following research keywords and combinations of concepts were used in the search engines: *disappearing traffic*, *evaporating traffic*, *car capacity reductions*, *road capacity reductions AND effect on car use*, *road narrowing AND effect on car use*, *induced demand*, and *induced demand AND elasticity*. In addition to keyword-based searches, the *snowballing* method was employed, whereby new articles were identified through references cited in relevant reports.

### 2.2. Disappearing traffic in general

This section provides an overview of studies that examine disappearing traffic in general. The most extensive study on this phenomenon was published in 1998, with a follow-up study in 2001 [Cairns et al., 2002]. The original study analysed 70 case studies from eleven countries to investigate the occurrence of disappearing traffic. The follow-up study highlighted that the choices people make following a reduction in road capacity are more complex than previously assumed. It categorised disappearing traffic into three scenarios.

In the first scenario, road space reallocation does not necessarily lead to a reduction in capacity, as changes in traffic management or adaptations in driving behaviour may offset the impact. Consequently, traffic intensities remain unchanged, and no disappearing traffic is observed. In the second scenario,

capacity is reduced, but there is sufficient spare capacity on alternative routes, maintaining overall traffic levels across the network. In this case, disappearing traffic is also minimal. In the third scenario, however, spare capacity on alternative routes is insufficient. Here, disappearing traffic is frequently observed due to behavioural changes, including shifts in mode choice, destination choice, and trip frequency. The study demonstrated that traffic levels decrease significantly following a reduction in road capacity, resulting in minimal deterioration in traffic congestion.

In 2017, TNO, a Dutch research institute, conducted a study on disappearing traffic, comprising a literature review on Dutch examples of capacity reductions and a workshop on the topic [Vonk et al., 2024]. The study highlighted that varying definitions of disappearing traffic make it difficult to compare different cases, and that the extent of disappearing traffic is highly dependent on local conditions. Furthermore, many studies do not adequately consider the role of alternative modes of transport. The research concluded that current knowledge on disappearing traffic is insufficient to incorporate it into traffic models effectively, advocating for further Dutch research on the subject. It also emphasised the importance of the measurement period, as a new equilibrium takes time to form. The study recommended that traffic levels be assessed three to six months after a capacity reduction to ensure that a new balance has been established.

As outlined in the introduction, the Dutch Institute for Mobility Policy (KiM) has explored various policies for implementing low-car urban environments [Jorritsma et al., 2023]. Figure 2.1 provides an overview of the policy measures examined and their effects on car ownership and usage. The measures categorised under roads and streets are particularly relevant to disappearing traffic. Road closures and street redevelopment are both classified as having an unknown effect on car usage.

	Effect on car ownership	Effect on car usage
<b>Built environment</b>		
Densification	reduction	reduction
Mixing of functions	reduction	reduction
<b>Parking</b>		
Remove existing parking space	unknown	reduction
Strict parking norms for new construction	reduction	reduction
Parking permits	reduction	unknown
Increase parking fees	reduction	unknown
Remote parking	unknown	unknown
<b>Roads and streets</b>		
Road closure	slight reduction	unknown
Car low city centre	unknown	unknown
30 kph streets	slight reduction	unknown
Redevelopment of streets	slight reduction	unknown

**Table 2.1:** Low car policies and its effect on car ownership and car use per person [Jorritsma et al., 2023] (translated from Dutch to English)

2.3. Case studies research into disappearing traffic

There have been multiple independent studies examining the effects of road capacity reductions. The majority of these are data-driven investigations, complemented by several revealed preference studies on disappearing traffic. However, studies in the latter category do not appear to identify significant impacts. A study conducted in the United Kingdom in 2021, which analysed changes in travel behaviour following the pedestrianisation of a street in the city centre of a small town with 65,000 inhabitants, did not find significant differences [Melia and Calvert, 2023]. Similarly, a study in Oslo, which utilised a street-space reallocation survey, observed only minor modal shifts [Tennøy and Hagen, 2020].

Conversely, multiple data-driven studies have identified behavioural adaptations to road capacity reductions. In Bristol, United Kingdom, a city with 617,000 inhabitants, the impact of closing a central bridge—which provided the only direct north-south and east-west connection through the city centre—for five weekdays was examined [Melia and Calvert, 2023]. The findings indicate a 6.8% reduction in traffic in the central area and a 2.3% reduction in the outer area. Given the short duration of the closure,

no long-term effects could be determined. This closure was well communicated to residents, enabling them to adjust their travel behaviour and withhold some trips during this period. Another study investigated the closure of the Maastunnel in Rotterdam in the southbound direction [Gemeente Rotterdam, 2018]. This research registered a 2.5% modal shift towards public transport and a 2.8% shift towards cycling. The following sections will discuss several larger case studies.

Another study was conducted in Oslo, Norway, where the capacity of the Smestad tunnel, an outer-ring road tunnel, was reduced from four to two lanes for nearly a year [Tennoy et al., 2020]. On the first day of the reduction, morning rush hour traffic decreased by 37% and evening rush hour traffic by 33%, with no significant increase in traffic on alternative routes. Due to extensive media coverage, many commuters altered their travel mode or worked from home, leading to smooth rush-hour conditions. This was widely reported in the press, and consequently, traffic volumes increased the following day, gradually returning to normal levels over subsequent weeks. This suggests that the remaining capacity in the tunnel was sufficient for daily traffic volumes. Another highway tunnel in Oslo experienced a similar lane reduction from four to two lanes between February 2016 and April 2017. This tunnel accommodated a larger daily volume of vehicles. During the closure, daily traffic declined by 26% to 34%. Despite this reduction, the average speed within the tunnel decreased, indicating increased congestion. The primary alternative route experienced an increase in traffic volumes of between 12% and 37%, while other relevant municipal roads saw minimal changes. Overall, a reduction of 4.2% in morning rush hour traffic and 2.2% in evening rush hour traffic was observed at selected traffic counting locations.

Nello-Deakin examined the effects of eleven road interventions in Barcelona, where traffic lanes were reduced and replaced with bike lanes, bus lanes, or expanded sidewalks [Nello-Deakin, 2022]. All these interventions were implemented during the COVID-19 pandemic, a period that saw increased emphasis on active travel modes. This study compared traffic counts from the second half of 2019 (pre-intervention) with those from the second half of 2021 (post-intervention). Traffic counting locations were categorised into four groups: intervention streets, adjacent streets (alternative routes), buffer area streets (alternative routes within 500 metres of the intervention street), and control area streets (control group locations more than 500 metres from the intervention). Monthly daily average traffic levels were calculated relative to the control group stations. On average, vehicular traffic on intervention streets declined by 14.8%. Adjacent streets experienced a minor increase of 0.7%, while buffer streets exhibited a slight decrease of 0.5%. These findings suggest an overall reduction in vehicular trips.

Recently, a study was published on the closure of the Weesperstraat and three adjacent streets in Amsterdam, the Netherlands [Gemeente Amsterdam, 2024]. This six-week pilot aimed to assess the impacts on car usage, network utilisation, modal shifts, liveability, and air and noise pollution. The research comprised 30 sub-studies, with most findings compared to data from two weeks in May 2023, immediately preceding the pilot. Results indicate that within the pilot area, there was an 18% reduction in unique vehicles and a 10% reduction in vehicle kilometres. Across the entire Amsterdam area, there was a 3% reduction in unique vehicles and a 5% reduction in vehicle kilometres. The most attractive diversion route experienced a 40% increase in traffic and an average delay of three minutes. Certain streets saw reductions in average speed, particularly along diversion routes. Conversely, some streets recorded increased average speeds, likely due to lower traffic volumes. No significant change was observed in public transport usage, possibly due to the limited duration of the pilot.

In 2003, the city of Seoul, South Korea, demolished an elevated highway running through the city centre and restored the Cheonggyecheon stream. The number of traffic lanes was reduced from four to two in each direction. A study was conducted to analyse changes in travel behaviour and identify lessons learned from this intervention [Chung et al., 2012]. Prior to the restoration, concerns were raised about potential congestion; however, residents adapted by altering their route, departure time, or travel mode—a phenomenon referred to in the study as self-compliance. Traffic data indicated an increase in subway ridership and a decline in car usage. Initially, the average travel speed on alternative routes deteriorated but eventually returned to previous levels. The study states: *“Self-compliance caused the system to revert back to its former condition, although this is unlikely to hold true for all urban restoration projects.”* This latter point emphasises that specific conditions must be met to prevent increased congestion. These conditions include careful planning and the availability of sufficient alternatives, such as alternative routes and high-quality public transport.



**Figure 2.1:** Cheonggyecheon stream restoration project



**Figure 2.2:** Self-compliance in response to road capacity reduction

## 2.4. Behavioural adaptation in response to road capacity reductions

This section examines research into the behavioural changes of travellers following a reduction in road capacity. In 2024, Amsterdam Bereikbaar conducted a study on the potential behavioural adaptations in response to future roadworks around Amsterdam [Claassen et al., 2024]. Although this study primarily focuses on temporary road capacity reductions, it provides valuable insights into the types of behavioural changes that may occur and the conditions under which they are likely to take place. The overall methodology of this research consisted of four stages. First, for each road construction project, the effects on route choice and network load were analysed, leading to an estimation of the expected additional travel time. Second, the origins and destinations of affected trips were examined. Third, based on the preceding analyses, the potential for behavioural change was assessed.

The study concludes that this potential is highly dependent on both the number of affected travellers and the extent of travel time loss. A marginal increase in travel time due to roadworks is unlikely to make alternative modes, such as cycling or public transport, significantly more attractive. Consequently, the greater the number of affected travellers and the longer the additional travel time, the higher the likelihood of behavioural adaptation. However, these are not the only determining factors. Other influential factors include the level of car dependency, trip purpose, personal financial constraints, the presence of fellow travellers, freight transport requirements, and occupations that necessitate car or freight vehicle use. The study also highlights that for origin–destination pairs where high-quality public transport or cycling infrastructure already exists, those who still choose to drive are more likely to be highly car-dependent or have no viable alternative. As a result, achieving substantial behavioural change in such cases is more challenging.

For each alternative mode, the study identifies the conditions under which it is likely to have a high potential for uptake. The (electric) bicycle is considered an attractive alternative when a significant proportion of origins and destinations are within a 15-kilometre range. The viability of buses, trams, and metro services depends on the location of the roadworks and the spatial relationship between origins, destinations, and public transport routes. These modes are most appealing for short-distance trips within the city and for travel from surrounding areas towards central locations. The train presents a feasible alternative when both the origin and destination are near railway stations and the total journey time is comparable to that of driving. Park and Ride (P+R) facilities are suitable for travellers originating outside the city and heading towards the city centre, provided these facilities are conveniently located before the roadworks. In addition to mode shifts, some travellers may opt to adjust their departure times to avoid peak-hour congestion.

## 2.5. Insights from capacity expansion: understanding induced demand

This research focuses on behavioural changes following a reduction in capacity. However, there is extensive research on the opposite intervention: increasing capacity. It is crucial to understand the outcomes of capacity enhancement, as these findings can subsequently be translated to interventions involving capacity reductions.

*"Traffic engineering theory is straightforward: a street is congested because the number of drivers exceeds its capacity. If you enlarge the street, you will eliminate congestion. Unfortunately, seventy-five years of evidence tells us that this almost never happens."* [Speck, 2018].

The reason congestion does not diminish is that the widened road will only experience a brief reduction in travel time immediately after the highway opens. As time progresses, the road that has been relieved of congestion attracts individuals who previously wished to use that route but were deterred by the existing congestion. This phenomenon is referred to as latent demand [Clifton and Moura, 2017]. A framework illustrating latent demand is presented in Figure 2.3.

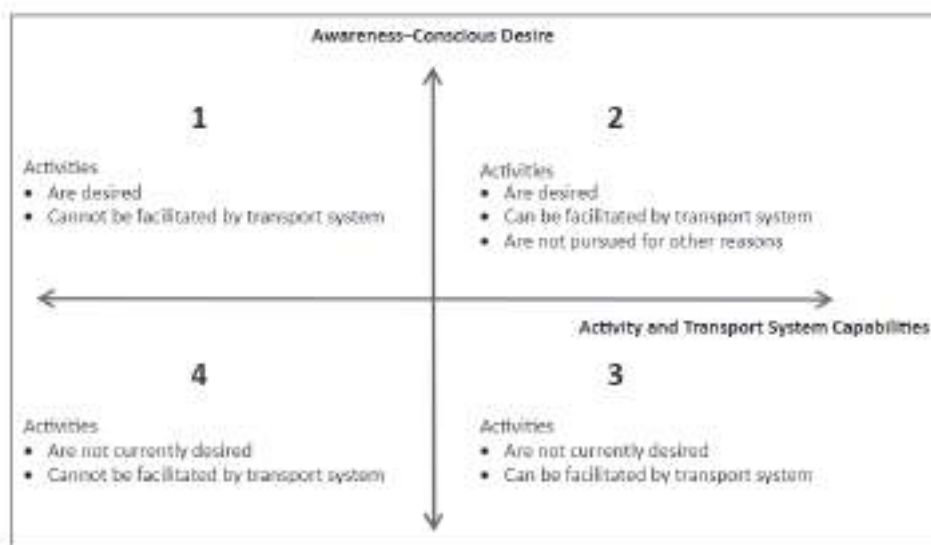


Figure 2.3: Framework latent demand [Clifton and Moura, 2017]

Latent demand is driven by individuals that choose another departure time, mode or stay home in order to not get stuck in traffic [Speck, 2018]. If capacity is increased, individuals and businesses could even move further from the city, following the vicious circle of congestion (see Figure 2.4). This phenomenon is called induced demand and is the opposite of disappearing traffic.



Figure 2.4: Vicious circle of congestion [Rodrigue, 2024]



The subsections below outline key aspects of road expansion and the resulting induced demand. Firstly, the type and order of increase in travellers is addressed in Subsection 2.5.1. Secondly, induced demand is analysed from an economic perspective in Subsection 2.5.2. Subsection 2.5.3 discusses potential methods for incorporating induced demand into traffic models. Finally, Subsection 2.5.4 will examine the aspects of induced demand that are relevant to the concept of disappearing traffic.

### 2.5.1. Generated traffic

The increase in travellers on the road will result in congestion that is, more or less, equivalent to that experienced previously; it returns to the former congestion equilibrium during peak hours. This increase in travellers is referred to as generated traffic. Generated traffic comprises diverted travel and induced travel [Litman, 2017]. Diverted travel represents the shift from other routes and times to the peak hour period of the widened road, while induced travel signifies an overall increase in vehicle usage. Induced travel is partially driven by the law of conservation of travel time and movement, which suggests that individuals maintain a constant daily average travel time of approximately 70 minutes [Ahmed and Stopher, 2014]. Consequently, reductions in congestion will stimulate greater mobility rather than saving travel time. Litman has researched the most significant types of generated traffic, as illustrated in Figure 2.2. He categorises generated traffic into four types: diverted trips (a shift in time or route), induced vehicle trips (trips that were already made but using a different mode than the car), longer trips (where the vehicular trip length has increased), and induced trips (where trip frequency increases). For each type, it is assessed whether the change is short-term or long-term and what the implications for travel and costs are.

Type of generated traffic	Explanation	Category	Time frame
Shorter route	Improved road allows drivers to use more direct route	Diverted trip	Short term
Longer route	Improved road attracts traffic from more direct routes	Diverted trip	Short term
Time change	Reduced peak period congestion reduces the need to defer trips to off-peak periods	Diverted trip	Short term
Mode shift (existing travel choices)	Improved traffic flow makes driving relatively more attractive than other modes	Induced vehicle trip	Short term
Mode shift (changes in travel choices)	Less demand leads to reduced rail and bus service, less suitable conditions for walking and cycling and more automobile ownership	Induced vehicle trip	Long term
Destination change (existing land use)	Reduced travel costs allow drivers to choose farther destinations. No change in land use patterns	Longer trip	Short term
Destination change (land use changes)	Improved access allows land use changes, especially urban fringe development	Longer trip	Long term
New trip (no land use changes)	Improved travel time allows driving to substitute for non-travel activities	induced trip	Short term
Automobile dependency	Synergetic effects of increased automobile oriented land use and transportation system	Induced trip	Long term

**Table 2.2:** Generated traffic overview [Litman, 2017] (table adapted)

Since the short term and long term in Figure 2.2 can vary in time period, Litman defined four orders or capacity expansions. This is shown in Table 2.3.

Order	Definition
First	Reduced congestion delay, increased traffic speeds
Second	Changes in time, route, destination and mode
Third	Land use changes. More dispersed, automobile-oriented development
Fourth	Overall increase in automobile dependency. Degraded walking and cycling conditions, reduced public transit service and social stigma associated with alternative modes

**Table 2.3:** Four different orders in capacity expansions [Litman, 2017]

Another aspect which is often researched with respect to induced demand is the elasticity of the additional traffic compared to the road capacity. The elasticity is the ratio between the generated traffic and the

new added capacity. A elasticity of 0 indicates no generated traffic after a capacity increase and an elasticity of 1 means that the new capacity is 100 percent filled with new road users. In Figure 2.5, the traffic growth after several years after completion of the project is shown for different levels of latent demand based on a literature study.

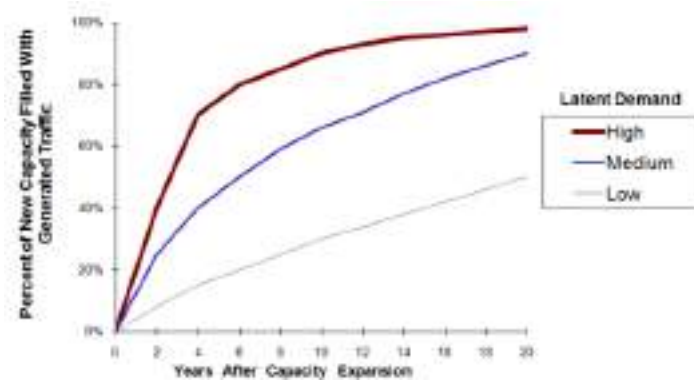


**Figure 2.5:** Elasticity of traffic volume with respect to road capacity [Litman, 2017]

Table 2.4 shows the results of a literature research to induced demand from Rodier et al. [2001] split out for short-term and long-term.

Author	Short-term	Long-term (3+ years)
SACTRA		0.5-1
Goodwin	0.28	0.57
Johnson and Ceerla		0.6-0.9
Hansen and Huang		0.9
Fulton et al.	0.1-0.4	0.5-0.8
Marshall		0.76-0.85
Noland	0.2-0.5	0.7-0.1

**Table 2.4:** Elasticity levels from different scientific research [Litman, 2017]

Table 2.4 and Figure 2.5 show a wide range in induced traffic levels. This corresponds to the results of the literature review of case studies of Dunkerley et al. [2018]. This study confirms that induced traffic exists and may be significant in some situations. The probability of occurrence is the highest in urban areas and on highly congested routes. When applied to the national highway network, the impact is often smaller.

### 2.5.2. Induced demand from economical perspective

Considering induced demand from an economic perspective, it can be defined as a movement along the travel demand curve. Here, the price axis encompasses not only monetary costs but also travel time and other user costs, while the horizontal axis represents traffic volume [Lee et al., 1999]. The fact that an expanded highway attracts additional travellers indicates that the demand for travel is elastic. Lee et al. (1999) divide this travel demand into two components. Exogenous factors—those not influenced by infrastructure, such as population growth, employment rate, availability of alternative modes, land use and income patterns—determine the location of the demand curve. Endogenous factors, such as travel time and travel costs, determine the specific point along the demand curve. Since changes in road capacity affect travel time, such interventions also influence the position on the demand curve. Short-run elasticity is generally lower than long-run elasticity, as travel demand becomes more flexible over time due to factors such as potential traffic growth.

Figure 2.6 illustrates the distinction between diverted trips and induced trips from an economic perspective. The general equilibrium demand curve accounts only for car trips, whereas the partial equilibrium demand curve includes all travellers in the market, such as those currently opting for alternative modes, different routes or departure times or those who choose not to travel due to congestion. The general equilibrium demand curve exhibits greater elasticity, as it offers a wider range of alternative options, resulting in increased flexibility. In the scenario presented in the figure, an increase in capacity leads to a reduction in the generalised cost of travel, from  $p_0$  to  $p_1$ . This, in turn, results in an increase in both partially new trips (induced travel) and diverted trips (diverted travel). Another factor influencing elasticity is whether the curve represents demand over a full day or only during peak periods. If only peak periods are considered, elasticity increases, as individuals have more choices available. The figure also demonstrates that when capacity is increased, consumer surplus rises, as the overall cost of car travel decreases, benefiting existing drivers and attracting new users.

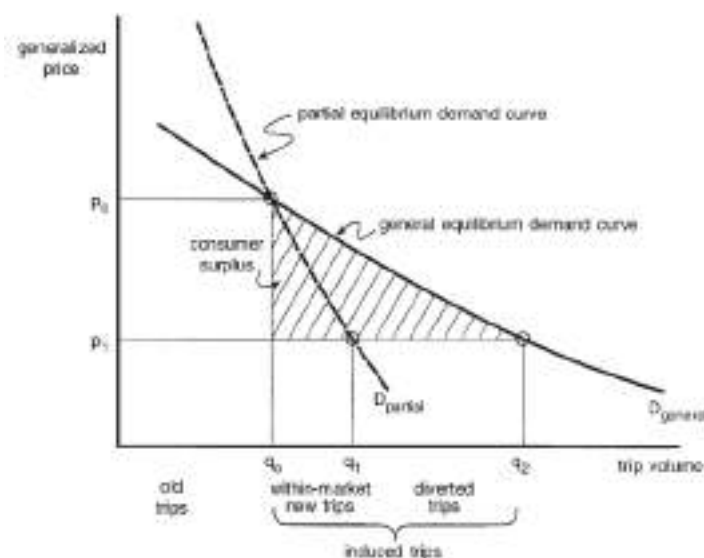


Figure 2.6: Partial and general equilibrium demand curves [Lee et al., 1999]

### 2.5.3. Modelling implementations induced demand

To gain deeper insights into induced demand, generated traffic should be incorporated into traffic models. These models should include a feedback loop in which congestion influences travel behaviour and long-term land use changes [Litman, 2017]. While most traffic models account for route and mode shifts, they often fail to consider trip frequency and the broader shift towards a more car-dependent society. As a result, long-term traffic volumes are currently underestimated due to the omission of induced vehicle travel. This has significant implications for cost-benefit analyses of road expansion projects, as the anticipated travel time savings are smaller than expected, while the environmental impact is greater than initially projected.

### 2.5.4. What can be learned from induced demand?

Understanding induced demand can significantly contribute to the development of the model for this research, as induced demand has been studied more extensively than disappearing traffic. Both terms are its opposites, however, the underlying mechanisms of both phenomena are fundamentally the same. When road capacity is expanded, the friction associated with driving is reduced, leading to an increase in vehicle numbers. Conversely, when capacity is reduced, friction increases.

Induced demand demonstrates that traffic is flexible and adapts to the available road capacity. A similar process is likely to occur when capacity is reduced; disappearing traffic may partially arise from individuals maintaining the same origin and destination but altering their mode of transport or departure time. Additionally, some individuals may reduce their overall travel. Adaptations to induced demand typically take between five and ten years. However, identifying the adaptation period for disappearing traffic is more challenging. It is possible that adjustments to disappearing traffic occur more rapidly, as travellers are confronted with increased travel times. In contrast, for induced demand, the process operates in the opposite direction.

## 2.6. Modelling disappearing traffic

As outlined in several studies above, disappearing traffic arises from the increased friction associated with car use. A reduction in road capacity leads to less available 'space' for vehicles, resulting in a decline in the efficiency of the car-based mobility system. For users, this translates into increased travel times.

When modelling disappearing traffic, at least two key aspects must be considered. The first is the additional travel time caused by a given reduction in capacity. The second is the calculation of a new mobility distribution, which encompasses alternative modes of transport as well as the option of not making the trip anymore. Methods to examine the increase in additional travel time and the methods for recalculating the mobility distribution are shown in Subsection 2.6.1 and 2.6.2.

### 2.6.1. Increase in travel time over network

The most common option for computing an increase in travel time due to a change in the infrastructure network is using a traffic model. The increase in travel time can be calculated based on a given network assignment. The most common traffic models are macroscopic models and microscopic models. Macroscopic models use aggregated traffic flow characteristics, comparable as how fluids flow, whereas microscopic models simulate each individual vehicle [Calvert et al., 2016].

Literature shows that modelling of congestion is important when considering disappearing traffic. Congestion can be modelled best by microscopic level, since these models capture behaviour of lane changes and headways better than macroscopic models [Ferrara et al., 2018]. Also, the trip individual information, like travel time per trip, is important information to compare different situations. Therefore, the best method to determine the increase of travel time on an individual level is by using a microscopic traffic model.

### 2.6.2. Mobility distribution

The second aspect of modelling disappearing traffic involves recalculating a new mobility distribution. Based on the additional travel time, users may opt for an alternative mode of transport or decide not to undertake the trip at all.

#### Modal split

In transport modelling, the logit model is frequently employed to determine the modal split [Cingel et al., 2019]. This model is grounded in the principle of Random Utility Maximisation, whereby decision-makers evaluate the utility associated with each available alternative  $i$  generating a set of utilities  $U_1, U_2, \dots, U_j$ . The total utility comprises an observable component  $V_i$  and an unobservable component  $\varepsilon_i$ . When  $\varepsilon_i$  is assumed to follow an Extreme Value Type I distribution, the modal split can be derived using the Multinomial Logit model, as expressed in Equation 2.1.

$$P_i = \text{Prob}(V_i + \varepsilon_i > V_j + \varepsilon_j, \forall j \neq i) = \frac{e^{V_i}}{\sum_j e^{V_j}} \quad (2.1)$$

### Modelling no travel alternative

The literature presents various approaches to modelling the alternative of staying at home instead of travelling. In particular, following the COVID-19 pandemic, there has been increased interest in incorporating the ‘no travel’ alternative into traffic models. Research conducted by TNO explored the possibilities of integrating this option and identified several methods (see Figure 2.7). Their findings suggest two principal approaches to including the ‘no travel’ alternative in traffic models. The first involves externally adjusting trip frequency prior to running the model (see Option 1), while the second integrates the ‘no trip’ alternative within the model itself—either at the distribution, modal split, or time-of-day stage (see Options 2, 3, and 4).

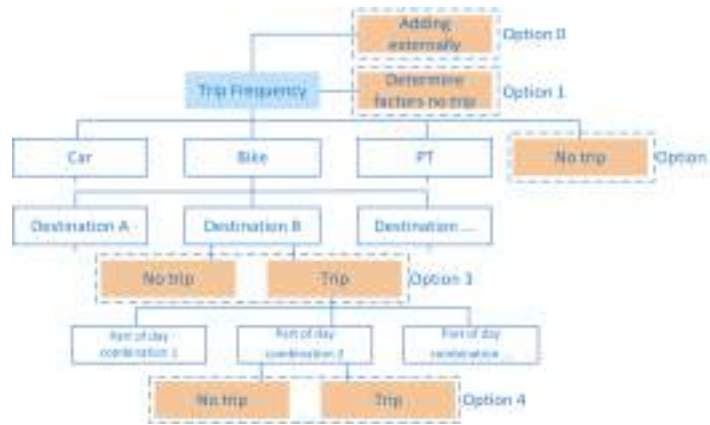


**Figure 2.7:** Possibilities of incorporating the no travel alternative in traffic models [Snelder and van der Tuin, 2023]

When modelling disappearing traffic, the additional travel time per Origin Destination pair (OD pair) is a crucial factor in determining the extent of disappearing traffic. Consequently, incorporating the ‘no trip’ alternative within the traffic model is the most suitable approach. Hensher et al. [2023] examined the effects of integrating a work-from-home factor into traffic models and identified a significant impact. Their study analysed the influence of socio-economic variables, day of the week, spatial location effects, and modal attributes on the utility of working from home.

## 2.7. Conclusions from literature

This section summarises the findings of the literature review, discussing the conditions under which disappearing traffic occurs and the key factors influencing its extent. Table 2.5 provides an overview of the most relevant studies on disappearing traffic.

Disappearing traffic may occur following a reduction in road capacity; however, this is not always the case. Based on the literature review, several conditions must be met for disappearing traffic to materialise. If any of these conditions are not fulfilled, the number of daily vehicular trips will remain unchanged:

1. *A road space reallocation must lead to a capacity reduction; road space reallocation might not always lead to a reduction in maximum throughput.*
2. *The original maximum intensity should be lower than the new set capacity*
3. *The realistic and plausible alternative routes lack sufficient capacity to accommodate the excess volume of cars*
4. *The difference between the maximum intensity and the new set capacity should be large enough so that a shift of departure time (between peak and non-peak hours) is not sufficient to not let the congestion increase*

The primary driver of disappearing traffic is the increase in congestion following a capacity reduction. When road space for cars is reduced, congestion rises if the number of car users remains constant. This leads to increased travel times, introducing additional friction for car travel. In response, individuals seek to minimise this friction by altering their travel behaviour. They may choose to change their route, departure time, mode of transport, or destination, reduce their travel frequency, or decide not to travel at all. Disappearing traffic mainly results from decisions made by individuals who derive relatively low added value from car travel. For these travellers, the inconvenience of congestion outweighs the benefits of driving, making alternative modes of transport, such as public transport, a more attractive option.

When individuals adjust their travel behaviour and reduce car trips, congestion on the affected road decreases, which in turn leads to a reduction in travel time. This process is iterative: congestion levels influence the number of travellers, and the number of travellers influences congestion. Over time, a new equilibrium is reached. The literature review also identifies key factors influencing the extent of vehicular trip reductions. These include number of hindered car travellers, additional travel time, accessibility by alternative modes, level of car enthusiast travellers, number of travellers forced to car, travel motive, rest capacity (on other roads) and rest capacity outside rush hour.

Author	Year	Title	Type of research	Main conclusions
Cairns, Atkins, Goodwin	2002	Disappearing traffic: the story so far	Literature to multiple case studies	An average reduction of 11% of overall traffic can be seen when capacity is reduced, but this is highly dependent on local environment
Vonk, Talen, Peirik	2017	Redevelopment projects and disappearing traffic	Literature study and expert interviews	Currently, the focus is on studying the effect on car use, but other modalities are studied less. Current knowledge about disappearing traffic is not sufficient to adapt traffic models to it.
Tennoy, Hagen	2020	Reallocation of road and street space in Oslo: measures for zero growth in urban traffic	Revealed preference study on case study	Only minor modal changes are found.
Tennoy, Hagen	2020	Effects and consequences of capacity reduction in the Smestad tunnel.	Data analysis on case study	One tunnel which was closed had enough capacity for the original number of daily vehicles. After reduction on first day, traffic grew fast back to original state. Another tunnel with a higher daily number of vehicles which reduced capacity lead to a drop of 2.2 to 4.2 percent in car use and more congestion on the closed-off road.
Faber, Jorritsma, Arendsen	2023	Autoluw beleid gemeenten: doelen, effecten en rollen	Literature to multiple case studies	The effect of closing and redesigning streets on car use is unknown, since it can also cause vehicles driving more distance due to the closed or narrowed road.
Nello-Deakin	2022	Traffic Evaporation Findings from tactical urbanism interventions in Barcelona	Data analysis on case study	Study to eleven road interventions in Barcelona where car roads were turned into bike lanes, bus lanes or side walks. On average a 14.8% reduction of car trips on intervention streets and only a minor increase on adjacent roads. Difficult point of this study is that it happened during Covid, which might influence results. Besides this, due to new bike lanes, not exclusively the effect of reducing road capacity could be investigated.
Melia, Calvert	2023	Does traffic really disappear when roads are closed?	Data analysis and revealed preference study on case study	Two studies, one to a pedestrianized street in a small town. This led to no significant reduction in car trips. Other study was to a closing of a bridge in the city center in a city of 617k inhabitants. This led to 6.8% traffic levels reduction in the central area and a 2.3% reduction in the outer area. But no long-term effects can be investigated, since the closure was only 5 weekdays.
Municipality of Amsterdam	2024	Research report – pilot block Weesperstraat	Data analysis on case study	Effects on closing a busy street in the city centre of Amsterdam of six weeks. There was a reduction of 18% unique vehicles in the pilot area. Overall, a reduction of 3% unique vehicles could be observed.

**Table 2.5:** Overview of studies on disappearing traffic and their main conclusions.

# 3

## Methodology

In this chapter, the methodology for the predictive model will be elaborated in detail. One of the key findings from the literature study is that the increased congestion, and the associated additional travel time, following a capacity reduction is the primary driver behind the decrease in car trips. Immediately after a road capacity reduction is introduced, an adaptation period is initiated. During this period, a portion of car users adjust their behaviour to mitigate the additional travel time. These individuals may alter their route, mode of transport, trip frequency or destination.

Congestion levels have a reciprocal relationship with the number of car trips: increased congestion typically leads to a decrease in car trips, while a reduction in car trips can alleviate congestion. Consequently, both aspects are unstable during the adaptation period. Over time, however, these variables stabilise as individuals stick to their adjusted behaviours and stop reacting to further changes in congestion. Once this stabilisation occurs, a new equilibrium is reached in both car usage and congestion. At this point, congestion levels often resemble those observed prior to the capacity reduction.

To simulate this process, the model consists of an iterative cycle of traffic assignment and recalculation of the mobility distribution. This new mobility distribution includes modal alternatives as well as a 'no trip' option, which takes into account alternative changes in travel behaviour, like changing destination, avoiding rush hour or staying home. The new mobility distribution provides feedback to the Origin-Destination (OD) matrix for car trips within the traffic assignment model. The theoretical framework is presented in Figure 3.1. The model comprises three iterative steps, explained below.

1. The first step of the model involves a traffic simulation. Based on the original OD matrix and a specified capacity reduction, travel times for each OD pair within the network are computed using a dynamic microscopic traffic model. The output of this step is an updated OD travel time matrix. This step is explained in detail in Section 3.1.1.
2. Based on the outcome of the simulations, travel times distributions of selected OD pairs are compared with a Kolmogorov-Smirnov test to see if an equilibrium has reached (see Section 3.1.2). If the travel time has stabilised, the iteration will stop. If not, the iterative process will continue.
3. Based on the updated travel time matrix for cars, the utility for car trips is recalculated for each OD pair in the model. Travel time matrices for cars, bicycles and public transport are retrieved from the V-MRDH model. Based on the travel times and travel distance, the utility of each OD pair for car, bike, public transport and choosing the 'no trip' option is calculated. Based on the updated utility for car trips, a logit model is applied to predict the new mobility distribution. The resulting mobility distribution produces an updated OD matrix for car trips which is the input of the new traffic simulation in step 1. This step is further explained in Section 3.1.3.

The parameters of the utility functions are estimated in the model calibration, further explained in Section 3.2. After that, the calibrated model is validated. The validation method is explained in Section 3.3.



Since three different traffic related models are mentioned in this methodology and the following chapters, this will be clarified by giving a name to the resulting model of this study, which estimates the level of disappearing traffic given a road capacity reduction. This model is called the DiTra model; the Disappearing Traffic model. This is to distinct it from the RODY (Rotterdam Dynamisch) model, which is the dynamic traffic simulation of the municipality of Rotterdam, and the V-MRDH model, which is the static transport and traffic model of the metropolitan area of Rotterdam and The Hague. The python code of the DiTra model is given in Appendix A.

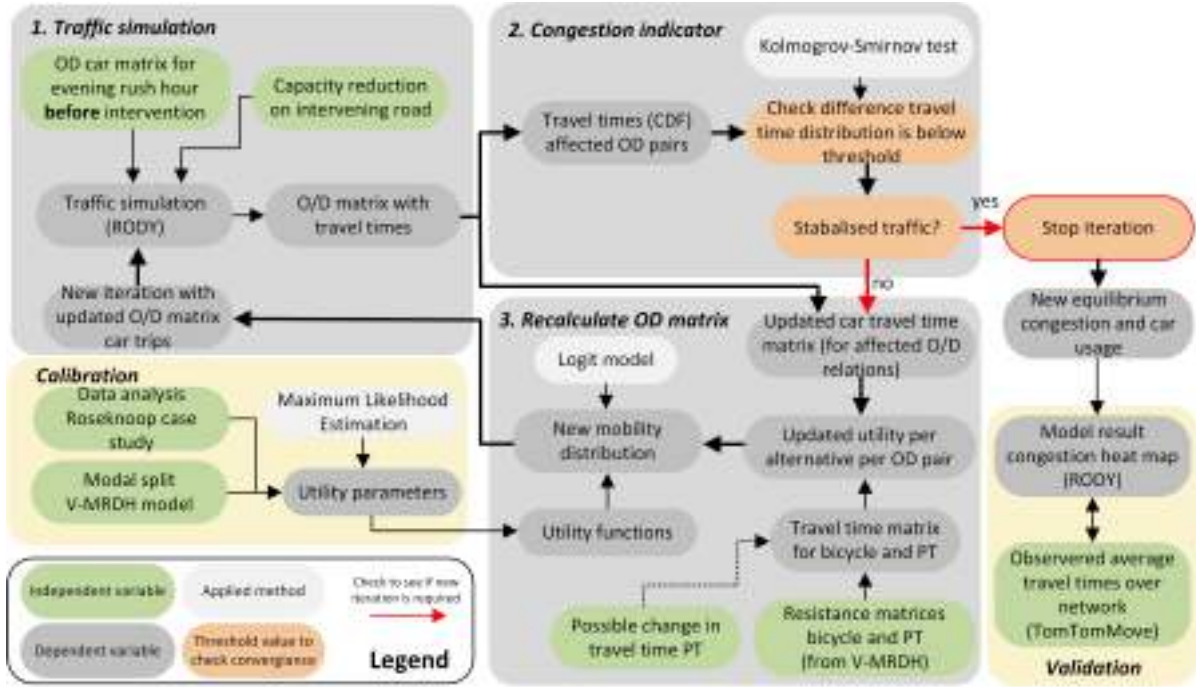


Figure 3.1: Framework of model to predict the new equilibrium in mobility distribution after a capacity reduction.

### 3.1. Model iteration process

The model consists of a three step iterative process. The three steps are elaborated in more detail below.

#### 3.1.1. Step 1: Traffic simulation

The first step in the process of the DiTra model is to determine the travel time for car trips over the network with the capacity reduction based on a given traffic demand. The network assignment, which represents one evening peak, determines the travel times based on the car usage. This simulation reflects how individuals get ‘informed’ about the conditions on the road of one evening peak hour. Based on the updated travel times, individuals can make a decision whether or not they change their behaviour. The overview of this section is displayed in Table 3.1.

In the initial iteration, the original OD matrix from before the capacity reduction is used. The input is implemented in the dynamic microscopic traffic model of Rotterdam, known as Rotterdam Dynamisch (RODY). RODY is developed in the Paramics Discovery software and simulates car traffic in the city of Rotterdam. This model is capable of providing more detailed insights into congestion than a static traffic model. It is constructed using data from the static regional traffic and transportation model Metropool-regio Rotterdam Den Haag (V-MRDH), covering the area of the metropolitan region of Rotterdam and The Hague in detail, and the rest of the Netherlands in reducing detail when the distance increases. RODY covers the area within the rectangular highway shape around Rotterdam, including adjacent neighbourhoods. The model incorporates 371 zones which is an aggregation of the 1381 zones of Rotterdam in the V-MRDH model [de Jong, 2021]. Based on the simulation run, the average travel time for each OD pair can be found based on the traffic conditions. This is the output of the simulation.

Model aspect	Description
Input	<ul style="list-style-type: none"> <li>Capacity change on intervening road</li> <li>OD matrix for car trips</li> </ul>
Modelling	Traffic assignment with a microscopic traffic model
Output	<ul style="list-style-type: none"> <li>The updated OD travel time matrix</li> </ul>

**Table 3.1:** Model aspects calculating travel times for car trips

### 3.1.2. Step 2: Check for stabilised traffic

In this step, it is assessed whether traffic has stabilised or if a new iteration is required. If a significant number of individuals alter their behaviour based on the updated travel times, this leads to a different traffic situation, indicating that a new equilibrium in car usage and congestion has not yet been reached. Conversely, if only a small proportion of individuals modify their behaviour, the traffic conditions will be comparable to those of the previous simulation, allowing the iteration process to cease. The stabilisation of traffic is evaluated based on the travel time output of the affected OD pairs in the RODY simulation.

Based on a selected link analysis in the baseline run of the original Rotterdam model, the OD pairs affected by the road capacity intervention are identified. A distinction is made between directly affected OD pairs (first order) and indirectly affected OD pairs (second order). The directly affected OD pairs originally use the road subject to intervention. The indirectly affected OD pairs consist of those that utilise alternative routes to the intervened road. Drivers on these alternative routes may experience additional travel time if traffic diverts from the intervened road.

Distinguishing between directly and indirectly affected OD pairs provides valuable insights, as the change in travel time differs between them. If the intervened road fully restricts car traffic, the travel time for directly affected OD pairs will inevitably increase due to the need to take an alternative route, resulting in a longer travel distance. In contrast, the indirectly affected OD pairs do not need to change their route unless travel time increases significantly. Therefore, in a stabilised traffic situation, the increase in travel time for indirectly affected OD pairs should be closer to the travel times baseline run compared to the directly affected OD pairs.

To quantify the changes in travel time over the network, the travel times of the vehicles of the (in)directly affected OD pairs are compared across iterations using an empirical Cumulative Distribution Function (CDF). The equation for the CDF is presented in Equation 3.1 [Dekking et al., 2005]. In this context, this means that for a travel time  $x$  the value  $F_n$  indicates the section of OD pairs that has a travel time less than or equal to  $x$ .

$$F_n(x) = \frac{\text{number of OD pairs} \leq x}{\text{total number of OD pairs}} \quad (3.1)$$

An example of CDF outputs of different runs is given in Figure 3.2.

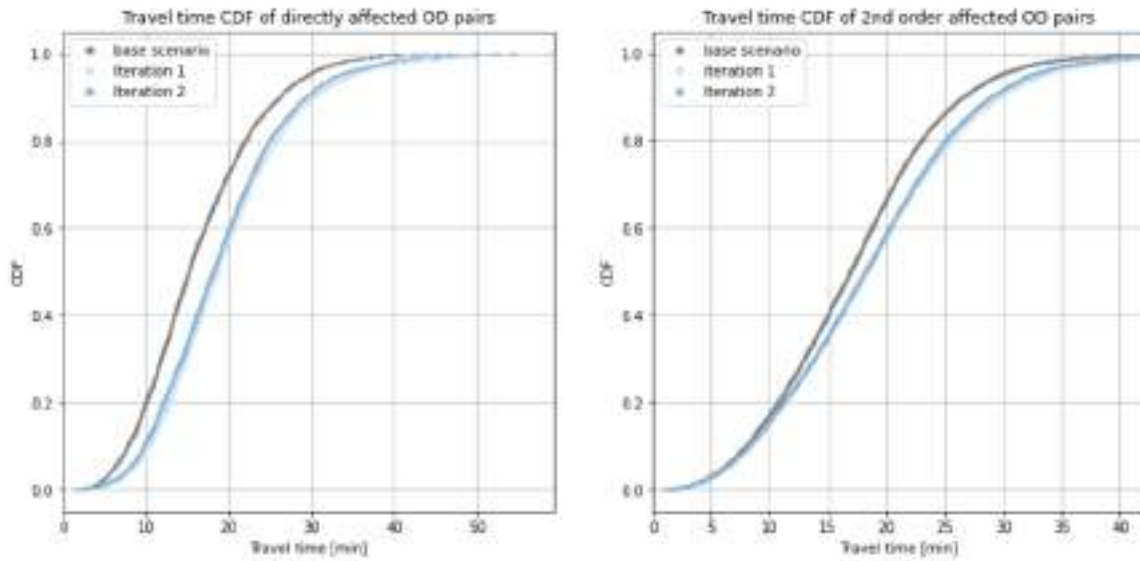


**Figure 3.2:** Example of CDF of travel times for the base scenario and multiple iterations for directly and indirectly affected OD pairs

To assess whether a new equilibrium has been reached, the iterations are compared by using the Kolmogorov-Smirnov test (KS-test). The KS-test calculates the maximum vertical distance between two samples of a CDF. This test is selected because it can identify differences in both location and shape of the CDF [Walpole et al., 2011]. When the KS value between iterations is smaller than the threshold value, the iteration terminates. The threshold value is determined in Section 4.1.

### 3.1.3. Step 3: Recalculation traffic demand

The third step of the iteration involves recalculating the the Origin-Destination (OD) matrix. Reaching this step in the simulation indicates that the travel time of car trips between the last two iterations differ significantly, suggesting that traffic has not yet reached a new equilibrium. This means that the last traffic simulation gives a new traffic situation to the individuals, and a portion of the individuals are going to change their behaviour based on this new traffic situation. This step calculates an updated number of individuals that adapt their travel behaviour, resulting in an altered car usage.

The RODY model only models the traffic around Rotterdam. However, Rotterdam experiences extensive interaction with its surrounding cities. In the RODY model, this is reflected in the high volume of external trips entering and exiting the network. To conduct an effective model split recalculation, it is crucial to account for the original origin or destination of external trips. For instance, an external trip from the countryside to Rotterdam is less likely to shift to public transport than a car trip originating near a train station. Coupling external highway zones to specific links in the cycling or public transport network would introduce ambiguity, as this disregards information about the remainder of the trip. To address this, the original origin and destination of external trips, derived from the OD matrix of the V-MRDH model, are utilised. This process expands the original RODY OD matrix from 371 x 371 zones to a matrix of 6101 x 6101 zones. This is further elaborated in Subsection 4.5.

The recalculation of the matrix is divided into two parts. Firstly, based on updated car travel times, the utility for the alternatives car and no trip is recalculated for each affected OD pair. The utility for public transport and bicycle trips is assumed to stay constant. Subsequently, the new distribution of alternatives - car, public transport, cycling and the no trip - is determined. The OD matrix for car trips is then updated in line with the revised mobility distribution. A comprehensive specification of the model is provided in Chapter 4. An overview of this section is presented in Table 3.2.

Model aspect	Description
Input	<ul style="list-style-type: none"> <li>• Original travel characteristics of car, bicycle and public transport per OD relation (from V-MRDH model)</li> <li>• Travel times car per OD relation from traffic simulation</li> <li>• Utility functions with its parameters (see Chapter 4)</li> </ul>
Modelling	Recalculating utility of car matrix, and applying logit model for new mobility distribution
Output	<ul style="list-style-type: none"> <li>• New mobility distribution</li> <li>• Updated OD matrix car trips</li> </ul>

**Table 3.2:** Model aspects calculating utility per mode per OD relation

## 3.2. Model calibration

This section will describe the methodology of the calibration of the model. The model calibration is implemented in Chapter 6. The utility functions in step three of the iterative process require a specified form and a corresponding set of parameters. These parameters will be identified through the calibration of the model. As outlined, the model incorporates four alternatives: car, public transport, bicycle, and a no trip alternative. The calibration will utilise two types of data. The first data source is model data derived from the V-MRDH model, including travel times of the three modal alternatives, car travel distance for a set of origin-destination (OD) pairs, and their corresponding modal split. The second data source comprises findings from the analysis of changing car travel patterns following the Roseknoop roadworks in the south of Rotterdam. This data includes the reduction in the number of vehicles entering the Roseknoop area during one evening peak, disaggregated by distance category. Given the lack of data on the increase in alternative modes, the calibration will consist of three steps, producing an initial model and a final model.

First, an initial model will be constructed, incorporating the alternatives of car, public transport and bicycle. Using the V-MRDH data on travel characteristics and modal split, the parameters of the utility functions will be calculated through Maximum Likelihood Estimation. This initial model will be applied to the calibration case study, calculating the modal shift from car trips to cycling and public transport trips for all OD pairs in the model.

The second step involves comparing the output of this initial DiTra model with the observed changes in trips derived from the data analysis. The data analysis observes the road capacity reduction at the Roseknoop in the south of Rotterdam (introduced further in Chapter 5). The data analysis consists of two parts. The first part aims to determine the number of car trips entering the Roseknoop influence area before and during the roadworks using traffic light data. The influence area is the area containing the Roseknoop itself and plausible alternative routes to avoid the Roseknoop. To account for seasonality, the change in traffic volume in the Roseknoop area will be compared with the course of traffic volumes at reference locations just outside of the city. The second part involves comparing the shares of trip lengths entering the influence area using data from TomTom Move. These data sources will be combined to identify the trip length distribution of vehicles entering the influence area. By comparing the period before the intervention with several months after the start of the roadwork phase, the absolute reduction in car trips per distance category will be established. This observed reduction in car trips will be compared to the calculated increase in bicycle and public transport trips generated by the initial DiTra model. The gap between the initial model's calculation and the observed reduction in car trips indicates that this segment of trips has left the influence area in the evening rush hour and did not change their mode. This implies that these individuals must have adapted their destination, departure time or trip frequency. Therefore, the gap between the initial model's calculation and the observed reduction in car trips represents the segment of trips opting for the no trip alternative. This results in a distribution of car trips per distance category that choose the no trip alternative.

Based on the information regarding the number of individuals opting for the no trip alternative across distance categories, the parameters of the final DiTra model will be estimated in step three of the calibration. This process involves taking the number of car trips per distance category that choose the no trip alternative, as determined in the previous step, and distributing these values across the OD pairs within each respective distance category. The resulting distribution is then used to calculate the

probability of choosing the no trip alternative for each OD pair. The Maximum Likelihood Estimation will be used to find the model parameters. Several forms of utility functions for the no trip alternative will be developed, and the best-performing form will be selected based on model fit.

### 3.3. Model validation

The model will be qualitatively validated. The reason for qualitative validation is that the validation case study is too small for any observable reduction in car trips due to the stochastic nature of traffic. Consequently, validation will be conducted by comparing the traffic conditions over the network as outcome of the RODY simulations with the observed traffic situation derived from TomTom Move data. Based on visual interpretation, the intensity and locations of traffic congestion will be compared. The model validation is performed in Chapter 7.

## Model specification

```

graph TD
    subgraph 1_Traffic_simulation [1. Traffic simulation]
        A[OD car matrix for evening rush hour before intervention] --> C[Traffic simulation (RCOV)]
        B[Capacity reduction on intervening road] --> C
        C --> D[O/D matrix with travel times]
        E[New iteration with updated O/D matrix car trips] --> C
    end

    subgraph Calibration
        F[Data analysis: Household travel study] --> G[Maximum likelihood estimation]
        H[Model split: V-NBD or model] --> I[Utility parameters]
        G --> I
    end

    subgraph 2_Congestion_indicator [2. Congestion indicator]
        J[Travel times (COV) affected O/D pairs] --> K[Kolmogorov-Smirnov test]
        K --> L{Check difference travel time distribution is below threshold}
        L --> M[Section 4.1 Threshold value]
        M --> N{Statistical traffic}
        N --> O[Stop iteration]
        N --> P[New iteration with updated O/D matrix]
    end

    subgraph 3_Recalculate_OD_matrix [3. Recalculate OD matrix]
        Q[Logit model] --> R[New mobility distribution]
        R --> S[Section 4.3, 4.4, 4.5 & 4.7]
        S --> T[Utility functions]
        T --> U[Section 4.2]
        U --> V[Possible change in travel time PT]
        V --> W[Section 4.6]
        W --> X[Resistance matrices: bicycle and PT from V-NBD or]
        X --> Y[Travel time matrix for bicycle and PT]
        Y --> Z[Updated utility per alternative per O/D pair]
        Z --> R
    end

    D --> J
    I --> T
    P --> A
    O --> AA[Model result congestion heat map (RCOV)]
    AA --> AB[Observed average travel times over network (from traffic flow)]
    AB --> AC[Validation]
  
```

**1. Traffic simulation**

OD car matrix for evening rush hour before intervention

Capacity reduction on intervening road

Traffic simulation (RCOV)

O/D matrix with travel times

New iteration with updated O/D matrix car trips

**Calibration**

Data analysis: Household travel study

Maximum likelihood estimation

Model split: V-NBD or model

Utility parameters

**2. Congestion indicator**

Travel times (COV) affected O/D pairs

Kolmogorov-Smirnov test

Check difference travel time distribution is below threshold

Section 4.1 (Threshold value)

Statistical traffic

Stop iteration

New iteration with updated O/D matrix

**3. Recalculate OD matrix**

Logit model

New mobility distribution

Section 4.3, 4.4, 4.5 & 4.7

Utility functions

Section 4.2

Possible change in travel time PT

Section 4.6

Resistance matrices: bicycle and PT from V-NBD or

Travel time matrix for bicycle and PT

Updated utility per alternative per O/D pair

Model result congestion heat map (RCOV)

Observed average travel times over network (from traffic flow)

Validation

**Legend**

Independent variable

Applied method

Check to see if any condition is reached

Dependent variable

Threshold value to check compliance

After a traffic simulation is performed, the cumulative distribution functions of travel times in the area are compared by the Kolmogorov-Smirnov (KS) test in step two of the process. The KS test outputs the maximum vertical distance between two CDFs. If this vertical separation is small, the traffic conditions have stabilised. Section 4.1 elaborates the threshold KS value. If the traffic conditions do not have stabilised, the traffic demand is recalculated. As discussed earlier, recalculating the OD matrix entails revising the utility values, based on updated travel times from the simulation. This is followed by the estimation of the new mobility distribution. The utility functions are presented in Section 4.2, and the calculation of the mobility distribution is further elaborated in Section 4.3. Section 4.4 describes the method applied to increase the convergence speed of the model. In Section 4.5, the external parts of the trips outside the RODY network are elaborated.

Section 4.6 and 4.7 describe optional features of the model, which are required in certain situations of road capacity reductions. The first feature is reducing the car traffic demand for initial iteration which can be applied when the effect of large road capacity interventions are going to be estimated. The second optional feature is adjusting the travel time matrix for the alternative modes if changes in these network occur simultaneously with the road capacity reduction.

## 4.1. Threshold value for congestion indicator

For the second step of the iteration process, a threshold Kolmogorov-Smirnov value must be established when the iteration should stop. If the KS value between two successive iterations falls below this threshold, it indicates that a new equilibrium has been reached, prompting the termination of the iterative process. This threshold is derived by assessing the variability observed across multiple parallel runs of the same scenario, alongside an evaluation of the convergence speed. As explained in Section 3.1.1, the model is performed with six parallel runs. The KS value between the ‘average’ run and each individual run is calculated, resulting in a standard deviation of  $\sigma = 0.0084$  for the directly affected OD pairs. Consequently, the maximum KS value for terminating the iterative process must exceed the standard deviation of a single simulation.

The threshold must strike a balance between model accuracy and computational efficiency. Given that each iteration requires approximately 4.5 hours to complete, computational efficiency is of considerable importance. Setting the threshold equal to the standard deviation would prolong the simulation unnecessarily. Based on an experiment with the model, in which multiple iterations were performed and the model’s convergence was analysed, the threshold was set at  $KS_{\text{threshold}} = 3\sigma = 0.0252$ . This convergence analysis is further elaborated in Appendix B.

## 4.2. Utility functions

In the third step of the iteration process, the utility for car trips is calculated based on travel times for each OD pair. The utility is derived by multiplying attribute levels - such as travel time - by the corresponding  $\beta$ -coefficients, which reflect the marginal utility of each attribute. The component of the utility that is not explained by these attributes is represented by the Alternative Specific Constant (ASC). The  $\beta$ -coefficients and ASCs are estimated by the model output of the V-MRDH model and through a case study that serves as the basis for model calibration, as elaborated in Chapter 6. These estimated parameters are subsequently used to compute the utility for each OD pair.

To incorporate the external parts of the car trips, i.e. the part of the trip which is performed outside of the RODY simulation area, the original total travel time matrix is derived from the V-MRDH model. The travel times from the traffic simulation are incorporated into this travel time matrix. This is achieved by subtracting the observed travel time in the baseline run (representing the standard Rotterdam network) and subsequently adding the travel time for each OD pair observed in the last iterative traffic simulation. This process ensures that the relative change in travel time is applied. For modal alternatives, travel time is the only attribute that is considered in the utility function. The formula for calculating the utility for car trips per OD pair is presented in Equation 4.1. This is a linear function, as further explained in Chapter 6.

$$V_{\text{car}}^{\text{OD}} = ASC_{\text{car}} + \beta_{\text{TT,car}} \cdot TT_{\text{car}}^{\text{OD}} \quad (4.1)$$

To estimate the new modal split, it is also necessary to calculate the utilities for bicycle and public transport trips for each OD pair. Since RODY exclusively simulates car traffic, the travel characteristics for these alternatives are sourced from the V-MRDH model. It is assumed that the travel characteristics of these alternative modes are minimally influenced by user volumes, as the public transport and bicycle networks are less susceptible to congestion compared to the road network. For example, increased public transport demand may result in crowding but typically has a negligible effect on travel time. For the case of Rotterdam, there is enough spare capacity in the public transport network, with most of the public transport lines having an occupancy rate of under 90% in rush hour [RET, 2024]. This makes the constant travel time for the alternative public transport a realistic assumption. Based on this assumption, the utilities for the alternative modes remain constant across iterations. The utility functions for public



transport and cycling are specified in Equations 4.2 and 4.3 respectively.

$$V_{PT}^{OD} = ASC_{PT} + \beta_{TT,PT} \cdot TT_{PT}^{OD} \quad (4.2)$$

$$V_{bike}^{OD} = ASC_{bike} + \beta_{TT,bike} \cdot TT_{bike}^{OD} \quad (4.3)$$

Furthermore, the no trip alternative is incorporated into the model. The utility of this option is expressed by the distance of the car trips and the increase in travel time resulting from reduced road capacity. The corresponding function is provided in Equation 4.4.

$$V_{notrip}^{OD} = ASC_{notrip} + \beta_{d,no\_trip} \cdot D_{car}^{OD} + \beta_{2,D,no\_trip} \cdot (D_{car}^{OD})^2 + \gamma \cdot \log(1 + \frac{\Delta T}{T_{car}^{OD}}) \quad (4.4)$$

This function incorporates a quadratic relationship with travel distance, as this best fits the data. Additionally, there is a logarithmic relationship with the increase in car travel time. The logarithmic component ensures that zero or near-zero increases in travel time result in a negative utility for the no trip alternative, thereby reducing the probability of selecting this option. As the additional travel time increases, the utility of the no trip alternative rises. The quadratic relationship with distance, along with the specific role of the logarithmic function in accounting for increases in travel time, is discussed in greater detail in Chapter 6.

### 4.3. Calculation new mobility distribution

Once the utility matrices for car trips and the no trip alternative have been updated, and the utility matrices for the alternatives are calculated, the probability of selecting each alternative per OD pair can be calculated using the logit model. The equation for the logit model is shown in Equation 4.5. Applying the logit model generates a new distribution of car, bike, public transport, and the no trip alternative for each OD pair. As the model includes a no trip alternative alongside the modal options, the term “mobility distribution” is used instead of “modal distribution” for the remainder of this report.

$$P_i = \text{Prob}(V_i + \varepsilon_i > V_j + \varepsilon_j, \forall j \neq i) = \frac{e^{V_i}}{\sum_j e^{V_j}} \quad (4.5)$$

There is a methodological difference in calculating the new mobility distribution between the V-MRDH model and the DiTra model. The V-MRDH model calculates the modal split using additional factors such as trip purpose and travel distance. These factors are transformed into generalised costs and distribution functions are applied per travel motive [Schoorlemmer et al., 2021]. In contrast, the DiTra model utilises utility functions and the logit model, as this provides greater flexibility in incorporating the no trip alternative.

Based on the total OD trip matrix, combining bike, car and public transport trips, derived from the V-MRDH model and the original travel characteristics from the V-MRDH model, the mobility distribution based on the utility functions in the DiTra model is computed for the base situation, the normal Rotterdam car network. The difference in calculation method compared to the V-MRDH model results in a slightly different base OD matrix for cars. This difference is small for the suburbs, but a higher difference can be observed for the city centre. The reason for this larger difference in the city centre is because of the car parking limit in the V-MRDH model. This reduces the car traffic towards the city centre based on the available parking places in this area.

If the OD matrix calculated from the utility functions in the DiTra model were directly applied to the initial traffic simulation of the DiTra model, this would lead to travel patterns that differ from those of the original RODY model. This is undesirable, as the original OD matrix in the RODY model is calibrated on the traffic situation in Rotterdam, therefore reflecting the actual traffic situation as best as possible.

Therefore, the number of car trips in the original RODY model is considered the primary reference. Based on the share of car trips derived from the utility functions in the DiTra model, the total OD trip

matrix (car, bike and PT trips combined) for the DiTra model, is recalculated per OD pair based on the number of car trips in the original RODY model and the probability of choosing the car alternative calculated by the utility functions in the DiTra model. This adjust the overall OD matrix, but ensures that only changes in travel time influence a change in number of car trips.

#### 4.4. Optimisation convergence

To calculate the new mobility distribution, information from previous simulations is also utilised to improve convergence speed. Applying Equation 4.5 to the newly calculated utility matrices yields new model split matrices. For the subsequent iteration, the model split matrices from previous iterations are also employed to compute the new model split for the current iteration, thereby expediting the process. The calculation of the new modal split matrices is based on Equation 4.6 [Srinivasan and Bonvin, 2003].

$$\tilde{u}_k = \tilde{u}_{k-1} + \bar{\alpha}_k \cdot \Delta \bar{u}_k \quad (4.6)$$

Here,  $\tilde{u}_k$  represents the modal split value applied in the next iteration, while  $\tilde{u}_{k-1}$  denotes the value used in the previous iteration.  $\Delta \bar{u}_k$  is the difference between the previous iteration  $\tilde{u}_{k-1}$  and the outcome of the next iteration without relaxation,  $\bar{u}_k$ .  $\bar{\alpha}_k$  is the weighting factor that determines the extent to which  $\Delta \bar{u}_k$  is incorporated into the new iteration. It is selected such that  $\bar{\alpha}_k = \frac{1}{k-1}$ , ensuring that each  $\bar{u}_k$  for  $k = 1 \dots K$  contributes equally to the new iteration.

#### 4.5. External trips in the RODY model

As discussed, the RODY model simulates traffic solely within the city of Rotterdam. In the DiTra model, it is essential that the original origin and destination are maintained, as otherwise, the mode shift calculations would become highly ambiguous. For recalculating the Origin-Destination matrix, the 371 x 371 matrix used in the RODY model is expanded to a 6101 x 6101 matrix for the DiTra model, which will be utilised to recalculate the OD matrix. The RODY model includes 256 internal zones, which are areas within Rotterdam that both generate and attract trips, as they contain residential, business, industrial or recreational functions. Additionally, the model incorporates 115 external zones, which represent highways, national roads and city roads where traffic demand enters or leaves the RODY network. The 6101 x 6101 matrix in the DiTra model is divided into four quadrants (see Table 4.1), each representing a different type of trip, depending on whether the origin or destination is located within the RODY network or outside it. Each quadrant is explained below.

	1	...	254	255	371		V0001	...	V7786
1	$a_{1,1}$	...	$a_{1,254}$	$a_{1,255}$	$a_{1,371}$		$b_{1,V0001}$	...	$b_{1,V7786}$
$\vdots$	$\vdots$	$\ddots$	$\vdots$	$\vdots$	$\vdots$		$\vdots$	$\ddots$	$\vdots$
254	$a_{254,1}$	...	$a_{254,254}$	$a_{254,255}$	$a_{254,371}$		$b_{254,V0001}$	...	$b_{254,V7786}$
255	$a_{255,1}$	...	$a_{255,254}$	$a_{255,255}$	$a_{255,371}$		$b_{255,V0001}$	...	$b_{255,V7786}$
371	$a_{371,1}$	...	$a_{371,254}$	$a_{371,255}$	$a_{371,371}$		$b_{371,V0001}$	...	$b_{371,V7786}$
V0001	$c_{V0001,1}$	...	$c_{V0001,254}$	$c_{V0001,255}$	$c_{V0001,371}$		$d_{V0001,V0001}$	...	$d_{V0001,V7786}$
$\vdots$	$\vdots$	$\ddots$	$\vdots$	$\vdots$	$\vdots$		$\vdots$	$\ddots$	$\vdots$
V7786	$c_{V7786,1}$	...	$c_{V7786,254}$	$c_{V7786,255}$	$c_{V7786,371}$		$d_{V7786,V0001}$	...	$d_{V7786,V7786}$

**Table 4.1:** OD matrix format applied in the DiTra model with internal RODY zones and V-MRDH zones (V) outside of Rotterdam. The values a, b, c and d correspond to od values for respectively internal-internal, internal-external, external-internal, external-external

The first quadrant contains trips between internal zones in Rotterdam. The origins and destinations are internal RODY zones. The OD values in this quadrant are a direct copy of the original RODY OD matrix applied in the RODY model. For the travel time matrix, for each zone, the V-MRDH centre zone is selected, which is used as the origin or destination to determine the travel time matrix based on the VMRDH model.

The second and third quadrant contain trip that start in Rotterdam and leave Rotterdam (2nd quadrant) or start outside of Rotterdam and ends in Rotterdam (3rd quadrant). The zones in the VMRDH model contains the full size of the Netherlands, where the zones are bigger, i.e. less detailed, moving further from the Metropolitan area of Rotterdam and The Hague. All of the V-MRDH zones outside of Rotterdam are assigned to a single external zone in the RODY model, in order to make a coupling between the OD matrix applied in the DiTra model and the RODY model which simulates the traffic. An illustrative map, zoomed in on Rotterdam, is shown in Figure 4.2.



**Figure 4.2:** Zone layout for the external RODY zones (zoomed in on Rotterdam). White zones are the RODY zones in Rotterdam. All other colours represent a coupling to a VMRDH zone to an external link

Assigning each zone outside of Rotterdam to an external RODY zone implies that if there is a trip from a specific zone outside of Rotterdam to Rotterdam, the car trip will use that link, which may be a highway, national road or city road, to enter the network. This is an assumption, as the destination in Rotterdam or traffic conditions may influence the external zone used to enter the network in practice. This can also be observed when the  $6101 \times 6101$  matrix is aggregated to the  $371 \times 371$  matrix, which yields slightly different results. This discrepancy arises because the original RODY  $371 \times 371$  matrix is generated based on a cutout of the V-MRDH model. It is crucial to retain the original  $371 \times 371$  matrix; otherwise, travel patterns may deviate from the normal situation, which would make the outcomes of the models incomparable. Therefore, the  $6101 \times 6101$  DiTra matrix is adjusted to ensure that the sum of cars entering the network via an external RODY link remains consistent. This is accomplished by applying a factor to the cells in the  $6101 \times 6101$  matrix. This factor is calculated by dividing the sum of the car trips entering a particular external zone, determined based on the  $6101 \times 6101$  matrix, by the value of car trips entering that particular zone in the original  $371 \times 371$  RODY matrix. Conversely, the same process applies to trips starting in Rotterdam and exiting the network through an external zone.

The fourth quadrant of the  $6101 \times 6101$  matrix consists of trips that go from one external RODY zone to another external RODY zone, which essentially represents through traffic in the network (with no origin or destination in Rotterdam). Under the assumption that only the capacity of roads within the city is reduced, through traffic is considered to remain unaffected, as traffic on highways and national roads surrounding Rotterdam will not be impacted by the additional travel time caused by the capacity reduction within the city.

In each iteration of the DiTra model, the  $6101 \times 6101$  matrix is recalculated based on the travel times from the simulation. Subsequently, the matrix is aggregated to the  $371 \times 371$  matrix, where the zones outside of Rotterdam are assigned to their respective external zone in the RODY model. With this new  $371 \times 371$  matrix, another cycle of the iterative process is initiated by the traffic simulation.

## 4.6. Optional: reducing initial car traffic demand

It is possible to initiate the first simulation not with the original OD matrix, but with a reduced matrix. This approach can be adopted when a significant road capacity reduction is introduced, in order to prevent gridlocks during the simulation. Gridlocks increase the simulation run time significantly and are therefore undesirable. Based on a specified percentage decrease, the trips that are directly affected are

adjusted. For example, the user can choose to reduce the initial OD matrix by 10%, thereby reducing the traffic demand on the directly affected OD pairs by 10%. The model user has the option to apply this reduction factor. However, the downside of implementing this reduction is that the outcome of the road capacity, when this is not communicated to people, is not known.

#### **4.7. Optional: adjusting the travel time matrix for the alternatives**

Another option that can be implemented in the model is the adjustment of travel times for specific trips within the cycling or public transportation network. Travel times may be increased when, for example, roadworks are combined with a simultaneous reduction in public transport service due to road capacity reductions. Conversely, if public transport service is increased to accommodate reduced car accessibility, travel times can be reduced for certain OD pairs. Similarly, in cases where cycling lanes are closed, travel times can be increased for specific OD pair relationships. These OD pairs can be selected by performing a selected link analysis on the car network within the RODY model.

# 5

## Case study

This chapter presents the results of the case study conducted as part of this research. The case study of this research are the roadworks of an intersection in the south of Rotterdam. In different phases, roadworks have obstructed car traffic for longer periods of time. The primary purpose of this case study is to provide both calibration and validation for the model and to gain insights into changes in travel behaviour during the roadworks.

This chapter is structured as follows. Section 5.1 introduces the case study. Sections 5.2 and 5.3 examine the impact of the roadworks on car traffic, with a focus on absolute reductions in trips and changes in the distribution of trip lengths, respectively. Subsequently, Section 5.4 addresses the data on traffic volumes for alternative modes, although the available data was insufficient to observe any meaningful effects.

### 5.1. Introduction case study

The location of the Roseknoop intersection is depicted in Figure 5.1. This intersection is situated in the southern part of Rotterdam, in an area known as the Roseknoop. It marks the junction of the Varkenoordseviaduct, Laan op Zuid, and the (2e) Rosestraat. Two photographs of the intersection are provided in Figures 5.2 and 5.3.

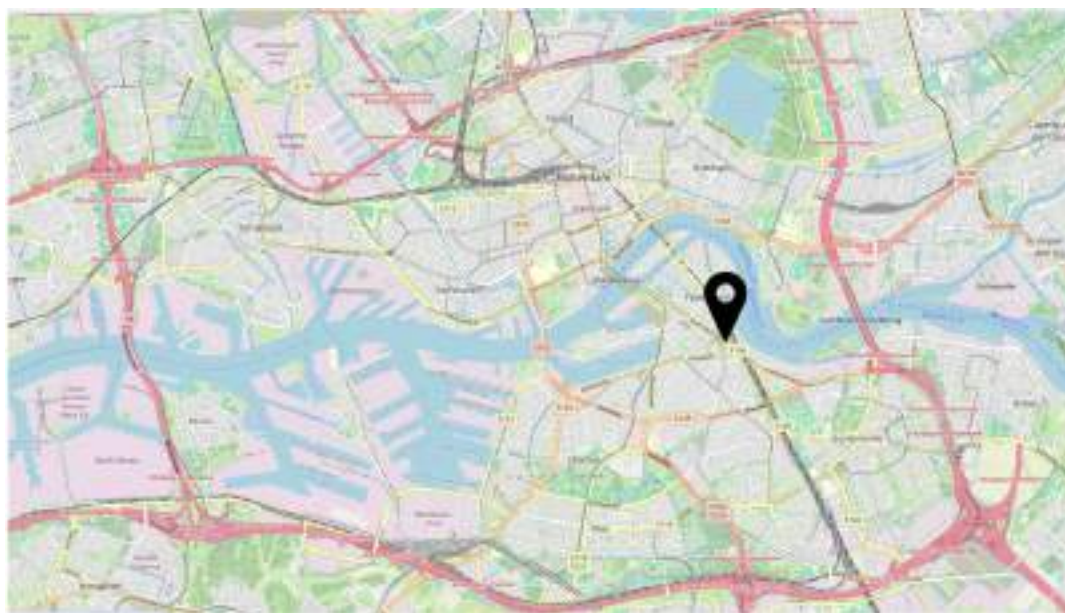


**Figure 5.1:** Location of Roseknoop [Openstreetmap, 2024]





**Figure 5.2:** Photograph of the Roseknoop intersection (1)  
(image by the author)



**Figure 5.3:** Photograph of the Roseknoop intersection (2)  
(image by the author)

Between January 2023 and July 2024, roadworks restricted car traffic at this intersection [Gemeente Rotterdam, 2024a]. The intersection was closed to car traffic in different phases. The municipality of Rotterdam expects that car traffic reduction occurred during the roadworks, as congestion impact was lower than expected. Despite being a temporary capacity reduction, the extended duration of the roadworks provides a sufficient time window to study the changes in travel behaviour. This case study was chosen because it represents one of the few capacity reductions in Rotterdam post-COVID-19. Many other road narrowing projects in the city occurred during the pandemic, making it challenging to assess the relationship between the reduction in car trips and the road capacity reductions.

From January 2023 to April 2023, phase 1 of the roadworks was implemented. During this phase, the side streets of the Roseknoop junction - the Rosestraat, Putselaan, Beijerlandse laan and Colosseumweg - were disconnected from the corridor formed by Laan op Zuid and the Varkenoordse viaduct (see Figure 5.4). Bus lines 66 and 77, as well as tram line 25 were diverted, while tram line 20 (Rotterdam Central station - Lombardijen) was suspended. Line 23 continued to operate along the corridor Laan op Zuid / Varkenoordse viaduct and line 125 was added as temporary service between Rotterdam Central Station and Stadion Feyenoord to make sure capacity along the Laan op Zuid / Varkenoordse viaduct was sufficient. For pedestrians and cyclists, the Roseknoop was accessible for the majority of the time. During certain periods, minor diversions were required. It is assumed that these diversions did not have a significant impact on travel time.



**Figure 5.4:** Roseknoop roadworks phase 1 where the side streets, indicated with the red arrows, of the Laan op Zuid - Varkenoordse viaduct corridor were closed for car traffic (background: Openstreetmap [2024]).

Between May 2023 and mid October 2023, phase 2 of the roadworks were carried out. During this phase, the capacity reduction was more significant than in phase 1, as, in addition to the disconnected side streets, traffic along the Laan op Zuid / Varkenoordseviaduct corridor was also blocked. This is illustrated in Figure 5.5. In this phase, tram services along the Laan op Zuid / Varkenoordseviaduct corridor were suspended. As a result, the tram network connecting the northern and southern parts of Rotterdam was disrupted, requiring an additional transfer to the metro for public transport trips between Rotterdam South and Rotterdam North.



**Figure 5.5:** Roseknoop roadworks phase 2 where the full junction was closed off for car traffic (background: Openstreetmap [2024]).

In mid October 2023, phase 1a started. This phases was comparable to the situation of phase 1, with the slight change that the side street Hilledijk was reconnected to the Putselaan. In January 2024, the 2e Rosestraat side street was connected to the Laan op Zuid / Varkenoordseviaduct corridor. This phase is called 1b.

## 5.2. Car trips: reduction in traffic volume

This section examines the impact of the roadworks on car traffic in the vicinity of the Roseknoop intersection. The data employed for this analysis consists of traffic signal data [Gemeente Rotterdam, 2024c]. Inductive loop detectors positioned in front of traffic signals register and record the number of vehicles passing through each lane of the signalised junction.

To assess the reduction vehicle numbers within the broader area surrounding the Roseknoop roadworks, the number of vehicles entering a cordon during the evening peak period is counted. A cordon is a bounded area that monitors traffic flows both into and out of the specified region. The cordon in this study contains the Roseknoop intersection as well as plausible alternative routes that serves as substitutes for it. Consequently, the measurement captures the number of vehicles that have altered their mode of transport, departure time, destination or trip frequency, without accounting for those that have simply chosen an alternative route to reach their destination. The study area, along with the designated measurement locations, is depicted in Figure 5.6.





**Figure 5.6:** Study area with measuring locations indicated (background: Openstreetmap [2024]).

By using the traffic signals at the boundary of the study area, an almost entirely enclosed cordon can be established, except for certain local roads that connect directly to the main road network without signalised intersections. As these roads primarily serve small neighbourhoods at the local level, it is assumed that they do not function as major diversion routes following the capacity reduction. Consequently, it is presumed that traffic volumes on these local roads remain constant and do not significantly affect the overall deviation of vehicles entering the cordon.

Since traffic signals serve as the primary data source, and detection loops are only positioned to register vehicles approaching the intersections rather than those departing, only inbound traffic to the cordon can be accurately measured. The main limitation of this method is that trips originating within the cordon and have a destination inside or outside this area, are not captured in the dataset. This can result in an underestimation of the overall reduction in trip numbers due to the roadworks.

The number of vehicles entering the cordon in the evening rush hour is analysed before, during the different phases and after the roadworks. The result is shown in Figure 5.7.



**Figure 5.7:** Number of vehicles entering Roseknoop cordon for evening peak period between 3 and 5PM (5 day rolling average).

The figure illustrates that, particularly during the second phase of the roadworks, a decline in the number of vehicles entering the cordon can be observed, a trend further reinforced by the summer holiday. Following phase two, the number of car trips increases; however, it does not return to the traffic levels recorded before May 2023.

The annual traffic fluctuation and annual growth influence makes it difficult to interpret these values. Therefore, reference measure points are selected to filter out these factors. These locations are the result of a trade-off between measuring the annual traffic fluctuation and growth in Rotterdam, but are relatively far away from the Roseknoop, so that the capacity reduction of the Roseknoop has minimal influence on the traffic levels measured at the reference locations. The data of the reference locations is further elaborated in Appendix C.

The traffic levels at the reference locations and those entering the Roseknoop cordon are compared by using the average traffic level in November 2022 as the reference point (represented as the 0% line in the figure). The results are presented in Figure 5.8.

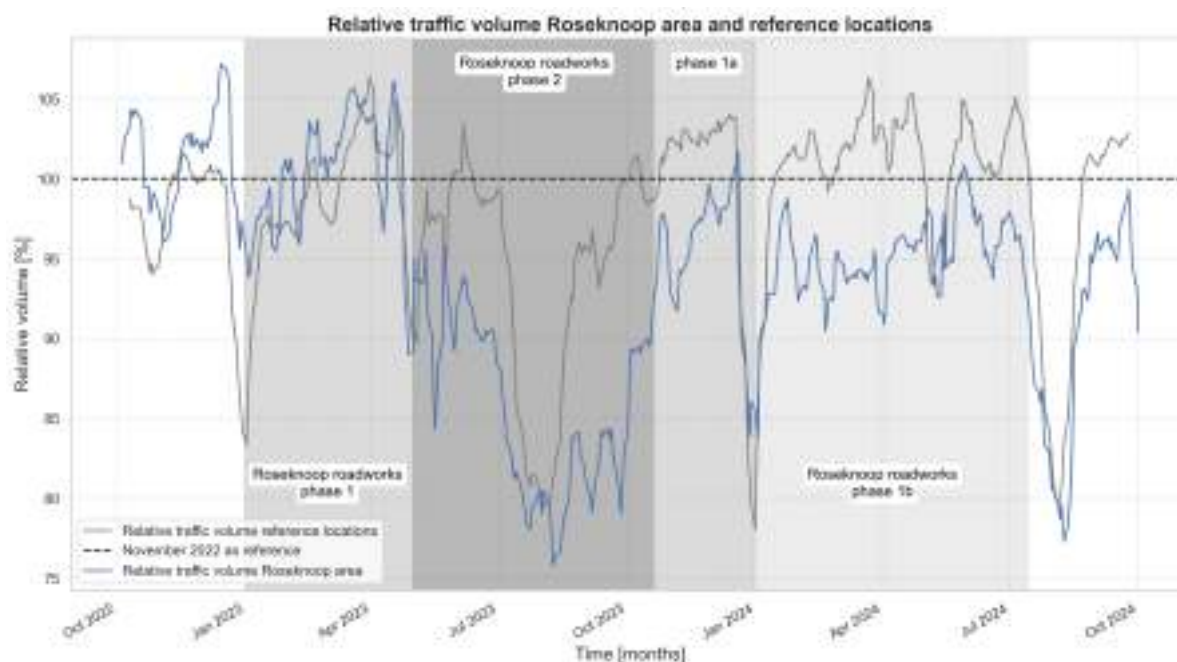


**Figure 5.8:** Traffic volume entering Roseknoop cordon [Gemeente Rotterdam, 2024c] and reference locations [NDW, 2024] in evening peak period (average traffic levels in November 2022 are used as reference).

This figure illustrates that, during phase 1 of the roadworks, the progression of traffic volume in the Roseknoop area closely follows that of the reference locations. However, in phase 2, a substantial difference becomes evident. The reference traffic intensity exceeds the traffic entering the cordon, except during the summer holiday period. After phase 2, a smaller yet significant reduction in car trips is observed, with the exception of the Christmas break. The graph indicates that during phase 2, a considerable proportion of travellers adapted their behaviour, and even after phase 2, traffic in the Roseknoop area remained lower than before. This suggests that a proportion of individuals did not revert to car use.

Notably, the decline in car traffic during the summer and winter breaks is less pronounced in the Roseknoop area compared to the reference locations. This can be explained by the fact that a share of individuals had already shifted away from car travel. During the summer and winter breaks, the reduction in congestion may have encouraged others who had previously shifted away from car use to start travelling by car again.

The difference between the two lines is depicted in Figure 5.9, which reinforces the above mentioned observations. During phase 1, no significant deviation is observed. Due to the stochastic nature of traffic, the reduction in car trips during this phase is likely too small to be detectable in the vehicle numbers that enter the cordon. The largest deviation occurs towards the end of phase 2, several months after the start and following the summer break. During this period, a 15% reduction in car trips is observed in the Roseknoop area compared to the reference locations, indicating that 15% fewer vehicles entered the area during the evening peak. This suggests that, as a result of the phase 2 roadworks, at least 4,400 car trips changed their departure time, travel mode, destination, or trip frequency.

After phase 2, with the introduction of phases 1a and 1b, the difference relative to the reference traffic levels stabilises at approximately 6%, corresponding to a reduction of between 1,800 and 2,100 vehicles. No significant difference in traffic levels is observed between phase 1a and 1b. Even after the roadworks the traffic entering the Roseknoop cordon remained under the reference traffic. However, this period is too small to make conclusions about the long term effects.

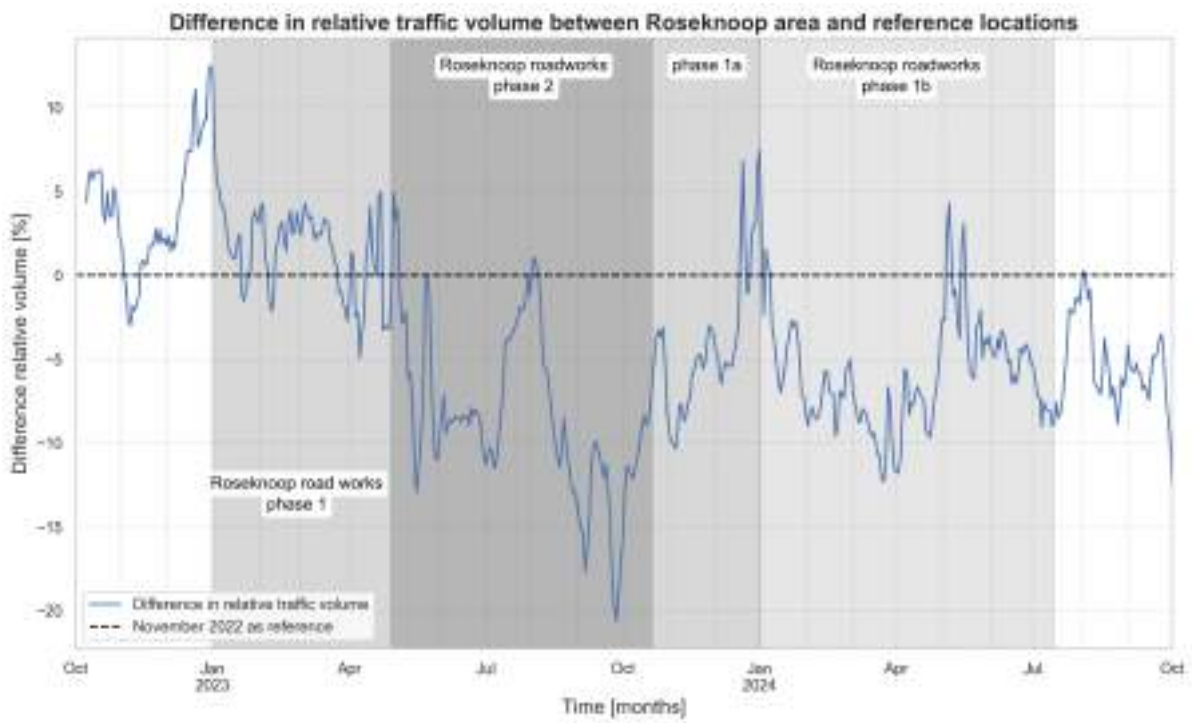
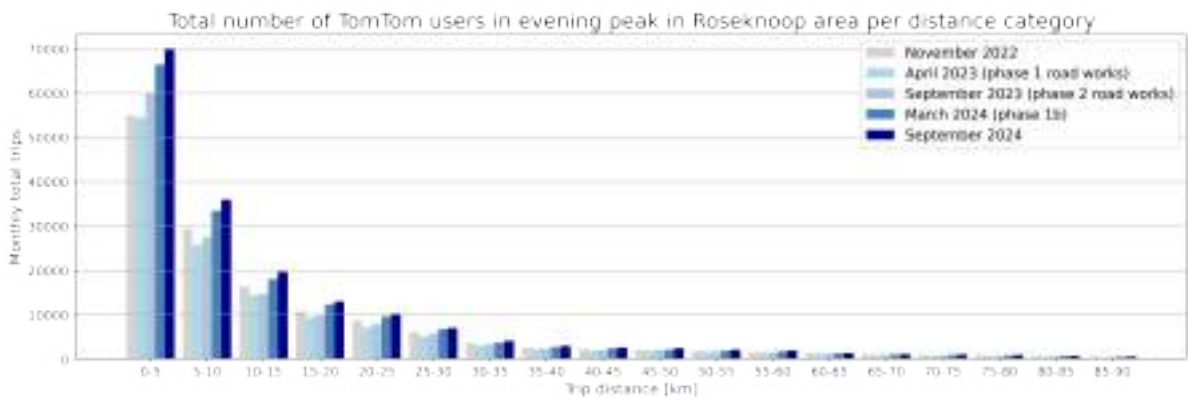


**Figure 5.9:** Difference in traffic level percentages between Roseknoop cordon and reference traffic measuring locations in evening peak period (data source: Gemeente Rotterdam [2024c] and NDW [2024]).

### 5.3. Car trips: change in trip length distribution

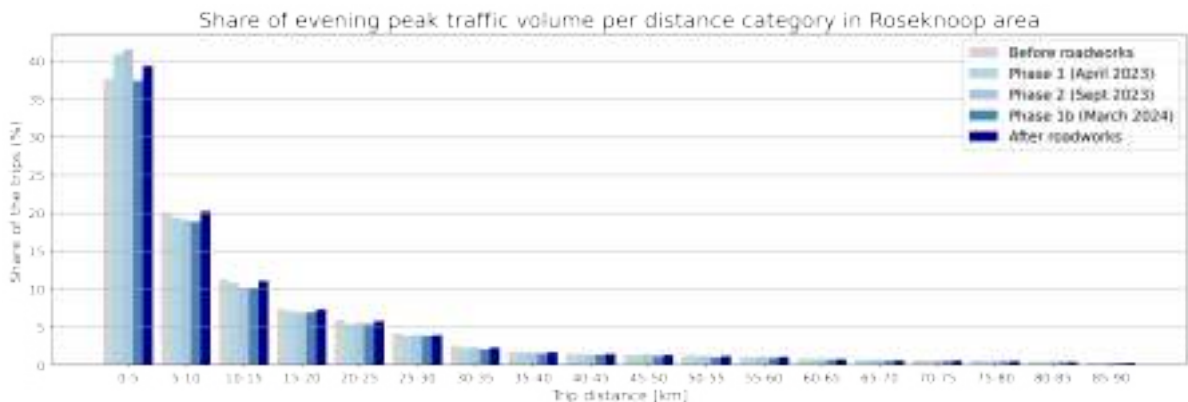
The second step involves identifying the types of trips that have been reduced by analysing the distribution of trip lengths before, during the various phases, and after the road capacity intervention. This analysis utilises data from TomTom Move. While TomTom Move does not capture all trips—since it only accounts for vehicles equipped with a built-in TomTom device—it provides an opportunity to assess trip patterns through the study area across the different phases of the intervention. It is assumed that the TomTom Move data offers a reliable reflection of overall trip behaviour in the region. This analysis yields valuable insights into the types of car trips that are no longer being undertaken.

Figure 5.10 illustrates the absolute number of trips through the study area (refer to Figure 5.6), segmented by categories of travel distance. Data has been collected for four distinct periods: November 2022 represents the situation prior to the road capacity intervention, while January 2023 marks the beginning of the first phase of the roadworks. By April 2023, the traffic patterns are considered to have stabilised at a new equilibrium for the first phase. Phase 2 began in May 2023, with September 2023 reflecting the new equilibrium for this second phase. Finally, September 2024 signifies the period following the completion of all roadworks.



**Figure 5.10:** Distribution of trip length before, during (two phases) and after road works Roseknop (data source: TomTom [2024])

A notable finding is the consistent exponential decline with distance in the number of trips across all time periods, with the majority of trips being under 10 kilometres. To account for variations in the number of days per month and potential increases in TomTom users, the distribution of trips across distance categories is expressed as a percentage of the total trips per month. This provides a more accurate reflection of changes in travel patterns, as illustrated in Figure 5.11.



**Figure 5.11:** Share of car trips by distance before, during (two phases) and after roadworks at Roseknop (data source: TomTom [2024])

The shares of traffic volume per distance is then multiplied by the monthly average evening peak traffic volume entering the Roseknop cordon (which was found in the traffic intensity analysis in Section 5.2). The result is the average evening peak traffic volume by distance category, shown in Figure 5.12.

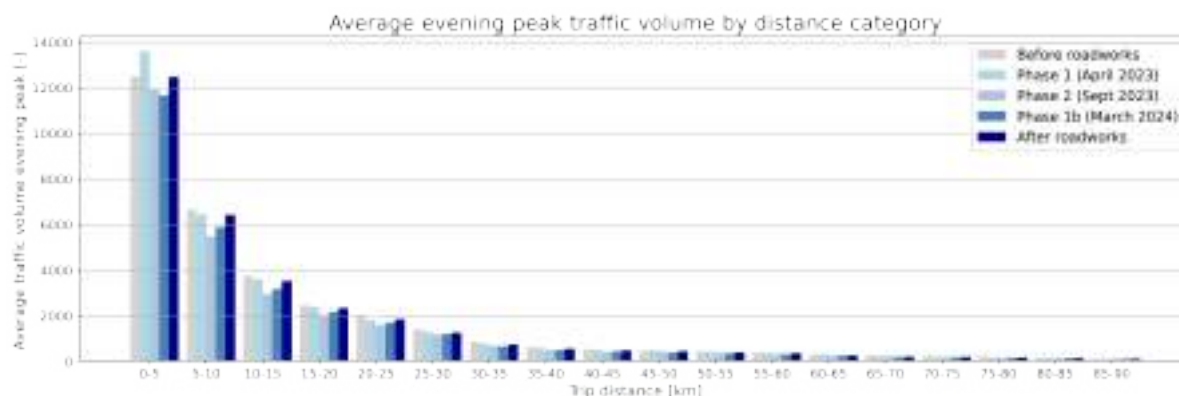


**Figure 5.12:** Average evening peak traffic volume in Roseknoop area by distance category. Average traffic volume per distance category during the evening peak, derived by combining shares [TomTom, 2024] with the measured total number of trips [NDW, 2024]. The data represents periods before, during (two phases) and after roadworks at Roseknoop

To facilitate comparison between the different phases, Figure 5.13 illustrates the change in trip lengths during each roadwork phase relative to November 2022 (pre-roadworks).

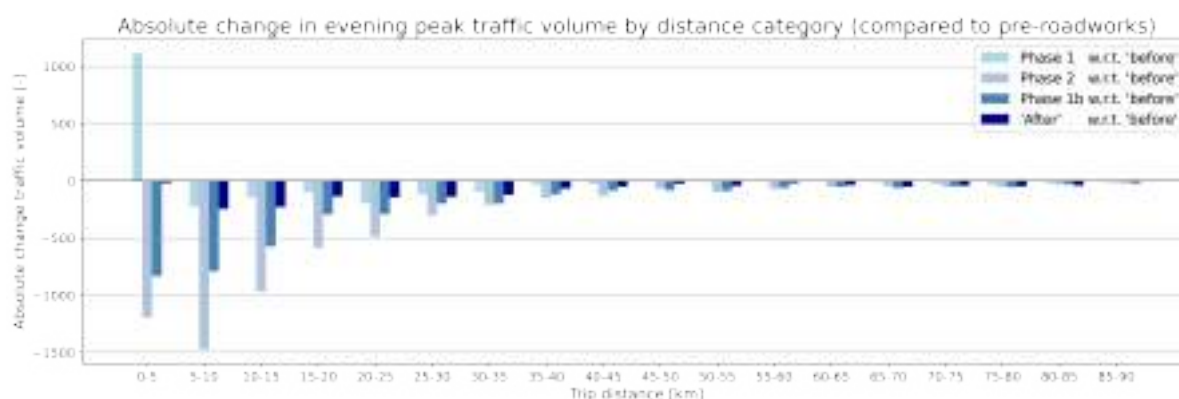


**Figure 5.13:** Absolute changes in traffic volume per distance category during the evening peak, compared to the month before roadworks at Roseknoop. Data derived from TomTom Move shares [TomTom, 2024] and measured total trips [NDW, 2024], covering periods before, during (two phases), and after the roadworks.

In this figure, several notable observations can be made. Across most of the roadwork phases, as well as the post-intervention phase, a reduction in trips is evident across all distance categories, with the exception of phase 1. During phase 1, there is an increase in trips of less than 5 kilometres, while trips exceeding 5 kilometres experience a reduction. A plausible explanation for the increase in car trips of less than 5 kilometres could be the diversion and disconnection of local bus services in the area, which likely made public transport a less attractive alternative.

Phase 2, which represents the most substantial reduction in road capacity, sees the greatest overall reduction in car trips, particularly for trips in the 5 to 10 kilometres range. For trips longer than 10 kilometres, the reduction is more modest across all distance categories. As noted in Section 5.2, during phase 1b (April 2024), traffic levels did not return to those observed before phase 2. In comparison to phase 2, phase 1b shows the most significant increase in trips within the 5 to 10 kilometres range.



In Figure 5.14, the relative change in traffic volume across distance categories is presented. The figure reveals that shorter trips (under 5 kilometres) experience the smallest relative reduction, whereas trips exceeding 10 kilometres show a more pronounced decline, particularly during the second phase of the roadworks. This contrasts with Figure 5.13, where the 0-5 kilometre range represents the largest category in absolute terms. This phenomenon can be attributed to the exponential negative relationship between trip frequency and distance, with the 0-5 kilometre range containing the highest number of trips. Although Figure 5.14 appears to indicate a significant dip in the longer distance categories, the absolute figures for these categories remain low.

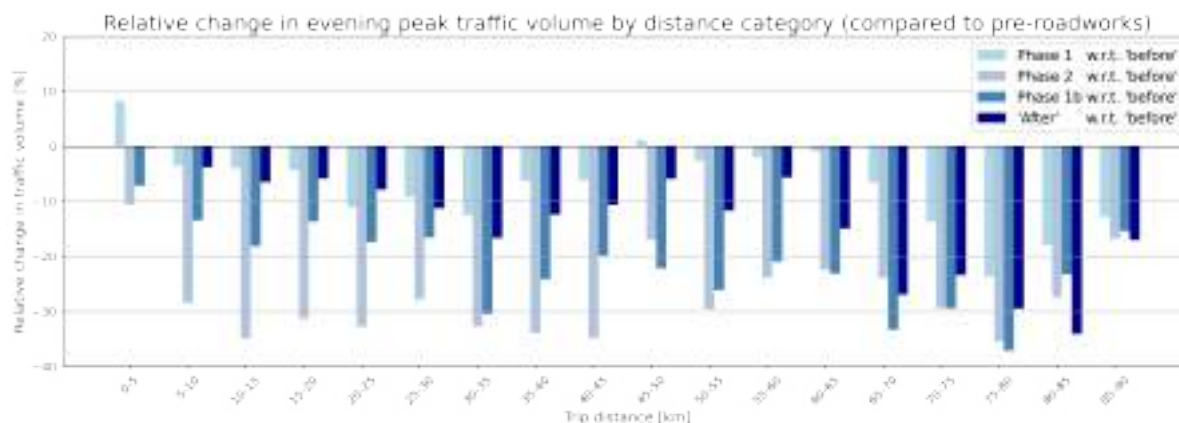


**Figure 5.14:** Relative changes in traffic volume per distance category during the evening peak, compared to the month before roadworks at Roseknoop. Data derived from TomTom Move shares [TomTom, 2024] and measured total trips [NDW, 2024], covering periods before, during the two phases and after the roadworks.

Thus, the results indicate that the 0–5 km range experiences the smallest relative reduction in car trips, whereas trips exceeding 5 km exhibit a more substantial and uniform decline of between 20–35% during the most intense phase of the roadworks. This suggests that shorter trips are more resilient to disruptions in road capacity, likely because trips under 5 km already have a strong potential for modal shift to cycling, meaning those who still choose to drive likely have fewer viable alternatives. In contrast, longer trips are more elastic and more readily avoided or substituted by alternative modes of transport. In contrast, longer trips demonstrate greater elasticity and are more readily foregone or substituted by alternative modes of transport.

## 5.4. Cycling and public transport trips

In addition to examining the decline in car usage, an analysis of the other transport modes was conducted to assess whether any shifts towards cycling or public transport could be detected. The number of counting locations for cyclists is significantly fewer than for cars, which limited the ability to identify meaningful trends. With regard to public transport, data related to tram lines in the area were obtained from the Rotterdam public transport operator, RET. The number of passengers on the affected lines was analysed; however, due to alterations in public transport services, such as rerouted and suspended tram and bus lines, no observable trends could be identified in this instance either.

For the remainder of this research, this implies that calibration or validation based on the increase in public transport and cycling trips is not feasible. Consequently, the calibration and validation will be grounded in the data analysis of car usage.

# 6

## Model calibration

This chapter outlines the calibration of the model, in which the parameters for the utility functions are estimated. The calibration is conducted for phase 2 of the Roseknoop roadworks. The model calibration is performed in three stages. Firstly, a model that considers the three modes—car, bicycle, and public transport—is developed. This model calculates the number of car trips that transition to alternative modes as a consequence of phase 2 of the Roseknoop roadworks. This is elaborated further in Section 6.1. In the second stage, the outcomes of the model from step 1 are compared with the observed traffic analysis. This is presented in Section 6.2. Based on the discrepancies between the data analysis and the model's output, the no trip alternative is calibrated in step 3. The no trip alternative in the model encompasses all car trips that no longer enter the Roseknoop area during the evening rush hour following the reduction in road capacity, and that did not shift to other modes. This alternative includes individuals who have stopped to make the trip, adjusted their departure times to avoid the evening rush hour, or chose an alternative destination outside the Roseknoop area as a result of the road capacity reduction. The method for determining the parameters for the no trip alternative is outlined in Section 6.3. An overview of the calibration process is provided in Figure 6.1. The figure illustrates the progression of the modal split and aims to facilitate understanding of the calibration methodology.



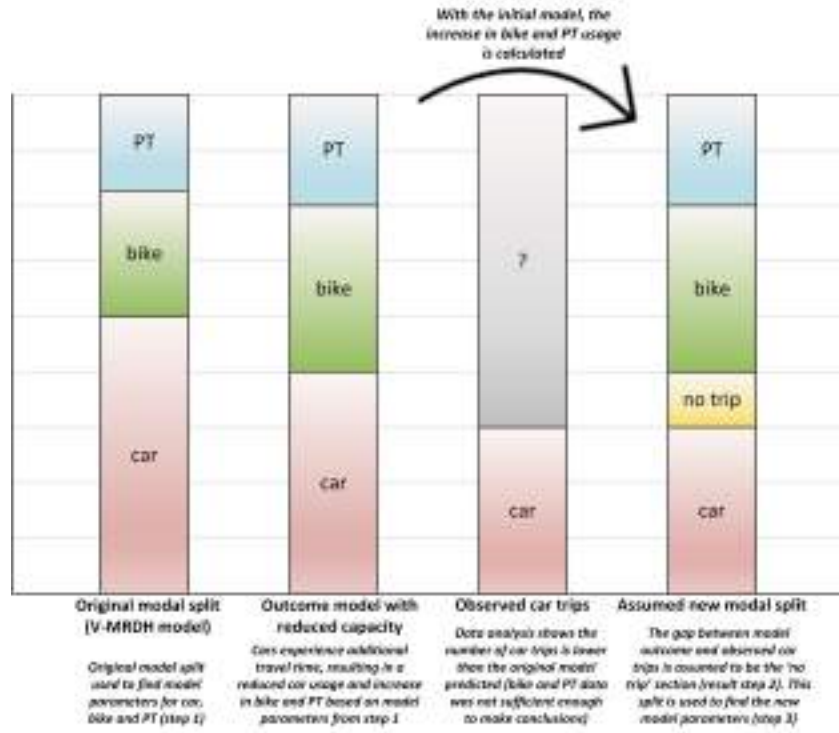


Figure 6.1: Illustration of modal split to clarify the methodology of calibrating this model

## 6.1. Step 1: Model with alternatives car, bike and public transport

In Chapter 4, the utility functions are introduced. The utility functions for the modalities are presented in the Equations 4.1, 4.2 and 4.3. This section outlines the estimation of the Alternative Specific Constants ( $ASC_{car}$ ,  $ASC_{PT}$ ,  $ASC_{bike}$ ) and the coefficients for the travel time ( $\beta_{TT,car}$ ,  $\beta_{TT,PT}$ ,  $\beta_{TT,bike}$ ) for the initial model.

$$V_{car}^{OD} = ASC_{car} + \beta_{TT,car} \cdot TT_{car}^{OD} \quad (4.1)$$

$$V_{PT}^{OD} = ASC_{PT} + \beta_{TT,PT} \cdot TT_{PT}^{OD} \quad (4.2)$$

$$V_{bike}^{OD} = ASC_{bike} + \beta_{TT,bike} \cdot TT_{bike}^{OD} \quad (4.3)$$

These parameters are determined based on the model outputs of the V-MRDH traffic model. The available data includes the travel time matrix for the three alternatives and the modal split per OD pair. The reason for not directly using the distribution functions from the V-MRDH model is because the functions are far more detailed. The functions are based on generalised costs and are split out per motive and car availability. The functions also combine the modal split with the distribution of trips [Schoorlemmer et al., 2021]. Incorporating all these factors would lead to a very comprehensive model, without the flexibility of adding a no trip alternative. Given that only travel times changes, the model output is used as data to estimate the parameters for defined utility functions for the alternatives.

The calibration is based on a set of OD pairs. The selected OD pairs are based on two criteria. The first criterion is that the OD pairs must have at least an origin or a destination in the city of Rotterdam (the RODY study area). Therefore, the chosen OD pairs are in the first, second and third quadrant of the overall OD trip matrix, as explained by Table 4.1. This ensures that the parameters are appropriate for the context of large cities, like Rotterdam. The second criterion is that the OD pair must have influence on generating trips. The minimum trip value for OD pairs is set to 0.2 to be selected. This means that at least in 1 out of 5 runs, there is a car trip generated for that OD pair. This ensures that most of the trips performed in the model are included, while excluding OD pairs with minimal impact on the OD

matrix. An illustrative data table of the selected OD pairs is provided in Table 6.1. It should be noted that this data is based on a model outputs, which inherently involve certain assumptions.

$OD_{\text{pair}}$	$TT_{\text{car}}$	$TT_{\text{PT}}$	$TT_{\text{bike}}$	$p_{\text{car}}$	$p_{\text{PT}}$	$p_{\text{bike}}$
1,3	7.439	73.021	13.525	0.261298	0.000000	0.738702
1,4	6.745	70.128	18.024	0.622820	0.000000	0.377180
1,5	6.898	70.162	19.443	0.565965	0.000000	0.434035
1,6	11.701	70.123	30.797	0.639180	0.000000	0.360820
1,9	7.711	77.628	21.190	0.837694	0.000000	0.162306
...	...	...	...	...	...	...
V7786,179	130.838	176.528	813.078	0.804296	0.195704	0.000000
V7786,180	128.913	177.085	812.763	0.484246	0.515754	0.000000
V7786,183	129.240	178.391	811.055	0.141459	0.858541	0.000000
V7786,184	131.360	177.528	810.003	0.633929	0.366071	0.000000
V7786,185	129.751	184.614	805.021	0.538717	0.461283	0.000000

**Table 6.1:** OD pair data used for the modal split calibration ('V' indicates VMRDH-zone)

Based on the OD pair data, the parameters are estimated using the Maximum Likelihood Estimation. This method finds the parameter values that maximize the likelihood function, as shown in Equation 6.1.

$$L(\theta|X) = \prod_{i=1}^n P(x_i|\theta) \quad (6.1)$$

To simplify computations and improve numerical stability, particularly when dealing with very small probabilities (which can result in very large or very small values in the product), the log-likelihood is used (see Equation 6.2).

$$\log L(\theta|X) = \sum_{i=1}^n \log P(x_i|\theta) \quad (6.2)$$

Several forms of utility functions are considered and compared. The types of utility functions are compared by calculating the modal fit for discrete choice models, see Equation 6.3.

$$\bar{\rho}^2 = 1 - \frac{L(\beta) - K}{L(0)} \quad (6.3)$$

The first set of utility functions are the linear functions, as in the form of Equation 6.4. The second set are non linear functions (see Equation 6.5).

$$V_{\text{mode}}^{\text{OD}} = ASC_{\text{mode}} + \beta_{t,\text{mode}} \cdot t_{\text{mode}}^{\text{OD}} \quad (6.4)$$

$$V_{\text{mode}}^{\text{OD}} = ASC_{\text{mode}} + \beta_{TT,\text{mode}} \cdot TT_{\text{mode}}^{\text{OD}} + \beta_{2,TT,\text{mode}} \cdot (TT_{\text{mode}}^{\text{OD}})^2 \quad (6.5)$$

The set of linear functions results in a model fit of  $\bar{\rho}^2 = 0.3307$ , while for the non-linear functions  $\bar{\rho}^2 = 0.3320$ . This represents a minor improvement in model performance. Both sets of utility functions are plotted against the travel time in Figure 6.2. Note that in this figure, the utility functions assume equal travel times for the three alternatives, which is often not the case in practice, for example, cars typically have shorter travel times than bicycles, particularly for longer distances. This figure illustrates that the difference between the two sets is not substantial, and the car utility is more evenly distributed across the travel time for the non linear utility function. Given the minimal variation, the linear utility functions are selected for the model.

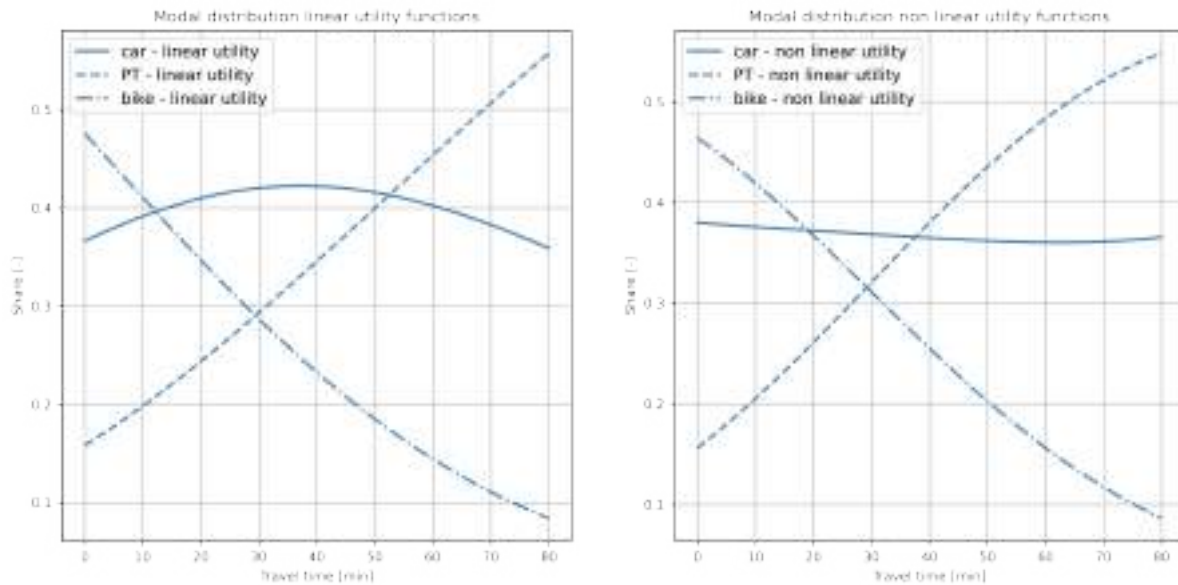


Figure 6.2: Comparison between linear and non linear utility functions

Table 6.2 shows the results of applying the Maximum Likelihood Estimation to the linear utility functions. Parameter  $ASC_{car}$  is set equal to zero, as this alternative is chosen as the reference choice. Consequently, the other ASC values represent the relative difference to the car alternative.

Parameter	Value	z-value	p-value
$ASC_{car}$	0	-	-
$ASC_{PT}$	-0.8405	-37.328	0.0
$ASC_{bike}$	0.2624	20.184	0.0
$\beta_{TT,car}$	-0.0487	-51.364	0.0
$\beta_{TT,PT}$	-0.0327	-51.098	0.0
$\beta_{TT,bike}$	-0.0701	-103.102	0.0

Table 6.2: Parameter estimates of modal split with robust standard errors, t-tests, and p-values.

All the parameters have an absolute t-test outcome greater than 1.96 and a p-value below 0.05, indicating the parameters are statistically significant. The estimated parameters also align with intuitive expectations. For instance, if the travel time is very short, the bike is preferred over the car, and the car chosen over public transport. Additionally, the  $\beta$  values are consistent with the underlying logic; all travel time coefficients are negative, signifying that longer travel times make an alternative less attractive. The parameter for bike is the most negative, as longer travel distances are unappealing for cycling trips. Public transport, on the other hand, has the least negative value, as it allows for activities such as working while travelling.

## 6.2. Step 2: discrepancy between model outcome and observed traffic

The second stage of the calibration process involves comparing the outcomes of the initial model for Roseknop phase 2 with the traffic intensity analysis conducted for the cordon surrounding the Roseknop.

For the traffic intensity analysis, data from TomTom Move is integrated with traffic signal data. TomTom Move provides the distribution of car trip distances, while the traffic signal data is utilised to determine the number of vehicles entering the Roseknop cordon during each evening rush hour. The traffic intensity for each distance category is presented in Figure 6.3 for the situation before the roadworks and several months after the start of phase 2 of the roadworks.

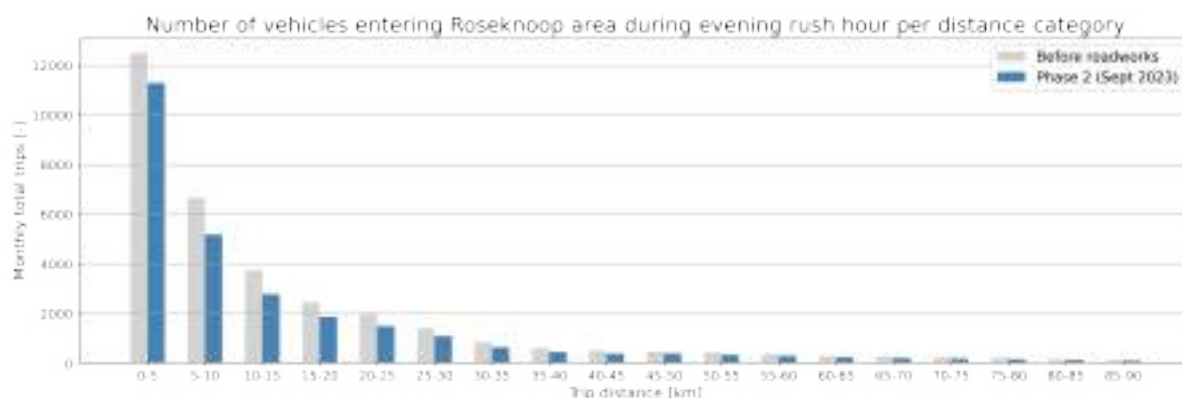


**Figure 6.3:** Number of vehicles entering Roseknoop cordon compared for before roadworks and during phase 2 of roadworks

Based on this information, a distribution in the reduction of trips per distance category can be made. This is shown in Figure 6.4.

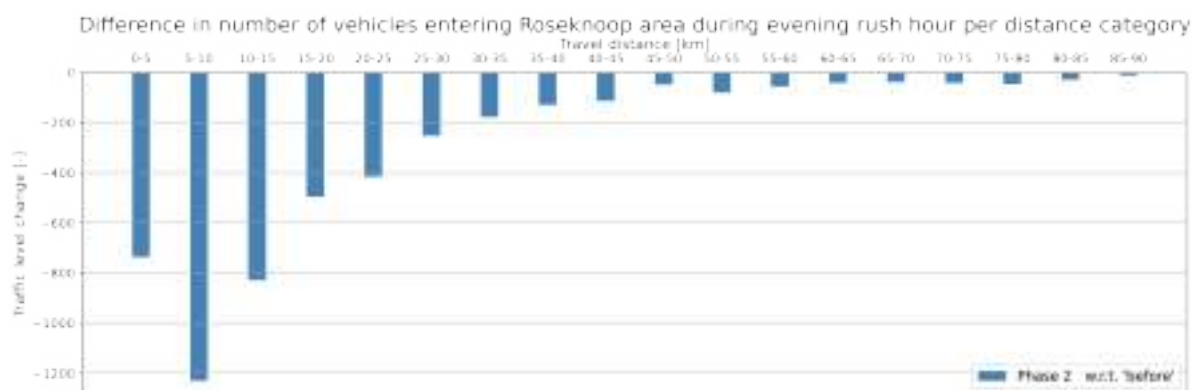


**Figure 6.4:** Difference in number of vehicles entering Roseknoop cordon compared for before roadworks and during phase 2 of roadworks

In addition to the data analysis, a model outcome of the capacity reduction of phase 2 of the roadworks is generated. The predictive model considers three travel alternatives—car, bicycle, and public transport—and estimates the reduction in car trips alongside the corresponding increase in trips by public transport and bicycle.

The data analysis counts the number of vehicles that enter the cordon between 3 and 6 PM. To compare the model results with the data analysis, trips in the simulation that enter the cordon between 3 PM and 6 PM are selected. The simulation runs from 2 PM to 7 PM, allowing for warm-up and cool-down periods before and after the evening rush hour. To extract the relevant trips, a factor is applied to generate an OD matrix for trips occurring between 3 PM and 6 PM. The OD pairs are then filtered to include only those that enter the cordon, i.e. OD pairs that drive on the set of links representing the cordon, in the base model.

This process results in two OD matrices: one representing trips entering the cordon between 3 PM and 6 PM prior to the road capacity reduction (from the base model) and another representing trips entering the cordon after the reduction (from the model output). The difference between these OD matrices allows for the calculation of the number of car trips that shift to bicycle or public transport, categorised by trip distance. The results are presented in Figure 6.5.



**Figure 6.5:** Model outcome roadworks phase 2 - number of car trips changed to public transport or bicycle

Next, the results of the data analysis and the model outcome are compared. As calibration is not possible for the increase in public transport and cycling trips, the discrepancy between the data analysis and the model outcome is interpreted as the portion of traffic that no longer uses the car during the evening rush hour but does not switch to another mode of transport. This discrepancy is indicated with the grey bars in Figure 6.6.

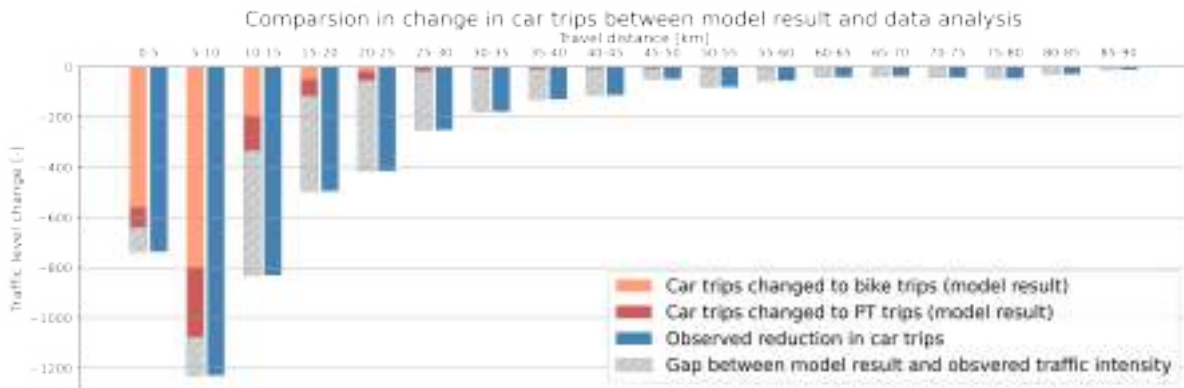


**Figure 6.6:** Comparison between model result and the traffic intensity analysis

When comparing the results of the model outcome and the traffic intensity analysis, it is notable that, in absolute terms, trips within the 10 to 25 km categories are predominantly underestimated. A possible explanation for this discrepancy is that, within the city (for trips below 10 km), viable alternatives exist due to the extensive cycling infrastructure and dense public transport network, making modal shifts more feasible. Conversely, for longer-distance trips, public transport and cycling become less attractive, particularly for those not residing near a train station.

As a result, shorter trips are more likely to shift to alternative transport modes, whereas longer trips are more inclined to adopt other behavioural adaptations, such as working from home or choosing destinations outside the city centre. For trip distances of 20 km or more, the overall reduction in trips is relatively small. However, car users who change their travel behaviour in these distance categories rarely switch to cycling or public transport, despite the data analysis indicating a reduction in car trips within these longer-distance categories.

The results of the discrepancy between the data analysis and the model outcome will be used to determine the parameters for the utility function associated with the no trip alternative.

### 6.3. Step 3: Final model including no trip alternative

The output of Section 6.2, the gap between the observed reduction in car trips and the calculated increase in PT and bicycle trips, will be used to determine the parameters for the utility function of the no trip alternative. First, the data is retrieved for the calibration in Subsection 6.3.1. The parameters are estimated in Subsection 6.3.2.

#### 6.3.1. Data for calibrating no trip alternative

The first step is to construct a data table comparable to Table 6.1, however now with additional information. An illustrative overview of the extended dataset is presented in Table 6.3. This dataset is filtered to include only OD pairs that experienced an increase in travel time due to the road capacity intervention. Each OD pair appears twice in the dataset: once representing the original situation, in which there is no increase in car travel time, and once reflecting the scenario where travel time has increased as a result of the road capacity intervention. This is the result of the initial model for the new equilibrium for the Roseknop roadworks phase 2. The construction of this table is explained below.

OD <sub>pair</sub>	D <sub>car</sub>	TT <sub>car</sub>	TT <sub>car</sub> <sup>eq</sup>	ΔT	TT <sub>PT</sub>	TT <sub>bike</sub>	p <sub>car</sub> <sup>model</sup>	p <sub>bike</sub> <sup>model</sup>	p <sub>PT</sub> <sup>model</sup>	trips <sub>tot</sub>	trips <sub>car</sub>	trips <sub>car</sub> <sup>disappeared</sup>	p <sub>no_trip</sub>	p <sub>car</sub> <sup>new</sup>
3,51	12.02	17.26	20.28	3.02	47.60	42.73	0.70	0.12	0.17	1.08	0.76	0.06	0.06	0.65
3,53	17.11	18.42	19.35	0.93	44.87	45.45	0.72	0.10	0.18	1.10	0.79	0.03	0.03	0.69
3,54	13.85	20.30	26.40	6.09	47.36	48.39	0.67	0.11	0.22	1.32	0.89	0.15	0.11	0.56
⋮	⋮	⋮	⋮	⋮	⋮	⋮	⋮	⋮	⋮	⋮	⋮	⋮	⋮	⋮
V7757,226	87.94	116.48	121.42	4.94	175.96	373.57	0.66	0.00	0.34	0.84	0.56	0.09	0.11	0.56
V7761,13	89.46	64.56	64.61	0.05	124.09	348.79	0.85	0.00	0.15	1.15	0.98	0.00	0.00	0.85
V7761,250	88.24	67.43	70.35	2.92	104.37	364.15	0.70	0.00	0.30	1.36	0.94	0.09	0.07	0.63

**Table 6.3:** OD pair data used for the extended modal split analysis ('V' indicates VMRDH-zone)

First of all, the travel time in the new equilibrium is added ( $TT_{car}^{eq}$ ). This represents the travel time outcome of the new equilibrium obtained using the model from step 1 of the calibration process. The difference between  $TT_{car}$  and  $TT_{car}^{eq}$  is  $\Delta T$ , which reflects the increase in travel time for the OD pair due to the road capacity reduction. Secondly,  $p_{car}^{model}$ ,  $p_{bike}^{model}$  and  $p_{PT}^{model}$  are included. These represents the probabilities of choosing each alternative, as calculated based on the utility functions and travel times within the initial model. Thirdly,  $trips_{tot}$  and  $trips_{car}$  are added and calculated, as they are necessary to determine the number of car trips that must have disappeared.  $trips_{tot}$  represents the original total number of trips (car, bike and public transport) for the given OD pair, while  $trips_{car}$  is the number of car trips for that OD pair, obtained by multiplying  $p_{car}^{model}$  by  $trips_{tot}$ .

Next, the number of car trips that must have disappeared can be calculated per OD pair. From Section 6.2, the number of car trips that additionally must disappear per distance category in the evening rush hour, can be derived. This is shown in Table 6.3. For each distance category, the OD pairs are selected and the disappeared cars are allocated proportionally based on the number of car trips ( $trips_{car}$ ) and the increase in travel time ( $\Delta T$ ). This proportional allocation is necessary due to the absence of additional information on how the reduction is distributed. This results in the column  $trips_{car}^{disappeared}$  in Table 6.3, representing the number of trips that must additionally disappear-beyond those that switch to cycling or public transport. Based on the value  $trips_{car}^{disappeared}$  and the total amount of trips ( $trips_{tot}$ ), the probability of opting for the no trip alternative ( $p_{no\_trip}$ ) can be calculated. The probability of choosing the no trip alternative is then subtracted from the probability of choosing the car, resulting in an updated probability of car use  $p_{car}^{new}$ . Consequently, for each OD pair, a revised mobility distribution is established ( $p_{car}^{new} - p_{bike}^{model} - p_{PT}^{model} - p_{no\_trip}$ ), which can be used for the calibration of the model parameters, including the no trip alternative.

#### 6.3.2. Determination of model parameters

With this updated dataset, the parameters can be recalibrated. The same method of Maximum Likelihood Estimation is applied as in Section 6.1. The form of the utility functions for the modal alternatives remain consistent with those in Equations 4.1, 4.2 and 4.3. However, their parameters are re-estimated. For the utility function of the no trip alternative, the formula as in Equation 4.4 is chosen.

$$V_{notrip}^{OD} = ASC_{notrip} + \beta_{D,notrip} \cdot D_{car}^{OD} + \beta_{2,D,notrip} \cdot (D_{car}^{OD})^2 + \beta_{\Delta T,notrip} \cdot \log(\beta_{\Delta T,2,notrip} + \frac{\Delta T}{TT_{car}^{OD}}) \quad (4.4)$$

This utility function is non-linear, incorporating a quadratic relationship with trip distance and a logarithmic function for the increase in travel time. The logarithmic function is selected because the utility should initially be negative for small values of  $\Delta T$ , ensuring that the probability of choosing the no trip alternative remains minimal under minor travel time increases.

To determine the most appropriate functional form, multiple specifications for the utility function of the no trip alternative were tested for model fit. A utility function with only a linear relationship with distance resulted in a model fit of 0.6731, while the inclusion of a quadratic term slightly improved the fit to 0.6763. Although this increase in model performance is modest, a comparison of the utility functions for different travel time increases (see Figure 6.7) reveals that the linear function effectively represents an average of the non-linear function.

Figure 6.6 demonstrated that the largest discrepancy between the data analysis and the model outcome occurs in the medium-distance trip categories (10–30 km). Consequently, the non-linear function provides a more realistic representation. The observed decline in utility for distances exceeding 40 km can be attributed to the fact that, at such distances, travel times are relatively high across all alternatives. As a result, the utility of the no trip option decreases for longer distances, preventing an unrealistically high probability of trip cancellation.

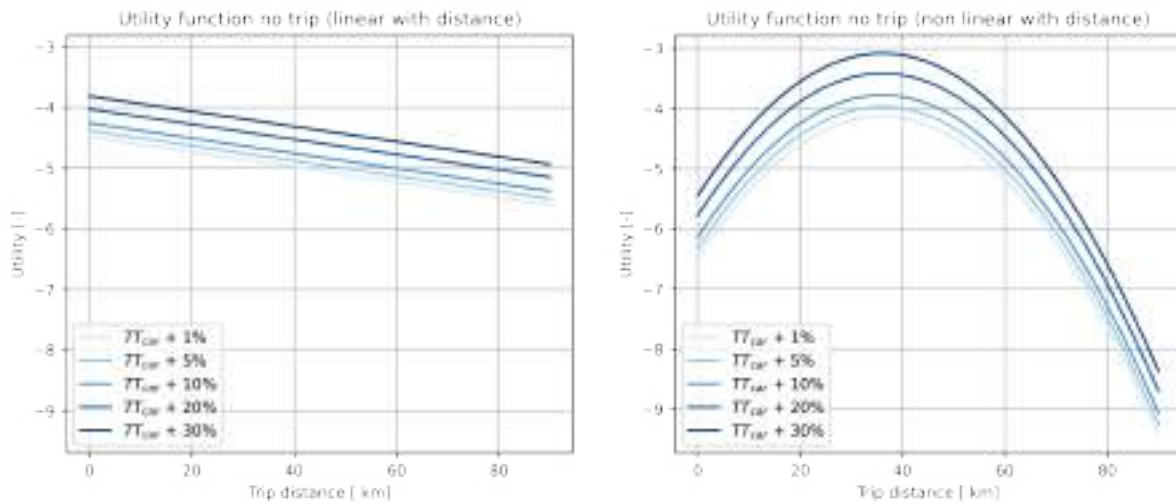


**Figure 6.7:** Comparing the linear and non linear utility function of the no trip alternative

Table 6.4 presents the results of the Maximum Likelihood Estimation.

Parameter	Value	z-value	p-value
$ASC'_{car}$	0	-	-
$ASC'_{PT}$	-0.8451	-44.05	0.0
$ASC'_{bike}$	0.2501	9.56	0.0
$ASC'_{notrip}$	-4.013	-61.45	0.0
$\beta_{TT,car}$	-0.0513	-29.79	0.0
$\beta_{TT,pt}$	-0.0331	-39.91	0.0
$\beta_{TT,bike}$	-0.0703	-78.53	0.0
$\beta_{D,notrip}$	0.1640	32.64	0.0
$\beta_{D,2,notrip}$	-0.002033	-32.64	0.0
$\beta_{\Delta T,notrip}$	0.9361	55.65	0.0
$\beta_{\Delta T,2,notrip}$	0.00005126	57.02	0.0

**Table 6.4:** Parameter estimates of modal split with robust standard errors, t-tests, and p-values.

As expected, the parameters of the utility functions for car, bike and public transport are relatively similar to the parameters found in Section 6.1. For the utility function of the no trip alternative, the value  $ASC_{\text{notrip}} = -4.013$  suggest that the probability of choosing not to travel is relatively low for short trips compared to opting for the car. This is a logical outcome, since the overall number of car trips that are ultimately not undertaken is relatively small in comparison to the total number of car trips. The parameters for distance,  $\beta_{D,\text{notrip}} = 0.1640$  and  $\beta_{D,2,\text{notrip}} = -0.002033$  indicate a parabolic relationship with the travel distance. The utility is highest for trips within the middle distance categories, which aligns with the findings in Figure 6.6, where a significant number of disappeared car trips are observed particularly within the 10-40 km range.

The parameter  $\beta_{\Delta T,\text{notrip}}$  represents the sensitivity of utility to an increase in travel time. With a value of  $\beta_{\Delta T,\text{notrip}} = 0.9361$ , it indicates that relative increases in travel time have a substantial influence on the likelihood of choosing the no trip alternative. The parameter  $\beta_{\Delta T,2,\text{notrip}} = 0.00005126$  introduces a small constant to the relative increase in travel time. This constant is extremely minor and only affects cases where the relative travel time increase is close to zero. It ensures a smooth transition from  $\Delta T = 0$  to small positive values, preventing an abrupt change in utility.

However, incorporating this constant  $\beta_{\Delta T,2,\text{notrip}}$ , results in a very small but non-zero probability of choosing the no trip alternative when  $\Delta T = 0$ . The theoretical maximum utility is  $V_{\text{notrip}} = -9.95$  at  $D_{\text{car}} = 40\text{km}$ . The final probability depends on the actual travel times of the alternatives. Assuming  $TT_{\text{car}} = 40\text{min}$ ,  $TT_{\text{PT}} = 25\text{min}$  and  $TT_{\text{bike}} = 70\text{min}$ , the resulting probability is  $P_{\text{notrip}} = 0.00015$ . This is an extremely low probability, and to prevent car trips from disappearing in the base scenario when no additional delay is present, probability values are rounded to two decimal places.

The final utility functions, including their parameters, are presented in Equations 6.6, 6.7, 6.8, 6.9.

$$V_{\text{car}}^{\text{OD}} = 0 - 0.0513 \cdot TT_{\text{car}}^{\text{OD}} \quad (6.6)$$

$$V_{\text{PT}}^{\text{OD}} = -0.8451 - 0.0331 \cdot TT_{\text{PT}}^{\text{OD}} \quad (6.7)$$

$$V_{\text{bike}}^{\text{OD}} = 0.2501 - 0.0703 \cdot TT_{\text{bike}}^{\text{OD}} \quad (6.8)$$

$$V_{\text{notrip}}^{\text{OD}} = -4.013 + 0.1640 \cdot D_{\text{car}}^{\text{OD}} - 0.002033 \cdot (D_{\text{car}}^{\text{OD}})^2 + 0.9361 \cdot \log(0.00005126 + \frac{\Delta T}{TT_{\text{car},\text{original}}^{\text{OD}}}) \quad (6.9)$$



## 6.4. Results calibrated model

To provide insights into the behaviour of the utility functions, several graphs are presented, which illustrate the mobility distributions for increasing values of additional travel time due to road capacity reductions. Six typical OD pairs have been selected from the model to represent a range of trip types: a short inner-city trip (Figure 6.8), a journey from the suburbs to the city centre (Figure 6.9), a trip from an adjacent city to Rotterdam's city centre (Figure 6.10), a journey originating from a distant city to Rotterdam (Figure 6.11), a trip from the countryside near Rotterdam to the city (Figure 6.12) and a trip from the countryside far from Rotterdam to the city (Figure 6.13). For each scenario, the mobility distributions are displayed for varying values of  $\Delta T$ . The mathematical functions corresponding to the graphs can be found in Appendix D.

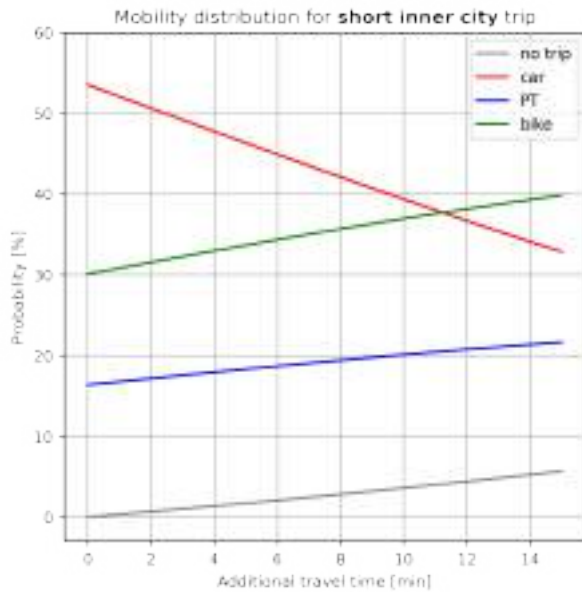


**Figure 6.8:** Mobility distribution for increasing additional travel time for short inner city trip of 3.5 km (from Rotterdam Feyenoord to Rotterdam Dijkzigt)

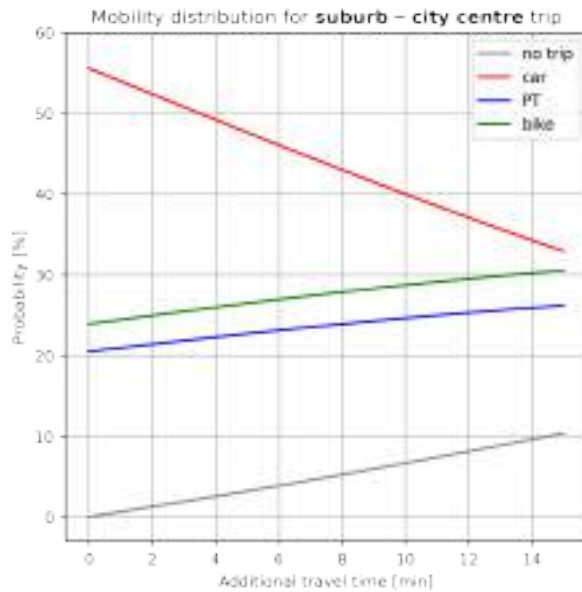


**Figure 6.9:** Mobility distribution for increasing additional travel time for trip from a suburb to city centre of 9.1 km (from Rotterdam Prinsenland to Rotterdam city centre)

The first two journey types take place within the city. The first is a short inner-city trip of 3.5 km, while the second is a trip from the suburbs to the city centre, covering 9.1 km. The graphs indicate that for the short inner-city trip, the majority of individuals shift from car use to cycling as travel time increases, followed by public transport and the no trip alternative. For the suburb-to-city centre trip, a similar shift from car use to cycling and public transport is observed; however, the no trip alternative is selected more frequently. This suggests that individuals residing further from the city centre are more likely to adjust their destination, departure time, or trip frequency compared to those living close to the city centre, as cycling becomes less attractive over longer distances.

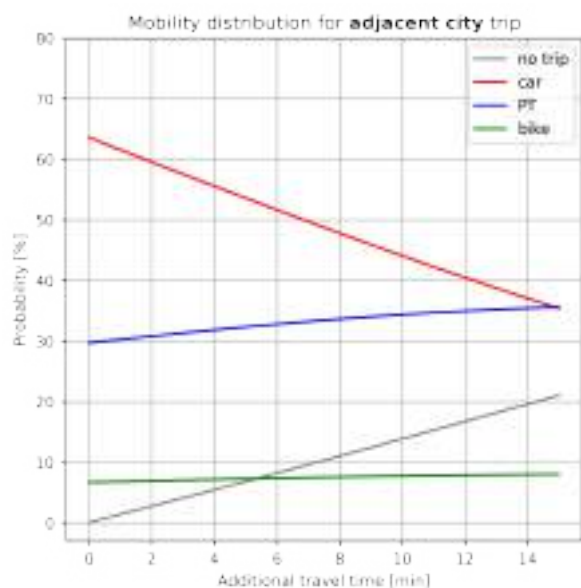


**Figure 6.10:** Mobility distribution for increasing additional travel time for adjacent city trip of 14.7 km (from Delft city centre to Rotterdam city centre)

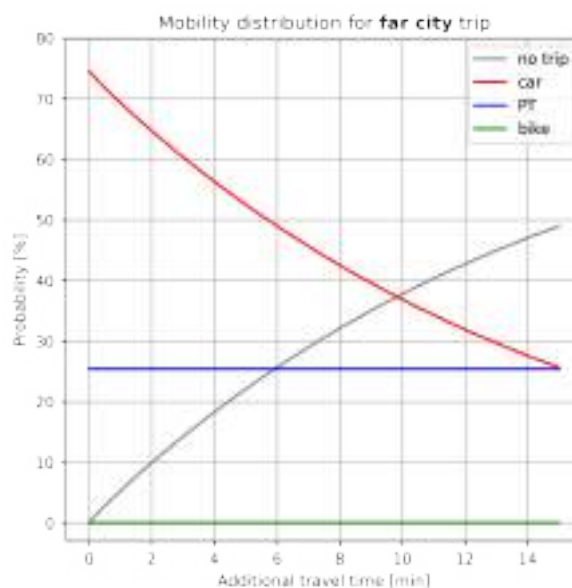


**Figure 6.11:** Mobility distribution for increasing additional travel time for a trip from a suburb of another large city to Rotterdam of 59.4 km (from Utrecht Overvecht to Rotterdam city centre)

Next, journeys from other cities to Rotterdam are analysed. The first originates from a city near Rotterdam, with a travel distance of 14.7 km. While public transport and cycling attract a small number of additional users, the majority of car users opt to change their departure time, destination, or trip frequency when travel time increases. For trips originating from a more distant city (59.4 km), the impact on car use is even greater. Public transport and cycling do not experience a significant increase in usage, while a substantial proportion of car users choose the no trip alternative.

For these longer distance journeys, the diminishing influence of additional travel time is evident, whereas for trips from adjacent cities, the relationship appears almost linear. This can be attributed to the fact that for shorter journeys, the impact of additional travel time remains significant as it increases. In contrast, for longer trips, this effect diminishes because the overall travel time is already substantial, and the relative impact of additional travel time becomes less pronounced. While a small increase in travel time may still prompt individuals to alter their destination, departure time or trip frequency—since alternative modes such as public transport or cycling would likely result in even longer travel times—the behavioural effect weakens as delays accumulate. For instance, when the additional travel time increases from 10 to 15 minutes, the behavioural effect is smaller than when it increases from 5 to 10 minutes. This is likely because travellers may have already adjusted to or accepted the initial 10-minute increase and are therefore more inclined to tolerate an additional five minutes.

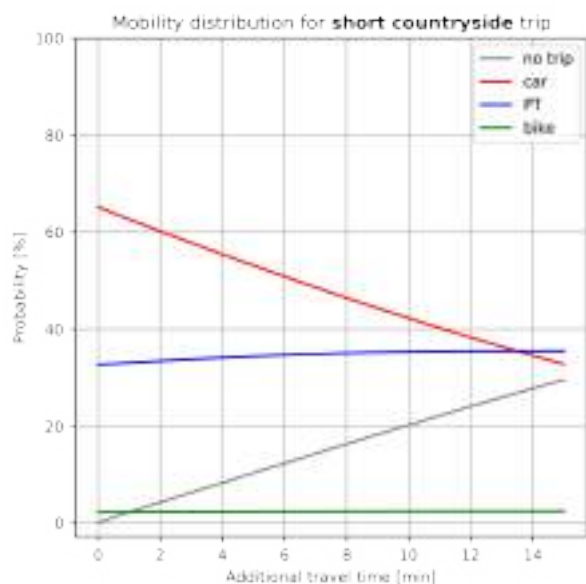


**Figure 6.12:** Mobility distribution for increasing additional travel time for a trip from the countryside close to the city of 17.7 km (from Mijnsheerenland to Rotterdam city centre)

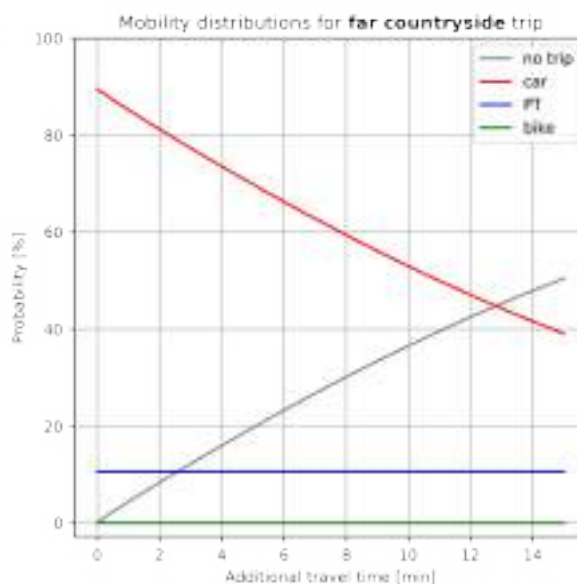


**Figure 6.13:** Mobility distribution for increasing additional travel time for a far trip from the countryside to a large city of 66.8 km (from Tholen (Zeeland) to Rotterdam)

The final set of trips concerns travel from the countryside to the city. The first case involves a short countryside trip with a well-connected public transport link to the city. In this scenario, an increase in travel time leads to a slight rise in public transport usage, while the majority of car users opt to adjust their destination, departure time, or trip frequency. The second case involves a journey from a more remote rural area (66.8 km from the city). The graphs illustrate that additional travel time has a significant impact on car use. Public transport gains no notable increase in users, while nearly all car users choose to opt-out for the trip altogether during the peak hour.

Overall, the probabilities suggest that for short journeys, an increase in travel time primarily results in a shift towards public transport and cycling. In contrast, for longer trips, the transition from car use to alternative modes remains minimal. Instead, these individuals are more likely to adjust their destination choices, departure time or trip frequency.

# 7

## Model validation

In this chapter, the model validation will be discussed. In Chapter 6, the model is calibrated using the Roseknoop roadworks phase 2. The Roseknoop roadworks phase 1 is employed to validate the calibrated model. Phase 1 represents the smaller of the two roadwork phases, where only the side streets of the Laan op Zuid / Varkenoordsviaduct corridor are closed to car traffic. An overview of the roadwork phase is provided in Figure 7.1. A more detailed explanation of the roadworks can be found in Chapter 5. This chapter will first present the results of applying the model to Roseknoop roadworks phase 1 in Section 7.1. Subsequently, the model results will be compared with the data analysis in Section 7.2. Section 7.3 will conclude with the findings of the model validation.

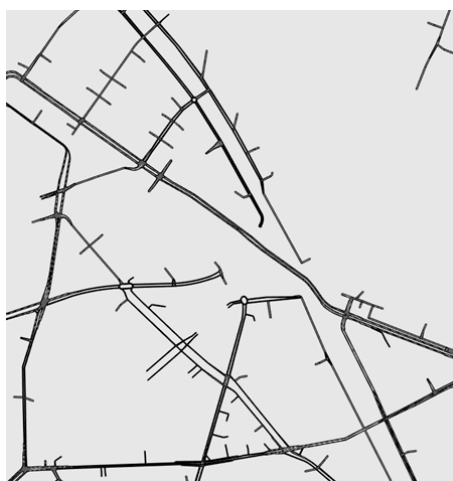


**Figure 7.1:** Adapted infrastructure network during phase 1 of Roseknoop roadworks

### 7.1. Model result Roseknoop roadworks phase 1

This section will present the model results for Roseknoop roadworks phase 1. The model inputs consist of the adapted infrastructure network, as shown in 7.1, and the original OD matrix. The following results were obtained.

For Roseknoop phase 1, the model required three iterations to reach the new equilibrium. The cumulative distribution functions for both directly and indirectly affected OD pairs are displayed in Figure 7.2.

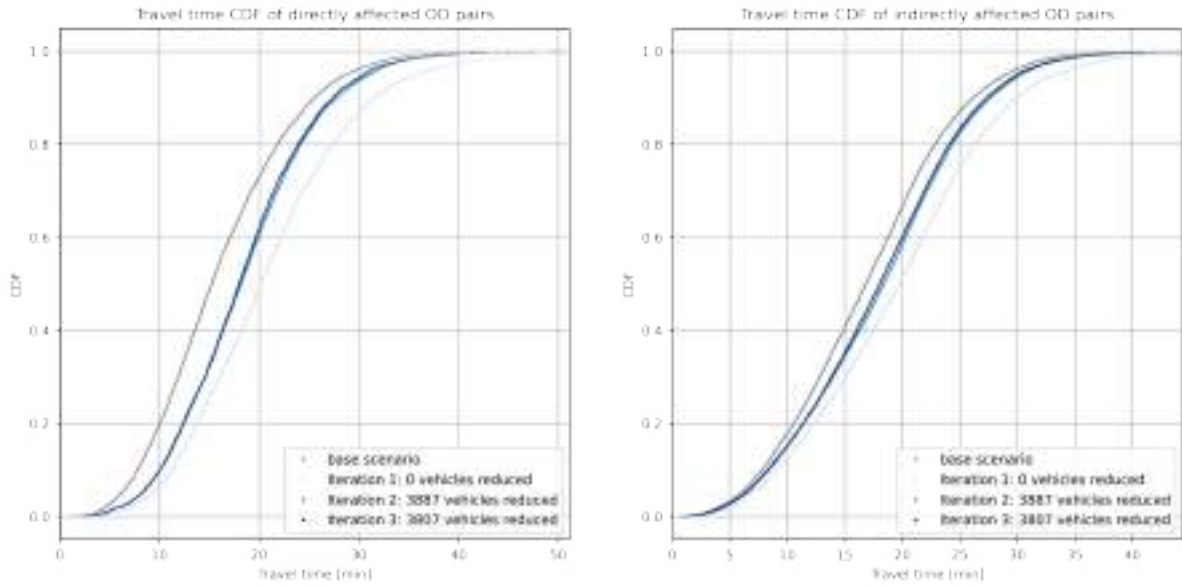


**Figure 7.2:** Cumulative distribution function of the travel times for directly and indirectly trips per iteration

This figure illustrates that iteration 2 and 3 have fairly similar outputs. Figure 7.3 shows the progression of the KS values for each iteration, with the KS value between the last two iterations indicated by the solid line. The figure demonstrates that at the third iteration, the KS value drops below the threshold, suggesting that the CDFs of the travel times between iteration 2 and 3 are so closely aligned that the traffic has stabilised and a new equilibrium is found. Additionally, the KS-value for each iteration, relative to the base scenario, is indicated in the figure by the dash-dotted line.

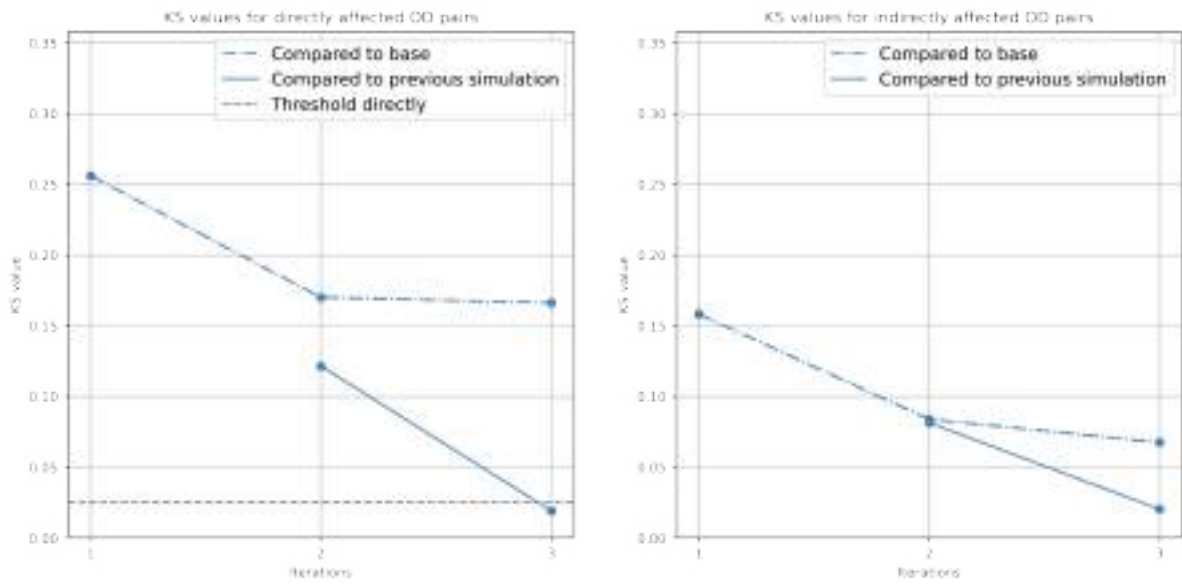


**Figure 7.3:** Progression of KS values between CDFs for the directly affected OD pairs (left) and indirectly affected OD pairs (right). The dashed-dotted line is the KS value between the base and the iteration.

In Table 7.1, an overview of the recalculation of the OD matrix during the different iterations is provided.  $\Delta\text{cartrips}_{\text{sim}}$  represents the reduction in car trips applied in the traffic simulation of the iteration. This simulation results in a certain increase in travel time for both directly and indirectly affected OD pairs. These are indicated in the table as  $\Delta T_{\text{directly}}$  and  $\Delta T_{\text{indirectly}}$ , respectively.  $\Delta\text{cartrips}_{\text{recalc}}$  reflects the outcome of the recalculated OD matrix, which results from the increased car travel time.  $\Delta\text{cartrips}_{\text{recalc}}^{\text{optimised}}$  shows the result of applying the optimisation, where information from the previous iterations is used to determine the new OD matrix (see Section 4.3 for an explanation of the optimisation process). This updated OD matrix is then used as input for the simulation of the next iteration.

Iteration	$\Delta\text{cartrips}_{\text{sim}}$	$\Delta T_{\text{directly}}$	$\Delta T_{\text{indirectly}}$	$\Delta\text{cartrips}_{\text{recalc}}$	$\Delta\text{cartrips}_{\text{recalc}}^{\text{optimised}}$
1	0	+ 4.79 min	+ 2.80 min	- 7774	- 3887
2	- 3887	+ 2.38 min	+ 1.15 min	- 3647	- 3807
3	- 3807	+ 2.43 min	+ 1.04 min	- 3229	- 3662

**Table 7.1:** Model results for the different iterations for phase 1 (all values are compared to the base scenario)

In the first iteration, the original OD matrix is applied in the traffic simulation. This leads to an average increase of 4.79 and 2.80 minutes for directly and indirectly affected OD pairs, respectively. The increase in travel times causes a significant reduction in car trips, amounting to 7,774 vehicles. For the next iteration, the average of the original and recalculated OD matrix is used. This OD matrix shows a reduction of 3,887 vehicles. The simulation of iteration results in a smaller impact on travel times, with an average increase of 2.38 min for directly affected and 1.15 min for indirectly affected OD pairs. This leads to a calculated reduction of 3,647 vehicles.

Through process optimisation, the new iteration results in a reduction of 3,807 car trips. This leads to a change in travel time to 2.43 minutes and 1.04 minutes for directly and indirectly affected OD pairs, respectively. These values are comparable to the previous travel time changes and yield a KS value of 0.019, which is below the threshold value of 0.025. Recalculating the OD matrix based on the outcomes of iteration 3 produces the final OD matrix, showing a reduction of 3,662 vehicles—equivalent to 4.4% of the total affected car trips (82,800). Of these, 1,910 car trips are directly hindered (out of 27,700 directly hindered car trips), while 1,752 car trips are reduced which drove on the alternative routes (out of 55,200 indirectly hindered car trips). An overview of the results from the third iteration is presented in Table 7.2.

mode	$\Delta\text{trips}$	directly affected	indirectly affected
car	- 3662	- 1910 (6.9%)	- 1752 (3.2%)
bicycle	+ 947	+ 514	+ 433
public transport	+ 722	+ 352	+ 369
no trip	+ 1993	+ 1044	+ 950

**Table 7.2:** Final result of the model applied to Roseknoop roadworks phase 1 (all values are compared to the base scenario)

The table shows a slightly higher reduction in directly affected car trips compared to indirectly affected car trips in absolute values. However, the total number of indirectly affected car trips is much higher than that of directly affected car trips. There is a 6.9% reduction of directly affected car trips and a 3.2% reduction of indirectly affected car trips. It is logical that the percentage reduction is higher for directly affected car trips, since the directly affected car trips refer to vehicles which must take alternative routes. This often results in higher travel times, even without considering potential additional congestion on the alternative routes.

Regarding the alternatives to driving, Table 7.2 shows that the 3,662 reduced car trips are redistributed as follows: 947 bike trips, 722 public transport trips and 1,993 people opting for the no trip alternative. Thus, the largest portion of people choose this latter alternative. The no trip alternative includes not only the decision to cancel the trip but also the possibility of adjusting the departure time outside of rush hour or changing destination outside of Roseknoop area. Therefore, this large value is expected. Other notable aspects include the distribution of directly and indirectly affected trips for the public transport. For the bike and no trip alternative, the increase in trips for directly affected individuals is higher than for

indirectly affected individuals, consistent with the reduction in car trips. However, for public transport, there is an increase of 369 trips of indirectly affected car trips and 352 directly affected car trips. This could be due to the fact that directly affected OD pairs typically have shorter distances than indirectly affected OD pairs. As a result, directly affected OD pairs are more likely to switch to biking, while indirectly affected OD pairs are more inclined to use public transport due to the longer distances.

## 7.2. Comparison traffic conditions model outcome to observations

The case study on phase 1 of the roadworks did not show a visible reduction in traffic intensity entering the cordon (see Figure 5.9 in the case study). However, the model does indicate a reduction in vehicular trips. This discrepancy can be explained by the fact that only vehicles entering the cordon are observed, whereas trips that start and end within the cordon, as well as trips that start within the cordon and exit it, are not accounted for. The model is calibrated on trips entering the cordon by determining the parameters of the utility functions. These utility functions are then applied to all affected trips. As a result, the DiTra model predicts a reduction in car usage, even though this reduction is not directly visible in the data analysis.

Due to the lack of comprehensive trip data, a quantitative analysis is challenging to perform. Therefore, a comparison of the traffic situation was conducted to facilitate qualitative validation. The average speeds from TomTom Move during the equilibrium month of phase 1 of the roadworks (April 2023) are compared to the congestion heat map generated by the DiTra model for the same phase. These two aspects differ in their representation: the average speeds from TomTom Move highlight streets where speed has deteriorated compared to free-flow conditions, measured at night, whereas the congestion heat map visualises the locations of stationary vehicles, which colours ranging from blue, green to red to indicate increasing congestion levels. While these aspects are not entirely directly comparable, both maps provide insights into the location and intensity of congestion within the road network.

Figure 7.4 presents the average travel speed between 4 and 5 PM compared to the free-flow speed, which is measured between 11 PM and 4 AM, for April 2023-four months after the implementation of phase 1. Since this data analysis is compared to the congestion heat map, only travel speeds between 0 and 60% of the free-flow speed are displayed, highlighting areas with the most significant delays and congestion. Figure 7.5 illustrates congestion at 5:30 PM as simulated by the DiTra model for the equilibrium state of phase 1. This heat map represents the 'average' congestion pattern derived from six different simulation runs. The average heat map is determined based on visual assessment of congestion across these runs. The heat maps from the individual runs are provided in Appendix E.



**Figure 7.4:** Delay situation April 2023 (equilibrium of phase 1) in the Roseknoop area [TomTom, 2024]



**Figure 7.5:** Average congestion heat map of Roseknoop roadworks phase 1 as a new equilibrium (iteration 3)

The congestion heat map highlights three key areas of significant congestion around the Roseknoop area. Near the Roseknoop, in Feijenoord, congestion levels have increased compared to the base model results. Notably, congestion has intensified on the Posthumalaan and at the junction of the Laan op Zuid with the Brede Hilledijk / Vuurplaat. These locations align with the observed congestion patterns in Figure 7.4. The second area of congestion appears on the left side of the map, around 's Gravendijkswal and near the Maastunnelplein. These locations also experience congestion in the



base model, as they are known to be busy even under normal conditions. The third area with additional congestion is around the Bree and Groene Hilledijk. In the observed traffic data, congestion is also visible at these locations, though it appears to be slightly more severe.

To further validate the model, Figure 7.6 presents the ‘average’ congestion heat map from the first iteration of the DiTra model. This iteration represents the traffic situation where traffic demand remains unchanged from before the roadworks were introduced.



**Figure 7.6:** Average congestion heatmap of Roseknoop roadworks phase 1 at 5 PM with original OD matrix (no disappearing traffic). Red circles indicate additional traffic congestion locations compared to the congestion heat maps of the new equilibrium.

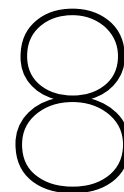
This heat map shows more congestion than Figure 7.5, which was expected given that the new equilibrium reflects a reduction of 3,662 vehicles in the simulation. Additionally, greater congestion is visible when compared to the observed speed differences in Figure 7.4. The three circles in Figure 7.6 highlight locations where more congestion appears in the majority of the model runs, compared to Figure 7.5. In contrast, the observed situation in Figure 7.4 does not indicate a significant reduction in average speed at these locations. This suggests that the traffic situation in the newly established equilibrium (Figure 7.5 aligns more closely with observed conditions than the scenario with the original traffic demand.

### 7.3. Conclusion model validation

Validating the model is challenging, as the roadworks phase used for validation is relatively small, resulting in no visible reduction in the number of cars entering the cordon in the data analysis. Therefore, the model was validated by comparing the observed average speeds with the congestion heat maps from the traffic simulation, considering both the original traffic demand and the reduced traffic demand at the new equilibrium. The heat map of the simulation revealed a clear overestimation of congestion for the original traffic demand, whereas the heat map of the new equilibrium aligned more closely with the observed data.

Based on these findings, it can be concluded that during phase 1 of the Roseknoop roadworks, a reduction in car trips during the evening rush hour did indeed occur, as predicted by the model. However, fully assessing the model's accuracy remains difficult. This is primarily due to the inability to validate the predicted increase in bicycle and public transport usage or the number of individuals who discontinued their trips in the Roseknoop area as a result of the road capacity interventions.





# Conclusion

The primary research question guiding this study is *How can the change in travel behaviour be accurately predicted following road capacity reductions in urban areas, and what insights can be drawn from these predictions?*. This question is addressed through the analysis of predefined sub-research questions. These questions are answered in Section 8.1. In Section 8.2, the assumptions of the model and the resulting limitations are explained. Section 8.3 provides the final conclusions of this report. This is followed by recommendations and implications for science and practice in Section 8.4 and Section 8.5 respectively.

## 8.1. Findings

This section will provide the findings of this study by answering all of the sub research questions.

### ***Under what conditions does disappearing traffic occur, and what are the key drivers behind this phenomenon?***

Extensive research has been conducted on the effects of road capacity reductions on car use. Numerous case studies have demonstrated changes in travel behaviour following such interventions [Chung et al., 2012] [Tennøy and Hagen, 2020] [Nello-Deakin, 2022] [Melia and Calvert, 2023] [Gemeente Amsterdam, 2024]. A recurring finding across these studies is the stabilisation of congestion after an initial adjustment period. While reductions in car usage are frequently observed, the extent to which this occurs is highly context-dependent.

It is important to note that disappearing traffic does not inevitably follow road space reallocations [Cairns et al., 2002]. For this phenomenon to occur, the following four conditions must be met:

1. Road space reallocation must result in a reduction of capacity
2. The original traffic intensity must exceed the newly established capacity.
3. Plausible alternative routes must lack sufficient capacity to absorb the surplus traffic.
4. The difference between the original intensity and the new capacity must be substantial enough that shifting departure times (between peak and non-peak hours) alone cannot prevent increased congestion.

The primary driver behind disappearing traffic is travellers desire to minimize friction during their journeys. Capacity reductions trigger shifts in travel behaviour as individuals seek to mitigate increased inconvenience [Nello-Deakin, 2022]. This behavioural adaptation typically takes several months [Vonk et al., 2024], during which congestion and car usage are in imbalance before reaching a new equilibrium.

**What are the essential components of a predictive model for estimating changing travel behaviour and how are its components interconnected?**

A methodology has been developed to replicate the process of finding a new equilibrium between traffic congestion and the car usage. The framework for constructing a predictive model to estimate the changing travel behaviour is presented in Figure 8.1. This model follows an iterative process of traffic assignment and recalculation of the mobility distribution to establish a new equilibrium. The model incorporates the three most common transport modes - car, bicycle and public transport - alongside a no trip alternative which reflects adjustments in departure time, travel destination or trip frequency.

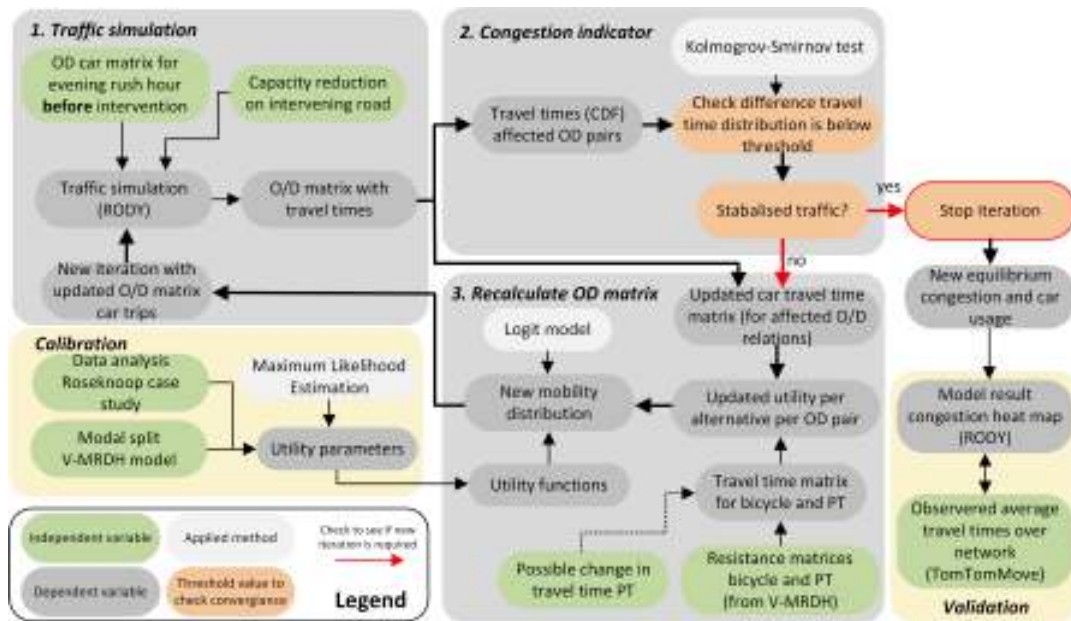


**Figure 8.1:** Framework of the model to predict the new equilibrium in mobility distribution following a capacity reduction.

The iterative process consists of three key steps. The first step involves traffic simulation where travel times for each Origin-Destination (OD) pair are derived based on a predefined OD matrix. In the second step, travel times of affected trips are compared between the two last iterations. If the travel times are comparable, traffic conditions have stabilised and a new equilibrium has been reached. Conversely, if the travel times differ significantly, congestion and car usage remain imbalanced and a new iteration is started. In the third step, travel times obtained from the traffic simulation are used to recalculate the OD matrix. Based on defined utility functions, the probabilities of the alternatives of each OD pair are calculated. This process generates, among other aspects, a revised OD matrix for car trips, which serves as input for the subsequent iteration.

**What insights do two case studies of road capacity reductions in Rotterdam provide about changing travel patterns?**

In the case study, the car usage before, during and after the Roseknoop roadworks is researched. Based on traffic light data, the number of vehicles entering the Roseknoop cordon is analysed. The Roseknoop cordon also contains the plausible alternative routes of the Roseknoop. These values are compared to reference locations to take out seasonality and annual traffic growth. The roadworks are divided in different phases. Phase 1 represents a smaller-scale roadwork phase, where only the side streets Rosestraat, Putselaan, Beijerlandse laan and Colosseumweg of the corridor Laan op Zuid / Varkenoordse viaduct were restricted for car traffic. In phase 2, the intersection was fully restricted to car traffic.

During phase 1, no significant reduction in number of cars entering the cordon is observed. However, once phase 2 begins, a reduction in car trips becomes evident, with a 15% difference of traffic volume between the car trips entering the cordon and the traffic intensity on the reference locations. This translates to 4.400 car trips that initially entered the cordon but subsequently changed their travel mode,

departure time, destination or trip frequency in the evening peak.

The case study also reveals that traffic does not fully return to its pre-restriction state after the restrictions are lifted. A portion of the original car users maintain their altered travel behaviour even when capacity is restored to normal levels. These observations were made up to one year after the capacity reduction was lifted; however, the long-term effects beyond this time frame have not been examined.

***What are the key characteristics of the calibrated predictive model?***

The calibrated predictive model demonstrates several key characteristics. These enable it to effectively capture and predict changes in mobility behaviour resulting from the additional travel time caused by road capacity reductions. One notable feature of the model is its sensitivity to trip distance, which significantly influences the nature of behavioural shifts.

For shorter trips, such as those within a city or between neighbouring cities, the model highlights a marked shift away from car usage towards alternative modes of transport, such as cycling and public transport. This behaviour is particularly evident for inner-city trips, where shorter distances make these alternatives more feasible. In contrast, for longer trips, the model indicates that individuals are less likely to adopt alternative modes of transport, such as public transport or cycling, due to the considerable increase in travel time these options would entail. For these types of trips, individuals are more inclined to adjust their destination, departure time, or trip frequency. For small increases in travel time, this shift is significant; however, as the additional travel time increases, this effect diminishes.

***How does the predictive model perform when applied to a case study in Rotterdam?***

The effectiveness of the model is tested by applying it to the Roseknoop roadwork phase 1, which occurred between January 2023 and June 2023. The data analysis of the traffic counts in the area for this phase was insufficient to facilitate a quantitative comparison of the results. Consequently, the traffic situation on the road was analysed instead. The congestion maps generated from the simulation demonstrate that congestion emerged at the same locations, with a magnitude comparable to that of the observed traffic congestion. Based on these findings, it can be concluded that the model's estimation of the reduction in car trips is robust when applied to phase 1 of the Roseknoop roadworks. However, the distribution of increases in trips for the alternatives remains challenging to validate due to the lack of comprehensive data.

***What insights can be drawn from the model's application for future urban planning and traffic management?***

This study provides several insights into the changes in travel behaviour in response to road capacity reductions. Road capacity reductions can lead to shifts in travel patterns when travel time for vehicles increases significantly. As a result of the increased travel time, the car becomes a less attractive mode of transport, prompting individuals to shift to alternative modes or alter their departure time, destination, or trip frequency. Following an initial adjustment period after the implementation of road capacity reductions, traffic congestion decreases and stabilises. However, average travel times in the surrounding areas continue to rise slightly, even for car trips on alternative routes. Ultimately, the road capacity reduction results in a new equilibrium, characterised by slightly more congestion and an associated increase in travel time. Nevertheless, this congestion is less severe than it would have been if car travel demand had remained unchanged following the capacity reduction. Based on the utility functions of the model, shorter trips are more likely to shift to alternative modes, while longer trips tend to adjust their destination, departure time or trip frequency.

## 8.2. Model assumptions and limitations

This section outlines the assumptions made during the construction of the DiTra model, along with the resulting limitations. First, general assumptions in traffic models are discussed, since the DiTra model builds upon the outcomes of these models. Following this, the specific assumptions inherent in the DiTra model are addressed.

The first assumption related to traffic models concerns the reflection of real-world patterns and the potential deviations from actual conditions. Although calibrated, the model cannot perfectly predict real-world patterns. There can be, for instance, errors in the Origin Destination matrices, or in the simulation of traffic movements in the dynamic traffic model. These assumptions may lead to discrepancies between the traffic conditions of the base scenario and real-world traffic patterns. Consequently, this could influence the travel times derived from the simulation and result in slight variations in the OD split within the new equilibrium after road capacity reductions. Moreover, traffic patterns will differ across days and months, making it challenging to achieve a perfect match. Consequently, a highly detailed model may not be particularly useful in this context. Furthermore, the travel characteristics per OD pair used from the V-MRDH model are also subject to inaccuracies, which can impact the modal split and influence the external segments of trips outside the RODY network.

Beyond the assumptions inherent in traffic models, the DiTra model also incorporates certain assumptions, particularly in Step 3 of the iterative process, where traffic demand is recalculated. First of all, this recalculation is based on utility functions. The utility functions for the different modes of transport consider only travel time as an attribute and are modelled as linear functions. This simplification may constrain the accuracy of estimating the probabilities of choosing alternative modes. Based on the outputs of these utility functions, the probabilities are calculated using the logit model. However, the logit model also has its assumptions. One assumption that may be debatable is the presumption that decision-makers possess complete knowledge of the characteristics of the available alternatives. Habitual behaviour may prevent individuals from considering other options, which could result in an overestimation of the likelihood of mode-switching. Another assumption, related to Step 3, concerns the treatment of external trips. In the model, a V-MRDH zone located outside of Rotterdam is assigned to a single external RODY zone. In practice, individuals may select alternative routes, influenced by varying levels of congestion on specific paths. This assumption may reduce the model's flexibility and could lead to an overestimation of congestion.

The calibration process, in which the parameters of the utility functions are estimated, also involves certain assumptions. Primarily, the calibration relies on a single case study. This approach renders the model susceptible to biases associated with the specific context of the case study, potentially limiting its generalisability. Additionally, the calibration method estimates the modal shift towards cycling and public transport using the initial model and the gap between the data analysis and the outcome of the initial model is considered to be the no trip section. Without comprehensive data to analyse the increase in cycling and public transport trips, it is hard to validate where the cars change to. The validation of the model similarly relies on a single case study, conducted at the same location as the calibration. This may reduce the robustness of the validation process.

A significant limitation concerns the long-term effects on congestion. The model is validated solely for the new equilibrium phases, offering no insights into traffic conditions two or three years after the road capacity reduction. Over time, the equilibrium may shift due to internal factors, such as drivers resuming car use and adapting to increased congestion. External factors, including population growth, spatial development and economic fluctuations, could also influence equilibrium and lead to differing congestion states.

The final limitation is the model's applicability, which is limited to road capacity reductions within and around the city centre. External-to-external trips are not affected by the model. Consequently, the effect of capacity reductions on motorways or at motorway junctions cannot be estimated with this model.

## 8.3. Final conclusions

This study has provided a comprehensive analysis of the phenomenon of disappearing traffic, the mechanisms underlying changes in travel behaviour following road capacity reductions and the performance of a predictive model designed to estimate these changes. The findings reveal that disappearing traffic occurs under specific conditions, primarily driven by travellers' adjustments to minimise friction in their journeys. Key condition is that congestion in the surrounding area increases if individuals do not adapt their behaviour. These findings emphasise the context-dependent nature of disappearing traffic and the importance of considering local traffic dynamics and behavioural patterns when planning interventions. The data analysis further reveals a noticeable reduction in car usage, with evidence that individuals have persistently adjusted their behaviour in response to these changes.

The predictive model developed in this study captures the iterative process of traffic stabilisation and the reallocation of mobility distribution. Its application to case studies, such as the Roseknoop roadworks in Rotterdam, demonstrates its ability to replicate traffic congestion patterns and reductions in car trips, offering valuable insights despite data limitations. The model effectively predicts shifts away from car usage for shorter trips and an increasing likelihood of behavioural adaptations—such as changes in departure times or destinations—for medium to long trips.

Overall, the study highlights the value of integrating dynamic traffic simulations with the recalculation of mobility distribution to estimate a new equilibrium in traffic congestion and car usage following road interventions. The data analysis and model indicate that, after the adaptation period, the impact on traffic congestion is limited. This indicates that, despite its limitations, traffic often behaves like a self-regulating system, adjusting to variations in demand and conditions. Despite a slight increase in overall travel time and congestion, it ultimately restores congestion to its typical levels. These findings provide valuable insights for the development of low-car urban environments.

## 8.4. Implications for science

This study contributes to the scientific understanding of changing travel behaviour in response to road capacity reductions, with the goal of achieving a low-car city. By integrating traffic simulation, convergence analysis, and traffic demand recalculation into a three-step framework, it provides a replicable approach for addressing dynamic travel behaviour under changing road network conditions. The findings reveal distinct behavioural responses to road capacity reductions. Shorter trips demonstrate a higher tendency to shift towards cycling and public transport, whereas longer trips show limited modal changes. Instead, these trips often result in adjustments to departure times, destinations or trip frequencies. This contrast improves the understanding of how travel behaviours vary with trip length. Furthermore, the case study revealed that, following road works, traffic volumes remained low, suggesting that individuals adapted to new travel behaviours, which subsequently became habitual, reducing their reliance on car usage.

This research offers potential to open up new directions for investigation into travel behaviour and traffic management. The implications resulting this study can be grouped in two categories; further exploration of the predictive model itself and research into the behavioural findings derived from the model.

Regarding the predictive model, the no trip alternative currently aggregates four aspects: changing departure time, destination and trip frequency. Ideally, these should be separated into distinct categories, particularly focusing on trip frequency reduction as separate alternative. Limited research exists on the value individuals place on different trip types. The increased occurrence of remote working, accelerated by the COVID-19 pandemic, could significantly influence mobility patterns and the distribution of travel demand. More information, for example by stated preference data, should be gathered regarding the value of not undertaking a particular trip before it can be integrated into this model.

Placing this model within a broader context, a key question arises: how can traffic demand models in general effectively incorporate the impacts of road capacity reductions? Current traffic models often lack sufficient flexibility in their traffic demand functions to respond to incremental increases in travel time. Future research should examine the effects of road capacity reductions across cities with varying urban forms, cultural attitudes towards travel behaviour, and policy priorities. Furthermore, it is essential to investigate how socio-economic factors and trip purposes influence traveller choices, providing insights

for more adaptive traffic models. These two aspects are the first two steps in incorporating this into models.

Turning to the findings derived from the model, further exploration is needed into the psychological barriers that prevent individuals from switching to alternative modes for longer trips. Is it preferable to encourage these travellers to maintain their current trips while switching modes, rather than altering their destination, departure time or trip frequency? In addition to this question, are shorter trips more likely to shift modes due to the quality and availability of cycling and public transport infrastructure, or is trip length the primary determinant? Comparative studies across cities with differing levels of infrastructure investment could investigate this. Additionally, the effects of combined interventions, such as reducing road capacity while simultaneously investing in cycling paths and public transport, need further examination. Similarly, the role of shared mobility options in shaping responses to road capacity reductions presents an interesting area for investigation.

Finally, the findings of this thesis offer a foundation for exploring the equity dimensions of travel behaviour. Do individuals from different demographic groups respond similarly to road capacity reductions or are certain groups disproportionately affected? This line of inquiry could contribute to the development of more inclusive and equitable urban mobility policies, ensuring that the benefits of sustainable transport systems are accessible to all.

## 8.5. Implications for practice

The model developed in this research provides policymakers with a valuable tool to estimate the effects of road narrowing projects for the municipality of Rotterdam and other municipalities in the Netherlands. Specifically, it allows for an accurate prediction of the new traffic equilibrium when road capacity is reduced. Unlike approaches that rely on predefined reduction factors for specific road links, this model directly calculates the new equilibrium and estimates the number of car trips that need to be reduced to avoid excessive congestion. By using these insights, municipalities can identify the percentage of car trips that should ideally be reduced before the start of the capacity reduction. Combining this with clear and early communication with road users, can shorten the adaptation period and mitigate significant congestion during the initial phase of implementation. Additionally, the model highlights locations where increased congestion may occur in the new equilibrium, enabling targeted traffic management interventions.

Furthermore, the observed lasting behavioural changes after capacity was restored suggest an additional opportunity for municipalities. By using these insights, policymakers can explore strategies to maintain and support these shifts, potentially promoting a broader transition to sustainable travel behaviours.

Finally, the study underscores the importance of integrating capacity reduction measures with improvements to alternative travel modes, such as cycling and public transport. The findings reveal that specifically shorter trips are likely to shift to these alternatives. This suggests that cities aiming to implement road capacity reductions should simultaneously invest in enhancing local cycling infrastructure and public transport network to encourage a shift in travel behaviour even more. Doing so can preserve overall accessibility, even as road capacity is reduced.

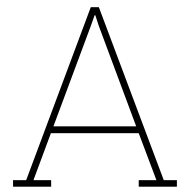
# Bibliography

- A. Ahmed and P. Stopher. Seventy minutes plus or minus 10 — a review of travel time budget studies. *Transport Reviews*, 34(5):607–625, 2014. doi: 10.1080/01441647.2014.946460. URL <https://doi.org/10.1080/01441647.2014.946460>.
- N. Bode, S. Buchel, G. Diercks, M. Lodder, D. Looibach, I. Notermans, R. van Raak, and C. Roorda. Staat van transitie: Dynamiek in mobiliteit, klimaatadaptatie en circulaire economie. Technical report, Dutch Reaserach Institute for Sustainability Transitions, 2019.
- S. Cairns, S. Atkins, and P. Goodwin. Disappearing traffic? the story so far. *Municipal Engineer 151*, 1: 13–22, 2002.
- S. Calvert, M. Minderhoud, H. Taale, I. Wilmink, and V.L. Knoop. Traffic assignment and simulation models. state-of-the-art background document, 2016.
- J. Chung, K.Y. Hwang, and Y.K. Bae. The loss of road capacity and self-compliance: Lessons from the cheonggyecheon stream restoration. *Transport Policy*, 21:165–178, 2012. ISSN 0967-070X. doi: <https://doi.org/10.1016/j.tranpol.2012.01.009>. URL <https://www.sciencedirect.com/science/article/pii/S0967070X12000108>.
- M. Cingel, J. Čelko, and M. Drličiak. Analysis in modal split. *Transportation Research Procedia*, 40: 178–185, 2019. ISSN 2352-1465. doi: <https://doi.org/10.1016/j.trpro.2019.07.028>. URL <https://www.sciencedirect.com/science/article/pii/S2352146519301899>. TRANSCOM 2019 13th International Scientific Conference on Sustainable, Modern and Safe Transport.
- Y. Claassen, E. Augustijn, N. van den Brink, and J. Feld. Potentie gedragsverandering bij werkzaamheden rondom amsterdam. Technical report, Amsterdam Bereikbaar, 2024.
- K. J. Clifton and F. Moura. Conceptual framework for understanding latent demand: Accounting for unrealized activities and travel. *Transportation Research Record*, 2668(1):78–83, 2017. doi: 10.3141/2668-08. URL <https://doi.org/10.3141/2668-08>.
- A. de Jong, S. te Riele, C. Huisman, C. van Duin, T. Husby, and L. Stoeldraijer. Regionale bevolkings- en huishoudensprognose 2022-2050 - steden en randgemeenten groeien verder, 2022.
- F. de Jong. Technische rapportage dynamisch model rotterdam. Technical report, Gemeente Rotterdam, 2021. Internal report.
- F. M. Dekking, C. Kraaikamp, H. P. Lopuhaä, and L.E. Meester. *A Modern Introduction to Probability and Statistics*. Springer, Delft, The Netherlands, 2005.
- F. Dunkerley, B. Whittaker, J. Laird, and A. Daly. Latest evidence on induced travel demand: An evidence review, May 2018. Project No.: 1-396, Report No.: 1.2, File Ref.: 70038415.
- Antonella Ferrara, Simona Sacone, and Silvia Siri. *Microscopic and Mesoscopic Traffic Models*, pages 113–143. Springer International Publishing, Cham, 2018. ISBN 978-3-319-75961-6. doi: 10.1007/978-3-319-75961-6\_5. URL [https://doi.org/10.1007/978-3-319-75961-6\\_5](https://doi.org/10.1007/978-3-319-75961-6_5).
- Gemeente Amsterdam. Onderzoeksrapport pilot weesperstraat. Technical report, 2024.
- Gemeente Rotterdam. Rapportage stedelijke bereikbaarheid. Technical report, Gemeente Rotterdam, 2018.
- Gemeente Rotterdam. Roseknoop, 2024a. URL <https://www.rotterdam.nl/roseknoop>.
- Gemeente Rotterdam. Hofplein, 2024b. URL <https://www.rotterdam.nl/hofplein>.



- Gemeente Rotterdam. Traffic flow data of traffic lights (yavc), 2024c.
- Gemeente Rotterdam. Stadsprojecten, 2024d. URL <https://www.rotterdam.nl/stadsprojecten>.
- L. Harms. Mobiel in de tijd: op weg naar een auto-afhankelijke maatschappij, 1975-2000. Technical report, Sociaal en Cultureel Planbureau, 2003.
- HealthEffectsInstitute. Traffic-related air pollution: A critical review of the literature on emissions, exposure, and health effects. 2010.
- D. A. Hensher, E. Wei, and W. Liu. Accounting for the spatial incidence of working from home in an integrated transport and land model system. *Transportation Research Part A: Policy and Practice*, 173:103703, 2023. ISSN 0965-8564. doi: <https://doi.org/10.1016/j.tra.2023.103703>. URL <https://www.sciencedirect.com/science/article/pii/S0965856423001234>.
- P. Jorritsma, K. Arendsen, and R. Faber. Autoluw beleid gemeenten: doelen, effecten en rollen. Technical report, Kennisinstituut voor Mobiliteitsbeleid (KiM), 2023.
- D. B. Lee, L. A. Klein, and G. Camus. Induced traffic and induced demand. *Transportation Research Record*, 1659(1):68–75, 1999. doi: [10.3141/1659-09](https://doi.org/10.3141/1659-09). URL <https://doi.org/10.3141/1659-09>.
- B. Van Liere, O. Beens, and A. Knol. Van wie is de stad? Technical report, Mileudefensie, 2017.
- T. Litman. Generated traffic and induced travel: Implications for transport planning. Technical report, Victoria Transport Policy Institute, 2017.
- S. Melia and T. Calvert. Does traffic really disappear when roads are closed? *Proceedings of the Institution of Civil Engineers - Municipal Engineer*, 176(1):1–9, 2023. doi: [10.1680/jmuen.21.00014](https://doi.org/10.1680/jmuen.21.00014). URL <https://doi.org/10.1680/jmuen.21.00014>.
- Giuliano Mingardo. Parking: an international perspective. chapter 8 - rotterdam, the netherlands. In Dorina Pojani, Jonathan Corcoran, Neil Sipe, Iderlina Mateo-Babiano, and Dominic Stead, editors, *Parking*, pages 133–145. Elsevier, 2020. ISBN 978-0-12-815265-2. doi: <https://doi.org/10.1016/B978-0-12-815265-2.00008-X>. URL <https://www.sciencedirect.com/science/article/pii/B978012815265200008X>.
- NDW. Nationaal dataportaal wegverkeer dexter, 2024. URL <https://dexter.ndw.nu>.
- S. Nello-Deakin. Exploring traffic evaporation: Findings from tactical urbanism interventions in barcelona. *Case Studies on Transport Policy*, 10(4):2430–2442, 2022. ISSN 2213-624X. doi: <https://doi.org/10.1016/j.cstp.2022.11.003>. URL <https://www.sciencedirect.com/science/article/pii/S2213624X22002085>.
- M. J. Nieuwenhuijsen, H. Khreis, E. Verlinghieri, and D. Rojas-Rueda. Transport and health: A marriage of convenience or an absolute necessity. *Environment International*, 88:150–152, 2016. ISSN 0160-4120. doi: <https://doi.org/10.1016/j.envint.2015.12.030>. URL <https://www.sciencedirect.com/science/article/pii/S0160412015301343>.
- Openstreetmap. Openstreetmap, 2024. URL <https://www.openstreetmap.org>.
- RET. Ret vervoerplan 2025, 2024.
- C.J. Rodier, J.E. Abraham, R.A. Johnston, and J.D. Hunt. Anatomy of induced travel using an integrated land use and transportation model in the sacramento region. In *80th Annual Meeting of the Transportation Research Board, Washington, DC*, volume 6, page 7, 2001.
- J.P. Rodrigue. *The Geography of Transport Systems*. Routledge, 6th ed. edition, 2024. doi: <https://doi.org/10.4324/9781003343196>.
- S. Schoorlemmer, F. de Vries, L. Witte, and J. van der Toorn. Verkeersmodel v-mrdh 3.0. Technical report, Goudappel, 2021. Internal report.
- M. Snelder and M. van der Tuin. Innovaties groeimodel. Technical report, TNO, 2023.

- J. Speck. *Understand Induced Demand*, pages 64–65. Island Press/Center for Resource Economics, Washington, DC, 2018. ISBN 978-1-61091-899-2. doi: 10.5822/978-1-61091-899-2\_27. URL [https://doi.org/10.5822/978-1-61091-899-2\\_27](https://doi.org/10.5822/978-1-61091-899-2_27).
- B. Srinivasan and D. Bonvin. Convergence analysis of iterative identification and optimization schemes. In *Proceedings of the 2003 American Control Conference, 2003.*, volume 3, pages 1956–1960 vol.3, 2003. doi: 10.1109/ACC.2003.1243360.
- Tennoy, E. Caspersen, and O. Hagen et al. Effects and consequences of capacity reduction in the smestad tunnel. Technical report, Institute of Transport Economics, 2020.
- A. Tennøy and O. Hagen. Reallocation of road and street space in oslo: Measures for zero growth in urban traffic. *OECD Publishing*, 14, 2020. doi: <https://doi.org/10.1787/6d7e9f43-en>.
- TomTom. Tomtom move, 2024. URL <https://move.tomtom.com>.
- T. Vonk, S. Talen, and F. Pierik. Herinrichtingsprojecten en verdwijnend verkeer. Technical report, TNO, 2024.
- Ronald E. Walpole, Raymond H. Myers, Sharon L. Myers, and Keying Ye. *Probability and Statistics for Engineers and Scientists*. Pearson, Boston, 9th edition, 2011.
- Fred Wegman, Fan Zhang, and Atze Dijkstra. How to make more cycling good for road safety? *Accident Analysis Prevention*, 44(1):19–29, 2012. ISSN 0001-4575. doi: <https://doi.org/10.1016/j.aap.2010.11.010>. URL <https://www.sciencedirect.com/science/article/pii/S0001457510003416>. Safety and Mobility of Vulnerable Road Users: Pedestrians, Bicyclists, and Motorcyclists.
- T. Zijlstra, J. Witte, and S. Bakker. De maatschappelijke effecten van het wijdverbreide autobezit in nederland (achtergrondrapport). Technical report, Kennisinstituut voor Mobiliteitsbeleid, 2022.



# Code DiTra model

Below, the iterative process of the python code is shown.

## A.1. Main code DiTra model

```
1 #!/usr/bin/env python
2 # coding: utf-8
3
4 # # DIsappearing TRAffic model (DiTra)
5
6 # Welcome to the DiTra model python file. This file can be used to run the model. Please read
   the manual before starting the DiTra model. \
7 # This file is built up in the following way:\
8 #     0. Loading packages \
9 #     1. Setting filepaths and simulation configurations \
10 #     2. Loading necessary data \
11 #     3. Running simulation
12 #
13 # You are only suppose to make changes in Chapter 1. (Setting filepaths and simulation
   configurations) and Section 2.2 (Loading affected OD pairs)
14
15 # ## 0. Loading packages
16
17 # The following cell loads the required data packages. Do not make changes. In case of errors
   , please install the packages.
18
19 # In[1]:
20
21
22 import subprocess
23 import sqlite3
24 import time
25 import pandas as pd
26 import numpy as np
27 from scipy import stats
28 import matplotlib.pyplot as plt
29 from matplotlib.colors import LinearSegmentedColormap
30 from matplotlib.legend_handler import HandlerPathCollection
31 import DiTraFunctions as dtr
32
33
34 # ## 1. Setting filepaths and simulation configurations
35
36 # In the following cell, the filepaths and simulation configurations are set. **Change the
   names to the correct paths and change the configuration names**. Keep the format (like r
   'C:\) equal as the original settings.
37
38 # In[2]:
39
40
```

```

41 # Define the path to the batch.exe file. This is the path to the map where you installed
    Params and then select the batch.exe file
42 batch_exe_path = r"C:\Program Files(x86)\Paramics\Microsimulation\Paramics\Discovery\
    24.0.6\bin\batch.exe"
43
44 # Select the path to where you stored the model file (both base and intervention file).
45 model_path_base = r"C:\Users\Sande\Paramics\Basis_model\Rotterdam.params" # the
    model without intervention (normal Rotterdam case)
46 model_path_intervention = r"C:\Users\Sande\Paramics\Roseknoop\phase1\full_simulation\1\
    Rotterdam_werkRoseknoopfase1.params" # the model with road capacity intervention
47
48 # Define file path where output is stored and run name (Do not add the '\log' here!)
49 output_file_base = r"C:\Users\Sande\Paramics\Basis_model"
50 output_file_intervention = r"C:\Users\Sande\Paramics\Roseknoop\phase1\full_simulation\1"
51
52 # Select the run configuration which you want to simulate: Open the intervention model RODY
    in params. The first run configuration in the list in the simulation tab corresponds to
    the value 1. The second run configuration to the value 2 etc.
53 run_config_id = 1
54
55 # Define the run configuration name. This name should be fully identical to the Prefix name
    in the simulation tab
56 run_config_name_base = 'AS_BASE_DEF_4'
57
58 # Define a run configuration name for the intervention output files
59 run_config_name_intervention = 'ERH_Phase1_final'
60
61
62 # **Optional: change PT travel time for directly affected OD pairs**
63
64 # In[3]:
65
66
67 increase_traveltime_PT = False # Set to True if you want to change the travel time for PT
    trips for directly affected OD pairs
68 TT_PT_increase = 8 # min
69
70
71 # **Optional: reduce initial traffic demand**
72
73 # In[4]:
74
75
76 # Recommended if a large capacity reduction is introduced and risk of gridlock arises
77 reduce_initial_od_matrix = False # Set this value to True if you want to reduce the initial
    traffic demand
78 reduction_directly_affected = 10 # [%] #Select the starting reduction of the DIRECTLY
    affected OD pairs (as percentage)
79
80
81 # # 2. Loading necessary data
82
83 # **2.1 Setting parameters and making empty simulation output lists**
84
85 # This cell sets the parameter values and makes output lists. Do not change.
86
87 # In[5]:
88
89
90 # Coefficients for utility functions (made up for now)
91 ASC = {'car' : 0, 'bike' : 0.2501, 'PT' : -0.8451, 'no_trip'
    : - 4.0132}
92
93 beta = {'car' : -0.0513, 'bike' : -0.0703, 'PT' : -0.0331, 'no_trip' : 0.1640,
    'no_trip2' : -0.002033, 'no_trip3' : 0.93614, 'no_trip4' : 0.00005126}
94
95 # Set the number of parallel RODY runs
96 runCount = 6
97
98 # Set the maximum number of iterations

```

```

99 num_iterations = 6
100
101 # Set the threshold for the p-value of the KS-test
102 threshold_directly = 0.0252
103
104 # Storing lists of values affected travel times (x) and corresponding cdf level (y) for
    directly and all affected od pairs respectively
105 x_cdf_directly = []
106 y_cdf_directly = []
107 x_cdf_indirectly = []
108 y_cdf_indirectly = []
109
110 # Storing lists of KS indicator per iteration
111 KS_iter_directly = []
112 KS_iter_indirectly = []
113 KS_base_directly = []
114 KS_base_indirectly = []
115
116 # Storing list of the number of cars that have disappeared
117 disappeared_cars = []
118
119 # Storing iterative OD split matrices
120 od_split_car_3d = []
121 od_split_bike_3d = []
122 od_split_pt_3d = []
123 od_split_notrip_3d = []
124
125
126 # **2.2 Loading affected OD pairs**
127
128 # The following two cells can be used to load the affected OD pair information. **Change file
    paths**
129
130 # In[6]:
131
132
133 # File paths to directly and all affected OD pairs. Change to correct paths
134 path_directly_affected = 'Data/Affected_OD_pairs/directly_affected_od_phase_1_od_trip_matrix.
    csv'
135 path_all_affected = 'Data/Affected_OD_pairs/total_affected_od_phase_1_od_trip_matrix.csv'
136
137 # Loading information of directly affected OD pairs
138 od_affected_directly, od_affected_directly_values = dtr.affected_od_pairs(
    path_directly_affected)
139
140 # Loading information of indirectly affected OD pairs
141 od_affected_all, od_affected_all_values = dtr.affected_od_pairs(path_all_affected)
142
143 # Setting the indirectly affected OD pairs
144 od_affected_indirectly = np.logical_and(od_affected_all, np.logical_not(od_affected_directly)
    )
145
146
147 # Optional: if you did not manage to load all affected OD pairs in one run, you can use the
    cell below to load them over different runs.
148
149 # In[7]:
150
151
152 # od_affected_all1, od_affected_all_values = affected_od_pairs('Data/total_affected_od_phase2
    od_trip_matrix.csv')
153 # od_affected_all1, od_affected_all_values = affected_od_pairs('Data/
    total_affected_od_phase2_1_od_trip_matrix.csv')
154 # od_affected_all2, od_affected_all_values = affected_od_pairs('Data/
    total_affected_od_phase2_2_od_trip_matrix.csv')
155 # od_affected_all3, od_affected_all_values = affected_od_pairs('Data/
    total_affected_od_phase2_3_od_trip_matrix.csv')
156 # od_affected_all4, od_affected_all_values = affected_od_pairs('Data/
    total_affected_od_phase2_4_od_trip_matrix.csv')
157

```

```

158 # od_affected_all = od_affected_all1 | od_affected_all2 | od_affected_all3 | od_affected_all4
    | od_affected_directly
159 # od_affected_indirectly = np.logical_and(od_affected_all, np.logical_not(
    od_affected_directly))
160
161
162 # **2.3 Loading od matrices and resistance matrices**
163
164 # The cell below loads all information required for the simulation. Do not change.
165
166 # In[8]:
167
168
169 # Load coppling V-MRDH to RODY
170 internal_zones, external_zones, copple_extern = dtr.load_coppling_extern_intern()
171
172 # Loading the original car matrix with internal RODY zones and external VMRDH zones (6101
    x6101 matrix)
173 od_car_original_vmrhdh = pd.read_csv('Data/OD_matrices/
    original_od_matrix_with_external_vmrhdh_zones.csv', index_col = 0) # 6101 x 6101 matrix
174 od_car_original_vmrhdh.columns = od_car_original_vmrhdh.index
175
176 # Loading resistance matrices
177 od_distance_car, od_time_original_vmrhdh, od_time_bike_vmrhdh, od_time_pt_vmrhdh,
    od_utility_car_original, od_utility_bike, od_utility_pt, od_split_car_original,
    od_split_bike_original, od_split_pt_original, od_bike_original_vmrhdh,
    od_pt_original_vmrhdh, od_total_original, od_split_notrip_original = dtr.
    loading_resistance_and_utility_matrices(ASC, beta, od_split_car_3d, od_split_bike_3d,
    od_split_pt_3d, od_split_notrip_3d, od_car_original_vmrhdh, TT_PT_increase,
    increase_traveltime_PT, copple_extern, internal_zones, external_zones,
    od_affected_directly)
178 od_time_original_vmrhdh.columns = od_time_original_vmrhdh.index
179
180 # Load the OD matrices which are not adjusted (na) (direct values from the 2h rush hour VMRDH
    model)
181 od_car_original_vmrhdh_na = pd.read_csv('Data/OD_matrices/od_matrix_with_external_vmrhdh_zones
    _na(not_adjusted).csv', index_col = 0) # 6101 x 6101 matrix
182 od_car_original_vmrhdh_na.columns = od_car_original_vmrhdh_na.index
183
184 od_bike_original_vmrhdh_na = pd.read_csv('Data/OD_matrices/
    od_matrix_bike_with_external_vmrhdh_zones_na(not_adjusted).csv', index_col = 0) # 6101 x
    6101 matrix
185 od_bike_original_vmrhdh_na.columns = od_bike_original_vmrhdh_na.index
186
187 od_pt_original_vmrhdh_na = pd.read_csv('Data/OD_matrices/
    od_matrix_pt_with_external_vmrhdh_zones_na(not_adjusted).csv', index_col = 0) # 6101 x 6101
    matrix
188 od_pt_original_vmrhdh_na.columns = od_pt_original_vmrhdh_na.index
189
190 # Calculate the modal split based on the not adjusted VMRDH 2h rush hour
191 od_split_car_original_vmrhdh = od_car_original_vmrhdh_na / (od_pt_original_vmrhdh_na +
    od_car_original_vmrhdh_na + od_bike_original_vmrhdh_na)
192 od_split_pt_original_vmrhdh = od_pt_original_vmrhdh_na / (od_pt_original_vmrhdh_na +
    od_car_original_vmrhdh_na + od_bike_original_vmrhdh_na)
193 od_split_bike_original_vmrhdh = od_bike_original_vmrhdh_na / (od_pt_original_vmrhdh_na +
    od_car_original_vmrhdh_na + od_bike_original_vmrhdh_na)
194 # Calculate the total number of trips (car, bike and pt) per od pair in the 4h RODY rush hour
    based on the modal split
195
196
197 # Retrieve the original OD matrices from paramics model
198 zone_id, od_car_original = dtr.loading_od_matrix_original(model_path_base)
199
200 # Loading ratios of main highway and parallel lane
201 ratio_330_331 = od_car_original.loc[:, 330] / (od_car_original.loc[:, 330] + od_car_original
    .loc[:, 331])
202 ratio_329_328 = od_car_original.loc[329, :] / (od_car_original.loc[329, :] + od_car_original
    .loc[328, :])
203 ratio_270_269 = od_car_original.loc[270, :] / (od_car_original.loc[270, :] + od_car_original
    .loc[269, :])
204

```

```

205 # Setting the original matrices as iterative matrices (these will be updated; for 1st
    iteration the original matrix will be used)
206 od_car_iterative = od_car_original.copy(deep=True)
207 od_car_iterative_vmrhdh = od_car_original_vmrhdh.copy(deep=True)
208 od_time_iterative_vmrhdh = od_time_original_vmrhdh.copy(deep=True)
209
210 # Adding the initial value for disappeared cars
211 if reduce_initial_od_matrix == False:
212     disappeared_cars.append(0)
213 if reduce_initial_od_matrix == True:
214     # Calculate the new OD matrix
215     od_car_reduced = dtr.reducing_od_matrix_start(od_car_original,
        reduction_directly_affected, od_affected_directly)
216     # Add to disappeared cars list
217     disappeared_cars.append(od_car_reduced.sum().sum() - od_car_original.sum().sum())
218     # Calculate the new OD split matrix
219     od_split_car_0 = od_car_reduced / od_total_original
220     # Update the reduced OD matrix in the Paramics model
221     #dtr.update_od_matrix_in_model(od_affected_all, od_matrix_new, zone_id,
        model_path_intervention)
222
223
224 # # 3. Running simulation
225
226 # In the following cells, the DiTra model is started. The first cell loads the information
    from the base run. The second cell starts the iterative process of traffic simulation and
    recalculation of the OD matrix. Do not make changes.
227
228 # In[9]:
229
230
231 # Loading the travel time matrix for the base run (normal Rotterdam model)
232 od_time_baserun = dtr.od_travel_times_sim(output_file_base, run_config_name_base, 99)
233
234 # Computing the first results of the congestion indicator
235 dtr.congestion_indicator(od_affected_directly, od_affected_all, od_time_baserun,
    x_cdf_directly, y_cdf_directly, x_cdf_indirectly, y_cdf_indirectly, KS_iter_directly,
    KS_iter_indirectly, KS_base_directly, KS_base_indirectly)
236
237
238 # In[10]:
239
240
241 # Main loop to run simulations and update OD matrix
242 num_iterations = 6
243 for iteration in range(1, num_iterations):
244     if iteration == 1:
245         print(f"Starting iteration 1: original OD matrix applied to the model with the
            capacity intervention")
246     else:
247         print(f"Starting iteration {iteration}")
248     print('')
249
250     # Start the traffic assignment simulation
251     #dtr.run_all_simulations(batch_exe_path, runCount, output_file_intervention,
        run_config_name_intervention, iteration, model_path_intervention)
252
253     # Retrieve OD travel time matrix for car trips from simulation
254     od_time_iterative_sim = dtr.od_travel_times_sim(output_file_intervention,
        run_config_name_intervention, iteration)
255
256     # Calculate congestion indicator based on the travel times of last simulation
257     dtr.congestion_indicator(od_affected_directly, od_affected_all, od_time_iterative_sim,
        x_cdf_directly, y_cdf_directly, x_cdf_indirectly, y_cdf_indirectly, KS_iter_directly,
        KS_iter_indirectly, KS_base_directly, KS_base_indirectly)
258
259     # Plot the congestion indicator output
260     dtr.plot_cdf_and_KS(x_cdf_directly, y_cdf_directly, x_cdf_indirectly, y_cdf_indirectly,
        KS_iter_directly, KS_iter_indirectly, KS_base_directly, KS_base_indirectly,
        disappeared_cars, threshold_directly)
261     plt.show()

```



```

262
263 # Check if new iteration is required
264 if (len(KS_iter_directly) == 0):
265     if KS_base_directly[0][0] < threshold_directly:
266         print(f'KS_value_between_base_and_iteration_is_{KS_base_directly[0][0]:.3f}_(
                lower_than_the_threshold_of_{threshold_directly})')
267         print('This means that the travel times through the area has not changed
                significantly. The intervention has not increased the
                congestion. No significant change in behaviour will occur.')
268         break
269     else:
270         print(f'KS_value_between_base_and_iteration_1_is_{KS_base_directly[0][0]:.3f}_(
                higher_than_the_threshold_of_{threshold_directly})')
271         print('The travel times are significantly changed due to the intervention.
                People will start adapting their behaviour.')
272         print('The OD matrix will be recalculated and a new iteration will start.')
273
274 else:
275     if KS_iter_directly[-1][0] < threshold_directly:
276         print(f'KS_value_{KS_iter_directly[-1][0]:.3f}<_{threshold_directly}.')
277         print('New equilibrium has found! Iteration will stop. The OD matrix will be
                recalculated for final results.')
278         # Recalculate OD matrix
279         od_split_car, od_car_iterative_vmrhdh, od_utility_car, od_bike_new_vmrhdh,
                od_pt_new_vmrhdh, od_notrip_new_vmrhdh, od_time_iterative_vmrhdh = dtr.
                recalculating_od_matrix(od_car_original_vmrhdh, od_car_iterative_vmrhdh,
                od_total_original, od_time_original_vmrhdh, od_time_baserun,
                od_time_iterative_sim, ASC, beta, od_affected_all, od_utility_car_original,
                od_utility_bike, od_utility_pt, od_split_bike_original, od_split_pt_original,
                od_split_car_3d, od_split_bike_3d, od_split_pt_3d, od_split_notrip_3d,
                internal_zones, external_zones, copples_extrn, od_time_iterative_vmrhdh,
                od_distance_car, disappeared_cars)
280         od_matrix_new = dtr.aggregate_od_matrix(od_car_iterative_vmrhdh, od_car_original,
                internal_zones, external_zones, copples_extrn, ratio_330_331, ratio_329_328,
                ratio_270_269)
281         print('-----')
282         print(f'Final result in change in travel behaviour:')
283         print('')
284         print(f'Total reduction of {(od_car_original.sum().sum() - od_matrix_new.sum().sum()
                ):.00f} car trips (compared to base scenario)')
285         print('')
286         print(f'Reduction of {(od_car_original[od_affected_directly].sum().sum() -
                od_matrix_new[od_affected_directly].sum().sum()):.0f} car trips directly
                hindered {(od_car_original[od_affected_directly].sum().sum() - od_matrix_new
                [od_affected_directly].sum().sum()) / od_car_original[od_affected_directly].sum()
                (.sum() * 100:.02f)}% of all directly hindered trips in evening rush hour')
287         print(f'Reduction of {(od_car_original[od_affected_indirectly].sum().sum() -
                od_matrix_new[od_affected_indirectly].sum().sum()):.0f} car trips indirectly
                hindered {(od_car_original[od_affected_indirectly].sum().sum() -
                od_matrix_new[od_affected_indirectly].sum().sum()) / od_car_original[
                od_affected_indirectly].sum().sum() * 100:.02f}% of all indirectly hindered
                trips in evening rush hour')
288         print('')
289         print(f'This is a reduction of {(od_car_original.sum().sum() - od_matrix_new.sum()
                .sum()) / od_car_original[od_affected_directly].sum().sum() * 100:.02f}% of car
                trips going over intervening road')
290         print('')
291         print(f'{od_bike_new_vmrhdh.sum().sum() - od_bike_original_vmrhdh.sum().sum():.00f}
                people shifted to bike')
292         print(f'{od_pt_new_vmrhdh.sum().sum() - od_pt_original_vmrhdh.sum().sum():.00f}
                people shifted to pt')
293         print(f'{od_notrip_new_vmrhdh.sum().sum():.00f} people moved away from Roseknoop
                area in evening rush hour')
294         break
295     else:
296         print(f'KS_value_{KS_iter_directly[-1][0]:.3f}>_{threshold_directly}.')
297         print(f'The simulation has not reached a new equilibrium. The OD matrix will be
                recalculated and iteration_{iteration} will start.')
298
299 print('')
300

```

```

301 # Recalculate OD matrix
302 od_split_car, od_car_iterative_vmrhdh, od_utility_car, od_bike_new_vmrhdh, od_pt_new_vmrhdh,
    od_notrip_new_vmrhdh, od_time_iterative_vmrhdh = dtr.recalculating_od_matrix(
    od_car_original_vmrhdh, od_car_iterative_vmrhdh, od_total_original,
    od_time_original_vmrhdh, od_time_baserun, od_time_iterative_sim, ASC, beta,
    od_affected_all, od_utility_car_original, od_utility_bike, od_utility_pt,
    od_split_bike_original, od_split_pt_original, od_split_car_3d, od_split_bike_3d,
    od_split_pt_3d, od_split_notrip_3d, internal_zones, external_zones, copple_extern,
    od_time_iterative_vmrhdh, od_distance_car, disappeared_cars)
303
304 # Aggregate the new 6101x6101 OD matrix to RODY format (371x371)
305 od_matrix_new = dtr.aggregate_od_matrix(od_car_iterative_vmrhdh, od_car_original,
    internal_zones, external_zones, copple_extern, ratio_330_331, ratio_329_328,
    ratio_270_269)
306
307 print(f'Next simulation will have {od_matrix_new.sum().sum():.0f} car trips')
308 print(f'Total reduction of {od_car_original.sum().sum()-od_matrix_new.sum().sum():.00f}
    car trips (compared to base scenario)')
309 print('')
310 print(f'Reduction of {(od_car_original[od_affected_directly].sum().sum()-od_matrix_new[
    od_affected_directly].sum().sum()):.0f} car trips directly hindered ({(
    od_car_original[od_affected_directly].sum().sum()-od_matrix_new[
    od_affected_directly].sum().sum())/od_car_original[od_affected_directly].sum().sum()
    *100:.02f}% of all directly hindered trips in evening rush hour)')
311 print(f'Reduction of {(od_car_original[od_affected_indirectly].sum().sum()-od_matrix_new[
    od_affected_indirectly].sum().sum()):.0f} car trips indirectly hindered
    ({(od_car_original[od_affected_indirectly].sum().sum()-od_matrix_new[
    od_affected_indirectly].sum().sum())/od_car_original[od_affected_indirectly].sum().
    sum()*100:.02f}% of all indirectly hindered trips in evening rush hour)')
312 print('')
313 print(f'This is a reduction of {(od_car_original.sum().sum()-od_matrix_new.sum().sum())
    /od_car_original[od_affected_directly].sum().sum()*100:.02f}% of car trips going over
    intervening road')
314 print('')
315 print(f'{od_bike_new_vmrhdh.sum().sum()-od_bike_original_vmrhdh.sum().sum():.00f} people
    shifted to bike')
316 print(f'{od_pt_new_vmrhdh.sum().sum()-od_pt_original_vmrhdh.sum().sum():.00f} people
    shifted to pt')
317 print(f'{od_notrip_new_vmrhdh.sum().sum():.00f} people moved away from Roseknop area in
    evening rush hour')
318
319 # Update the OD matrix in the .paramics intervention file
320 #dtr.update_od_matrix_in_model(od_affected_all, od_matrix_new, zone_id,
    model_path_intervention)
321
322 print('')
323 print(f"Completed iteration {iteration}")
324 print('')
325 print('-----')
326 print('')
327 print("All iterations completed.")
328
329
330 # In[ ]:

```

## A.2. Code functions for DiTra model

```

1 import subprocess
2 import sqlite3
3 import time
4 import pandas as pd
5 import numpy as np
6 from scipy import stats
7 import matplotlib.pyplot as plt
8 from matplotlib.colors import LinearSegmentedColormap
9 from matplotlib.legend_handler import HandlerPathCollection
10
11
12 def loading_od_matrix_original(model_path_base):
13     """

```

```

14     Loads the original OD matrix from the base paramics model
15
16     Parameters:
17         model_path_base (string): text line to indicate where the paramics base model is
            stored
18
19     Returns:
20         zone_id (array)           : the id numbers paramics uses for the zones
21         od_car_original (DataFrame) : the original OD matrix for car trips applied in the
            base scenario
22
23     """
24     # Retrieve demandZones table from SQLite-database
25     conn = sqlite3.connect(model_path_base)          # Connect to the SQLite-database
26     query = "SELECT * FROM demandZones"             # Retrieve the demandZones table data
27     demand_zones = pd.read_sql_query(query, conn)    # Set demandZones table into dataframe
28     conn.close()                                    # close connection
29
30     # Retrieve SQLite-id for zones in the model
31     zone_id = demand_zones['originZoneId'].unique()
32
33     # Selecting Evening Peak demand
34     demand_zones_ep = demand_zones[(demand_zones['demandId'] == 4) & (demand_zones['matrixId'
        ] == 0)]
35
36     # Transforming demandZone table into Origin-Destination matrix and setting zone labels
37     od_car_original = demand_zones_ep.pivot_table(index='originZoneId', columns='destZoneId',
        values='demand', fill_value=0)
38     od_car_original = od_car_original.reindex(index=zone_id, columns=zone_id, fill_value=0)
39     od_car_original.index = np.arange(1, 372, 1)
40     od_car_original.columns = np.arange(1, 372, 1)
41
42     return zone_id, od_car_original
43
44
45
46
47 # Function to load the original resistance matrices for car and other modalities from the
    Resistance map (retrieved from V-MRDH)
48 def loading_resistance_and_utility_matrices(ASC, beta, od_split_car_3d, od_split_bike_3d,
    od_split_pt_3d, od_split_notrip_3d, od_car_original_vmrhd, TT_PT_increase,
    increase_traveltime_PT, copple_extern, internal_zones, external_zones,
    od_affected_directly):
49     """
50     Loads the original resistance matrices for car, bike and PT
51     and calculates the utility, model split and OD matrices for all alternatives
52
53     Parameters:
54         ASC (dictionary)           : dictionary with ASC values for alternatives
55         beta (dictionary)          : dictionary with beta values for alternatives
56         od_split_car_3d (list)     : OD split matrix for car for storing all iterations
57         od_split_bike_3d (list)    : OD split matrix for car for storing all iterations
58         od_split_pt_3d (list)     : OD split matrix for car for storing all iterations
59         od_split_notrip_3d (list) : OD split matrix for car for storing all iterations
60
61     Returns:
62         od_time_original_vmrhd (DataFrame): OD travel time matrix for car
63         od_distance_car (DataFrame):       OD car distance matrix
64         od_time_bike_vmrhd (DataFrame):    OD travel time matrix for bike
65         od_time_pt_vmrhd (DataFrame):      OD travel time matrix for PT
66         od_utility_car_original (DataFrame): OD utility matrix for car
67         od_utility_bike (DataFrame):       OD utility matrix for bike
68         od_utility_pt (DataFrame):         OD utility matrix for PT
69         od_split_car_original (DataFrame): OD split matrix for car
70         od_split_bike_original (DataFrame): OD split matrix for bike
71         od_split_pt_original (DataFrame):  OD split matrix for PT
72         od_total_original (DataFrame):     OD trip matrix for all alternatives
73         od_bike_original_vmrhd (DataFrame): OD trip matrix for bike
74         od_pt_original_vmrhd (DataFrame):  OD trip matrix for PT
75     """
76     # Loading original resistance matrices for car

```

```

77 od_time_original_vmrhdh = pd.read_csv('Data/Resistance_matrices/
78     od_time_car_rody_with_vmrhdh_zones.csv', delimiter=',', index_col= 0)
79 od_time_original_vmrhdh.columns = od_time_original_vmrhdh.columns.astype('int')
80
81 # Loading car distance matrix
82 od_distance_car = pd.read_csv('Data/Resistance_matrices/
83     od_distance_car_rody_with_vmrhdh_zones.csv', delimiter=',', index_col= 0)
84 od_distance_car.columns = od_distance_car.columns.astype('int')
85
86 # Loading original resistance matrix for bike
87 od_time_bike_vmrhdh = pd.read_csv('Data/Resistance_matrices/
88     od_time_bike_rody_with_vmrhdh_zones.csv', delimiter=',', index_col= 0)
89 od_time_bike_vmrhdh.columns = od_time_bike_vmrhdh.columns.astype('int')
90
91 # Loading original resistance matrix for public transport
92 od_time_pt_vmrhdh = pd.read_csv('Data/Resistance_matrices/
93     od_time_pt_rody_with_vmrhdh_zones.csv', delimiter=',', index_col= 0)
94 od_time_pt_vmrhdh.columns = od_time_pt_vmrhdh.columns.astype('int')
95
96 # Calculating original utility matrices
97 od_utility_car_original = ASC['car'] + beta['car'] * od_time_original_vmrhdh
98 od_utility_bike = ASC['bike'] + beta['bike'] * od_time_bike_vmrhdh
99 od_utility_pt = ASC['PT'] + beta['PT'] * od_time_pt_vmrhdh
100 # Calculating the original utility matrix for notrip (which is all -999)
101 delta_T = od_time_original_vmrhdh - od_time_original_vmrhdh
102 od_utility_notrip_original = np.where(delta_T < 0, -999,
103     ASC['no_trip'] + beta['no_trip'] * od_distance_car + beta['no_trip2'] *
104     od_distance_car**2 + \
105     beta['no_trip3'] * np.log(beta['no_trip4'] + delta_T / (
106     od_time_original_vmrhdh)))
107
108 # Calculate total utility
109 od_utility_total = np.exp(od_utility_car_original) + np.exp(od_utility_bike) + np.exp(
110     od_utility_pt)
111
112 # Calculate the updated utility (do not change this cell)
113 if increase_traveltime_PT == True:
114     od_utility_pt = change_PT_traveltime(od_time_pt_vmrhdh, od_affected_directly,
115     coplex_extern, internal_zones, external_zones, ASC, beta, TT_PT_increase)
116
117 # Calculating od_split_car based on utility functions
118 od_split_car_original = np.round(np.exp(od_utility_car_original) / od_utility_total
119     , decimals = 6)
120 od_split_bike_original = np.round(np.exp(od_utility_bike) / od_utility_total
121     , decimals = 6)
122 od_split_pt_original = np.round(np.exp(od_utility_pt) / od_utility_total
123     , decimals = 6)
124 od_split_notrip_original = np.round(np.exp(od_utility_notrip_original) / od_utility_total
125     , decimals = 2)
126
127 od_split_car_3d.append(od_split_car_original)
128 od_split_bike_3d.append(od_split_bike_original)
129 od_split_pt_3d.append(od_split_pt_original)
130 od_split_notrip_3d.append(od_split_notrip_original)
131
132 # Calculating original total matrix based on od_split_car_original
133 od_total_original = od_car_original_vmrhdh / od_split_car_original
134
135 # Calculating the original OD matrix for bike and PT
136 od_bike_original_vmrhdh = od_split_bike_original * od_total_original
137 od_pt_original_vmrhdh = od_split_pt_original * od_total_original
138 od_notrip_original_vmrhdh = od_split_notrip_original * od_total_original
139
140 return od_distance_car, od_time_original_vmrhdh, od_time_bike_vmrhdh, od_time_pt_vmrhdh,
141     od_utility_car_original, od_utility_bike, od_utility_pt, od_split_car_original,
142     od_split_bike_original, od_split_pt_original, od_bike_original_vmrhdh,
143     od_pt_original_vmrhdh, od_total_original, od_split_notrip_original
144
145 def affected_od_pairs(filepath_affected_od):
146     """

```

```

133     Loads the OD pair files which are affected by the road capacity intervention
134
135     Parameters:
136         filepath_affected_od (string): text line to indicate where the affected od pair file
            is stored
137
138     Returns:
139         od_affected_bool (DataFrame) : OD matrix with True values for affected OD pairs and
            False for unaffected OD pairs
140         od_affected (DataFrame)      : OD matrix with the OD values for only the affected OD
            pairs
141
142     """
143     od_affected = pd.read_csv(filepath_affected_od, delimiter=',', index_col= 1)
144     od_affected = od_affected.drop(['Matrix_Number'], axis=1)
145     od_affected.columns = od_affected.index
146     od_affected_bool = od_affected.astype(bool)
147     return od_affected_bool, od_affected
148
149 # Function to run the simulation
150 def run_simulation(batch_exe_path, runNumber, runCount, database_path, logDir, model_path):
151     """
152     Starts the simulation for one particular run
153     Parameters:
154         runNumber (int)          : ID number for one parallel run
155         runCount (int)           : the total number of parallel runs of one iteration
156         database_path (string)   : path to database location on computer
157         logDir (string)          : path to storage location of one parallel run
158         model_path (string)      : path to location of Paramics model
159
160     Returns:
161         process: runs an individual parallel run of an iteration
162     """
163     cmd = f'"{batch_exe_path}" "{model_path}" --runConfigId {runNumber} --logDir "{logDir}" --runNumber
        {runNumber} --runCount {runCount} --statisticsFileName "{database_path}" --
        groupRunTemporaryFileName "randomtempname"'
164     #print('model path:', cmd)
165     process = subprocess.Popen(cmd, shell=True)
166     return process
167
168
169 def run_all_simulations(batch_exe_path, runCount, output_file, run_config_name, iteration,
    model_path):
170     """
171     Starts the simulation for a set of parallel runs
172
173     Parameter:
174         run_Count (int)          : the total number of parallel runs of one iteration
175         output_file (string)     : path to file where output is stored
176         run_config_name (string) : name of the simulation configuration
177         iteration (int)          : the iteration number
178         model_path (string)      : path to location of paramics model
179
180     Returns:
181         process: runs all the parallel runs of an iteration
182     """
183     # Set an empty list to store the processes
184     processes = []
185
186     # Set the database path based on the run_config_name
187     database_path = f'{output_file}\\log\\{run_config_name}_{iteration}.sqlite3'
188     #print('database_path', database_path)
189     # Loop over the runNumbers and start the Paramics simulation
190     for runNumber in range(1, runCount + 1):
191         # Set the Directory for the individual run output
192         logDir = f'{output_file}\\log\\{run_config_name}_{iteration}_run{runNumber}'
193         # Start the simulation
194         processes.append(run_simulation(batch_exe_path, runNumber, runCount, database_path,
            logDir, model_path))
195         time.sleep(1)
196     # Wait for all processes to be ready before continuing
197     for process in processes:

```

```

197     process.wait()
198
199 def od_travel_times_sim(output_file, run_config_name, iteration):
200     """
201     Function to load the travel times from the output file from the RODY simulation
202
203     Parameters:
204         output_file (string)      : text line to indicate where the output file is stored
205         run_config_name (string)  : text line with the configuration name as in the Paramics
206                                     model
207         iteration (int)           : the iteration number
208
209     Returns:
210         od_travel_times (DataFrame): OD matrix (371 x 371) with the average travel times per
211                                     OD pair
212     """
213     # Retrieve the tripsAll data with the travel times per trip
214     if iteration == 99:
215         conn = sqlite3.connect(f'{output_file}\\log\\{run_config_name}.sqlite3') # Connect
216                                     to the SQLite-database
217     else:
218         cmd = f'{output_file}\\log\\{run_config_name}_{iteration}.sqlite3'
219         conn = sqlite3.connect(cmd)
220         query = "SELECT * FROM tripsAll" #
221         Retrieve the tripsAll table data
222         all_trips = pd.read_sql_query(query, conn) #
223         Set tripsAll into dataframe
224         conn.close() #
225         Close connection
226
227     # Calculate the OD matrix travel times (in minutes) (fill-up and cool down hours removed)
228     all_trips.index = all_trips['departureTime']
229     all_trips_ph = all_trips[(all_trips.index > 15 * 3600) & (all_trips.index < 18 * 3600)]
230     od_avg_travel_times = all_trips_ph.groupby(['fromZone', 'toZone'])['timeTaken'].mean().
231         reset_index()
232     od_travel_times = od_avg_travel_times.pivot(index='fromZone', columns='toZone', values='
233         timeTaken')
234
235     #Adding zones which are currently missing in the matrix
236     all_zones = list(range(1, 372))
237     od_travel_times = od_travel_times.reindex(index=all_zones, columns=all_zones)
238
239     # Transform travel times from seconds to minutes
240     od_travel_times = od_travel_times / 60
241
242     return od_travel_times
243
244 def congestion_indicator(od_affected_directly, od_affected_all, od_travel_times,
245     x_cdf_directly, y_cdf_directly, x_cdf_indirectly, y_cdf_indirectly, KS_iter_directly,
246     KS_iter_indirectly, KS_base_directly, KS_base_indirectly):
247     """
248     Function to calculate the KS value as congestion indicator
249
250     Parameters:
251         od_affected_directly (DataFrame) : 371 x 371 Boolean matrix with values True for
252                                             directly affected OD pairs and False not directly
253                                             affected OD pair
254         od_affected_all (DataFrame)      : 371 x 371 matrix matrix with values True for all
255                                             affected OD pairs and False not affected OD
256                                             pair
257         od_travel_times (DataFrame)      : 371 x 371 matrix with the travel times from the
258                                             last simulation
259         x_cdf_directly (array)           : sorted travel times from small to large of
260                                             directly affected OD pairs
261         y_cdf_directly (array)           : corresponding CDF value of travel times in
262                                             x_cdf_directly of directly affected OD pairs
263         x_cdf_indirectly (array)         : sorted travel times from small to large of
264                                             indirectly affected OD pairs
265         y_cdf_indirectly (array)         : corresponding CDF value of travel times in

```

```

    x_cdf_indirectly of indirectly affected OD pairs
250     KS_iter_directly (array)      : KS values between last two CDFs of iterations for
        directly affected OD pairs
251     KS_iter_indirectly (array)    : KS values between last two CDFs of iterations for
        indirectly affected OD pairs
252     KS_base_directly (array)      : KS values between CDF last iteration and base
        scenario for directly affected OD pairs
253     KS_base_indirectly (array)    : KS values between CDF last iteration and base
        scenario for indirectly affected OD pairs
254 Returns:
255     Updated KS and CDF values in stored arrays
256     """
257     # For directly affected OD pairs:
258     # Make a 1d array of travel times for affected od pairs
259     od_travel_times_affected = od_travel_times[od_affected_directly].values.flatten()
260     od_travel_times_affected = od_travel_times_affected[~np.isnan(od_travel_times_affected)]
261
262     # Sorting the data, calculating CDF and appending to list
263     od_travel_times_affected = np.sort(od_travel_times_affected)
264     cdf = np.arange(1, len(od_travel_times_affected) + 1) / len(od_travel_times_affected)
265     x_cdf_directly.append(od_travel_times_affected)
266     y_cdf_directly.append(cdf)
267
268     # Calculating the KS-stat if there are at least two iterations done
269     if len(x_cdf_directly) > 2:
270         ks_stat = stats.ks_2samp(x_cdf_directly[-2], x_cdf_directly[-1])
271         KS_iter_directly.append(ks_stat)
272
273     # Calculating the KS-stat between base and current iteration
274     if len(x_cdf_directly) > 1:
275         ks_stat = stats.ks_2samp(x_cdf_directly[0], x_cdf_directly[-1])
276         KS_base_directly.append(ks_stat)
277
278     # For indirectly affected OD pairs:
279     od_affected_indirectly = np.logical_and(od_affected_all, np.logical_not(
        od_affected_directly))
280
281     # Make a 1d array of travel times for affected od pairs
282     od_travel_times_affected = od_travel_times[od_affected_indirectly].values.flatten()
283     od_travel_times_affected = od_travel_times_affected[~np.isnan(od_travel_times_affected)]
284
285     # Sorting the data and calculating CDF
286     od_travel_times_affected = np.sort(od_travel_times_affected)
287     x_cdf_indirectly.append(od_travel_times_affected)
288     cdf = np.arange(1, len(od_travel_times_affected) + 1) / len(od_travel_times_affected)
289     y_cdf_indirectly.append(cdf)
290
291     # Calculating the KS-stat between previous and current iteration
292     if len(x_cdf_indirectly) > 2:
293         ks_stat = stats.ks_2samp(x_cdf_indirectly[-2], x_cdf_indirectly[-1])
294         KS_iter_indirectly.append(ks_stat)
295
296     # Calculating the KS-stat between base and current iteration
297     if len(x_cdf_indirectly) > 1:
298         ks_stat = stats.ks_2samp(x_cdf_indirectly[0], x_cdf_indirectly[-1])
299         KS_base_indirectly.append(ks_stat)
300     return
301
302
303 def plot_cdf_and_KS(x_cdf_directly, y_cdf_directly, x_cdf_indirectly, y_cdf_indirectly,
    KS_iter_directly, KS_iter_indirectly, KS_base_directly, KS_base_indirectly,
    disappeared_cars, threshold_directly):
304     """
305     Function to plot the travel time CDF's and print the KS values calculated in the
        congestion_indicator() function
306
307     Parameters:
308         x_cdf_directly (array)      : sorted travel times from small to large of
            directly affected OD pairs
309         y_cdf_directly (array)      : corresponding CDF value of travel times in
            x_cdf_directly of directly affected OD pairs

```



```

310     x_cdf_indirectly (array)      : sorted travel times from small to large of
        indirectly affected OD pairs
311     y_cdf_indirectly (array)      : corresponding CDF value of travel times in
        x_cdf_indirectly of indirectly affected OD pairs
312     KS_iter_directly (array)      : KS values between last two CDFs of iterations for
        directly affected OD pairs
313     KS_iter_indirectly (array)    : KS values between last two CDFs of iterations for
        indirectly affected OD pairs
314     KS_base_directly (array)      : KS values between CDF last iteration and base
        scenario for directly affected OD pairs
315     KS_base_indirectly (array)    : KS values between CDF last iteration and base
        scenario for indirectly affected OD pairs
316     disappeared_cars (array)      : stored reduction of car trips applied in each
        iteration
317     threshold_directly (float)    : threshold KS value to indicate when the iteration
        stops
318
319     """
320     # Get the number of iterations (excluding the base scenario)
321     num_iterations = len(x_cdf_directly) - 1
322     max_iterations = 5 # Max 6 iterations
323
324     # Adjust the range for the colormap to get lighter blue for the first iteration
325     start_color = 0.2 # Start from a lighter blue (adjustable value)
326     end_color = 1.2 # End with a dark blue
327
328     # Get the KS value (compared to base scenario)
329     KS_value_base_indirectly = []
330     KS_value_base_directly = []
331     for i in range(num_iterations):
332         KS_value_base_indirectly.append(KS_base_indirectly[i][0])
333         KS_value_base_directly.append(KS_base_directly[i][0])
334
335     # Get the KS value (compared to previous iterations)
336     KS_value_iter_indirectly = []
337     KS_value_iter_directly = []
338     for i in range(num_iterations - 1):
339         KS_value_iter_indirectly.append(KS_iter_indirectly[i][0])
340         KS_value_iter_directly.append(KS_iter_directly[i][0])
341     iteration_list = list(range(0, num_iterations))
342     iteration_list_diff = list(range(1, num_iterations))
343
344     # Set figure size and color map
345     plt.figure(figsize=(14, 14))
346     cmap = plt.get_cmap("Blues")
347
348     # Plot the KS values of the directly affected OD pairs
349     plt.subplot(221)
350     plt.plot(iteration_list, KS_value_base_directly, marker = 'o', color = 'steelblue', lw
        =1.7, linestyle='-.', label = 'Compared to base')
351     plt.plot(iteration_list_diff, KS_value_iter_directly, marker = 'o', color = 'steelblue',
        linestyle='-', label = 'Compared to previous simulation')
352     plt.axhline(threshold_directly, color = 'grey', ls = '--')
353
354     custom_handles = [
355         plt.Line2D([], [], color='steelblue', linestyle='-.', label='Compared to base'),
356         plt.Line2D([], [], color='steelblue', linestyle='-', label='Compared to previous
        simulation'),
357         plt.Line2D([], [], color='grey', linestyle='--', label='Threshold directly')]
358     plt.legend(handles=custom_handles, fontsize=13)
359     plt.xticks(iteration_list)
360     plt.title('KS values for directly affected OD pairs')
361     plt.xlabel('Iterations')
362     plt.ylabel('KS value')
363     plt.ylim(0, KS_value_base_directly[0] * 1.4)
364     plt.grid()
365
366     # Plot the KS values of the indirectly affected OD pairs
367     plt.subplot(222)
368     plt.plot(iteration_list, KS_value_base_indirectly, marker = 'o', color = 'steelblue', lw
        =1.7, linestyle='-.', label = 'Compared to base')
369     plt.plot(iteration_list_diff, KS_value_iter_indirectly, marker = 'o', color = 'steelblue'

```

```

        ,linestyle= '-',label = 'Compared_to_previous_simulation')
369
370 plt.title('KS_values_for_indirectly_affected_OD_pairs')
371 plt.xlabel('Iterations')
372 plt.ylabel('KS_value')
373 custom_handles = [
374     plt.Line2D([], [], color='steelblue', linestyle='-.', label='Compared_to_base'),
375     plt.Line2D([], [], color='steelblue', linestyle='-', label='Compared_to_previous_
        simulation'),
376     plt.Line2D([], [], color='grey', linestyle='--', label='Threshold_indirectly')]
377 plt.legend(handles=custom_handles, fontsize=13)
378 plt.xticks(iteration_list)
379 plt.ylim(0, KS_value_base_directly[0] * 1.4)
380 plt.grid()
381
382 # Plot the CDF graphs of the travel time for directly affected OD pairs
383 plt.subplot(223)
384 plt.plot(x_cdf_directly[0], y_cdf_directly[0], marker=".", linestyle="none", markersize =
        0.3, color = "grey", label = "base_scenario")
385 for i in range(1, num_iterations + 1):
386     color = cmap(start_color + (end_color - start_color) * (i - 1) / (max_iterations - 1)
        )
387     plt.plot(x_cdf_directly[i], y_cdf_directly[i], marker=".", linestyle="none",
        markersize=0.3, color=color, label=f'Iteration_{i}:_{disappeared_cars[i-1]:.0f}_
        vehicles')
388
389 plt.title('Travel_time_CDF_of_directly_affected_OD_pairs')
390 plt.xlabel('Travel_time_min')
391 plt.ylabel('CDF')
392 plt.xlim(0, x_cdf_directly[1].max() * 2/3)
393 legend = plt.legend(markerscale=10)
394 plt.grid(True)
395
396 # Plot the CDF graphs of the travel time for indirectly affected OD pairs
397 plt.subplot(224)
398 plt.plot(x_cdf_indirectly[0], y_cdf_indirectly[0], marker=".", linestyle="none",
        markersize = 0.3, color = "grey", label = "base_scenario")
399 for i in range(1, num_iterations + 1):
400     color = cmap(start_color + (end_color - start_color) * (i - 1) / (max_iterations - 1)
        )
401     plt.plot(x_cdf_indirectly[i], y_cdf_indirectly[i], marker=".", linestyle="none",
        markersize=0.3, color=color, label=f'Iteration_{i}')
402
403 plt.title('Travel_time_CDF_of_indirectly_affected_OD_pairs')
404 plt.xlabel('Travel_time_min')
405 plt.ylabel('CDF')
406 plt.xlim(0, x_cdf_indirectly[1].max() * 2 / 3 )
407 legend = plt.legend(markerscale=10, loc = 'lower_right')
408 plt.grid(True)
409 plt.show()
410
411 # Print the KS values
412 print('KS_values_Directly_Indirectly')
413 print('Affected_pairs_Affected_pairs')
414
415 for i in range(len(KS_base_directly)):
416     print(f'Base_{i+1}_{KS_base_directly[i][0]:.3f}_{KS_base_indirectly[i][0]:.3f}')
417 print('')
418 for i in range(len(KS_iter_directly)):
419     print(f'Iteration_{i+1}_{i+2}_{KS_iter_directly[i][0]:.3f}_{KS_iter_indirectly[i][0]:.3f}')
420
421
422
423 def recalculating_od_matrix(od_car_original_vmrhdh, od_car_iterative_vmrhdh, od_total_original,
        od_time_original_vmrhdh, od_time_baserun, od_time_iterative_sim, ASC, beta,
        od_affected_all, od_utility_car_original, od_utility_bike, od_utility_pt,
        od_split_bike_original, od_split_pt_original, od_split_car_3d, od_split_bike_3d,
        od_split_pt_3d, od_split_notrip_3d, internal_zones, external_zones, copple_extern,
        od_time_iterative_vmrhdh, od_distance_car, disappeared_cars):

```

```

424 """
425 Function to recalculate the OD matrix
426
427 Parameters:
428     od_car_original_vmrhdh (DataFrame) : original OD matrix (6101x6101)
429     od_car_iterative_vmrhdh (DataFrame) : iterative OD matrix (6101x6101)
430     od_total_original (DataFrame) : total original OD matrix (6101x6101) of car, pt
431     and bike trips
432     od_time_original_vmrhdh (DataFrame) : original travel time matrix (6101x6101)
433     od_time_baserun (DataFrame) : travel time matrix (371x371) from base run (
434     normal Rotterdam network)
435     od_time_iterative_sim (DataFrame) : travel time matrix (371x371) from model run (
436     adjusted Rotterdam network)
437     ASC (dictionary) : storage of the Alternative Specific Constants
438     model parameters
439     beta (dictionary) : storage of the beta model parameters
440     od_affected_all (DataFrame) : 371 x 371 matrix matrix with values True for all
441     affected OD pairs and False not affected OD pair
442     od_utility_car_original, od_utility_bike, od_utility_pt (DataFrame) :
443     original utility OD matrix (6101x6101)
444     od_split_bike_original, od_split_pt_original (DataFrame) :
445     original OD split matrix (6101x6101)
446     od_split_car_3d, od_split_bike_3d, od_split_pt_3d, od_split_notrip_3d (list): OD
447     split matrices (6101x6101) of all iterations
448     internal_zones, external_zones (Int64Index): index with all internal/external RODY
449     zones
450     copple_extern (DataFrame) : coppling between external RODY zones and
451     corresponding V-MRDH zones
452     od_time_iterative_vmrhdh (DataFrame) : iterative car travel time matrix (6101
453     x6101)
454     od_distance_car (DataFrame) : car distance matrix (6101x6101)
455     disappeared_cars (array) : stored reduction of car trips applied in
456     each iteration
457
458 Returns:
459     od_split_car (DataFrame): iterative OD split car matrix (6101x6101)
460     od_car_iterative_vmrhdh (DataFrame): iterative OD car trip matrix (6101x6101)
461     od_utility_car (DataFrame): (6101x6101)
462     od_bike_new_vmrhdh, od_pt_new_vmrhdh, od_notrip_new_vmrhdh (DataFrame): (6101x6101)
463     od_time_iterative_vmrhdh (DataFrame): (6101x6101)
464
465 """
466 # Calculate the difference in travel time between this iteration and the base scenario
467 (371 x 371 matrix)
468 od_time_difference = od_time_iterative_sim - od_time_baserun
469 # Select the affected OD pairs
470 affected_pairs = od_affected_all.stack()[od_affected_all.stack() == True]
471
472 # Update the od_time_difference_affected_pairs (371x371 matrix) in the
473 od_car_iterative_with_vmrhdh (6101x6101 matrix)
474 # Loop over the affected OD pairs
475 for (rody_origin, rody_destination) in affected_pairs.index:
476     # Select the internal to internal trips (1st quadrant)
477     if rody_origin in internal_zones and rody_destination in internal_zones:
478         original_time = od_time_original_vmrhdh.loc[rody_origin, rody_destination]
479         difference_time = od_time_difference.loc[rody_origin, rody_destination]
480         updated_time = original_time + difference_time
481         if updated_time > 0:
482             # Add the updated travel time between base run and iterative run to the
483             overall skim matrix
484             od_time_iterative_vmrhdh.loc[rody_origin, rody_destination] = updated_time
485     # Select the internal to external trips (2nd quadrant)
486     if rody_origin in internal_zones and rody_destination in external_zones:
487         # Select the VMRDH zones corresponding to the RODY destination (external zone)
488         vmrdh_destinations = copple_extern.loc[rody_destination].dropna().astype(int)
489         original_times = od_time_original_vmrhdh.loc[rody_origin, vmrdh_destinations +
490         1000000]
491         difference_time = od_time_difference.loc[rody_origin, rody_destination]
492         updated_times = original_times + difference_time

```

```

478         # Only if the updated times are positive, update the values
479         if (updated_times > 0).all():
480             # Add the updated travel time between base run and iterative run to the
              overall skim matrix
481             od_time_iterative_vmrhd.loc[rody_origin, vmrdh_destinations + 1000000] =
              updated_times
482         # Select the external to internal trips (3rd quadrant)
483         if rody_origin in external_zones and rody_destination in internal_zones:
484             # Select the VMRDH zones corresponding to the RODY destination (external zone)
485             vmrdh_origins = copple_extern.loc[str(rody_origin)].dropna().astype(int).values
486             original_times = od_time_original_vmrhd.loc[vmrdh_origins.transpose() +
              1000000, rody_destination]
487             difference_time = od_time_difference.loc[rody_origin, rody_destination]
488             updated_times = original_times + difference_time
489             # Only if the updated times are positive, update the values
490             if (updated_times > 0).all():
491                 # Add the updated travel time between base run and iterative run to the
              overall skim matrix
492                 od_time_iterative_vmrhd.loc[vmrdh_origins.transpose() + 1000000,
              rody_destination] = updated_times
493
494         # Recalculate car utility of affected car trips
495         od_utility_car = ASC['car'] + beta['car'] * od_time_iterative_vmrhd
496
497         # Recalculate no trip utility based on increase in travel time (delta_T)
498         delta_T = od_time_iterative_vmrhd - od_time_original_vmrhd
499         od_utility_notrip = np.where(delta_T < 0, -999,
500         ASC['no_trip'] + beta['no_trip'] * od_distance_car + beta['no_trip2'] * od_distance_car
              **2 + \
501             beta['no_trip3'] * np.log(beta['no_trip4'] + delta_T / (
              od_time_original_vmrhd)))
502         od_utility_notrip = pd.DataFrame(od_utility_notrip, index = od_utility_car.index, columns
              = od_utility_car.index)
503
504         # Calculate the total utility (in e-)
505         od_utility_total = np.exp(od_utility_car.values) + np.exp(od_utility_bike.values) + np.
              exp(od_utility_pt.values) + np.exp(od_utility_notrip.values)
506
507         # Calculating the new OD split based on simulation outcome
508         od_split_car_sim = np.round(np.exp(od_utility_car) / od_utility_total, decimals
              = 6)
509         od_split_bike_sim = np.round(np.exp(od_utility_bike) / od_utility_total, decimals
              = 6)
510         od_split_pt_sim = np.round(np.exp(od_utility_pt) / od_utility_total, decimals
              = 6)
511         od_split_notrip_sim = np.round(np.exp(od_utility_notrip) / od_utility_total, decimals
              = 2)
512
513         # Calculating the new OD split where is prevented that people change from bike and PT to
              staying at home
514         od_split_bike_sim = np.maximum(od_split_bike_sim, od_split_bike_original)
515         od_split_pt_sim = np.maximum(od_split_pt_sim, od_split_pt_original)
516         od_split_notrip_sim = np.round(1 - od_split_car_sim - od_split_bike_sim - od_split_pt_sim
              , decimals = 2) # Herbereken P_notrip
517
518         # Append the OD split matrix to the overall od split matrices (for all iterations)
519         od_split_car_3d.append(od_split_car_sim)
520         od_split_bike_3d.append(od_split_bike_sim)
521         od_split_pt_3d.append(od_split_pt_sim)
522         od_split_notrip_3d.append(od_split_notrip_sim)
523
524         # Calculating the new OD split where the relaxation factor is applied for the next
              iteration
525         od_split_car = np.mean(od_split_car_3d, axis = 0)
526         od_split_bike = np.mean(od_split_bike_3d, axis = 0)
527         od_split_pt = np.mean(od_split_pt_3d, axis = 0)
528         od_split_notrip = np.mean(od_split_notrip_3d, axis = 0)
529
530         # Calculating new OD matrix for car trips
531         od_car_new_vmrhd = od_split_car * od_total_original

```

```

533 od_bike_new_vmrhdh = od_split_bike * od_total_original
534 od_pt_new_vmrhdh = od_split_pt * od_total_original
535 od_notrip_new_vmrhdh = od_split_notrip * od_total_original
536 od_car_iterative_vmrhdh.update(pd.DataFrame(od_car_new_vmrhdh, index=od_car_iterative_vmrhdh
    .index, columns=od_car_iterative_vmrhdh.columns))
537
538 disappeared_cars.append(od_car_new_vmrhdh.sum().sum() - od_car_original_vmrhdh.sum().sum())
539 return od_split_car, od_car_iterative_vmrhdh, od_utility_car, od_bike_new_vmrhdh,
    od_pt_new_vmrhdh, od_notrip_new_vmrhdh, od_time_iterative_vmrhdh
540
541
542
543 def aggregate_od_matrix(full_od_matrix, od_car_original, internal_zones, external_zones,
    copple_extern, ratio_330_331, ratio_329_328, ratio_270_269):
544     """
545     Function to aggregate the VMRDH format matrix (6101 x 6101) to the RODY format matrix
    (371 x 371)
546
547     Parameters:
548         full_od_matrix (DataFrame) : the 6101 x 6101 matrix which needs to be aggregated
549         internal_zones (Int64Index) : Index with all internal RODY zones
550         external_zones (Int64Index) : Index with all external RODY zones
551         copple_extern (DataFrame) : DataFrame with an overview of external RODY zones and
    associated VMRDH zones
552         ratio_330_331 (pandas.Series): List with all the origins and their ratio of choosing
    external zone 330 over 331 to enter network
553         ratio_329_328 (pandas.Series): List with all the origins and their ratio of choosing
    external zone 329 over 328 to enter network
554         ratio_270_269 (pandas.Series): List with all the origins and their ratio of choosing
    external zone 270 over 269 to enter network
555
556     Returns:
557         od_matrix_new (DataFrame): the aggregated 371 x 371 matrix which can be implemented
    in RODY
558     """
559     # Create list of all RODY zones
560     all_rody_zones = list(internal_zones) + list(external_zones)
561
562     # Create a new OD matrix in RODY format
563     od_matrix_new = pd.DataFrame(index=all_rody_zones, columns=all_rody_zones)
564
565     # Add all the OD values for internal to internal pairs into new OD matrix
566     od_matrix_new.loc[internal_zones, internal_zones] = full_od_matrix.loc[internal_zones,
    internal_zones]
567
568     # Second quadrant: trips from inside of Rotterdam leaving Rotterdam
569     for rody_origin in internal_zones:
570         for rody_destination in external_zones:
571             # Skip all external zones that enter Rotterdam (no trips leaving Rotterdam)
572             if rody_destination in [306, 284, 269, 270, 267, 257, 339, 328, 329, 258]:
573                 continue
574
575             vmrdh_destinations = copple_extern.loc[str(rody_destination)].dropna().astype(int)
    .values
576             # Make deivision for A15/A16 highway external zone between main highway and
    parallel lane
577             if rody_destination == 330:
578                 total_value = full_od_matrix.loc[rody_origin, vmrdh_destinations + 1000000].
    sum() * ratio_330_331.loc[rody_origin]
579                 od_matrix_new.loc[rody_origin, rody_destination] = total_value
580                 #print(f'({rody_origin}, {rody_destination}). ratio:{ratio_330_331.loc[
    rody_origin]}. total_value = {total_value} ')
581
582             elif rody_destination == 331:
583                 total_value = full_od_matrix.loc[rody_origin, vmrdh_destinations + 1000000].
    sum() * (1 - ratio_330_331.loc[rody_origin])
584                 od_matrix_new.loc[rody_origin, rody_destination] = total_value
585                 #print(f'({rody_origin}, {rody_destination}). ratio:{1 - ratio_330_331.loc[
    rody_origin]}. total_value = {total_value} ')
586             else:
587                 total_value = full_od_matrix.loc[rody_origin, vmrdh_destinations + 1000000].

```

```

        sum()
        od_matrix_new.loc[rody_origin, rody_destination] = total_value
588
589
590 # Third quadrant: trips from outside of Rotterdam to Rotterdam
591 for rody_destination in internal_zones:
592     for rody_origin in external_zones:
593         # Skip all rody zones of highways that leave Rotterdam
594         if rody_origin in [307, 285, 271, 268, 256, 340, 330, 331, 259]:
595             continue
596
597         vmrdh_origins = copple_extern.loc[str(rody_origin)].dropna().astype(int).values
598         # Make deviation for A15/A16 highway external zone on parallel highway and main
            highway
599
600         if rody_origin == 329: # Hoofdrijbaan
601             total_value = full_od_matrix.loc[vmrdh_origins.transpose() + 1000000,
                rody_destination].sum() * ratio_329_328.loc[rody_destination]
602             od_matrix_new.loc[rody_origin, rody_destination] = total_value
603             #print(f'({rody_origin}, {rody_destination}). ratio:{ratio_329_328.loc[
                rody_destination]}. total_value = {total_value} ')
604
605         elif rody_origin == 328: # Parallelbaan
606             total_value = full_od_matrix.loc[vmrdh_origins.transpose() + 1000000,
                rody_destination].sum() * (1 - ratio_329_328.loc[rody_destination])
607             od_matrix_new.loc[rody_origin, rody_destination] = total_value
608             #print(f'({rody_origin}, {rody_destination}). ratio:{ratio_329_328.loc[
                rody_destination]}. total_value = {total_value} ')
609
610         elif rody_origin == 270: # Hoofdrijbaan
611             total_value = full_od_matrix.loc[vmrdh_origins.transpose() + 1000000,
                rody_destination].sum() * ratio_270_269.loc[rody_destination]
612             od_matrix_new.loc[rody_origin, rody_destination] = total_value
613
614         elif rody_origin == 269: # Parallelbaan
615             total_value = full_od_matrix.loc[vmrdh_origins.transpose() + 1000000,
                rody_destination].sum() * (1 - ratio_270_269.loc[rody_destination])
616             od_matrix_new.loc[rody_origin, rody_destination] = total_value
617
618         else:
619             total_value = full_od_matrix.loc[vmrdh_origins.transpose() + 1000000,
                rody_destination].sum()
620             od_matrix_new.loc[rody_origin, rody_destination] = total_value
621
622 # Adding the OD values for external zones which do not have external VMRDH zones attached
            to it
623 current_index = set(od_matrix_new.index.tolist())
624 full_range = set(range(1, 372))
625 missing_zones = sorted(full_range - current_index)
626
627 #For each missing zone, retrieve the corresponding values from original_od_matrix and add
            them to od_matrix_new
628 for missing_zone in missing_zones:
629     # Retrieve the row and column for the missing zone from original_od_matrix
630     if missing_zone in od_car_original.index:
631         # Add the missing row to od_matrix_new (row for the missing zone)
632         od_matrix_new.loc[missing_zone] = od_car_original.loc[missing_zone]
633     if missing_zone in od_car_original.columns:
634         # Add the missing column to od_matrix_new (column for the missing zone)
635         od_matrix_new[missing_zone] = od_car_original[missing_zone]
636
637 # Ensure the matrix is sorted after adding the missing zones (optional)
638 od_matrix_new = od_matrix_new.sort_index(axis=0).sort_index(axis=1)
639
640 # Adding the trips from external to external
641 od_matrix_new.loc[external_zones, external_zones] = od_car_original.loc[external_zones,
            external_zones]
642
643 return od_matrix_new
644
645
646

```

```

647 # Function to update OD matrix in the .paramics file
648 def update_od_matrix_in_model(od_affected, od_new, zone_id, model_path_intervention):
649     """
650     Function update the recalculated OD matrix in the Paramics file of the model with the
651     intervention
652
653     Parameters:
654         od_affected (DataFrame) : 371 x 371 matrix matrix with values True for the affected
655         OD pairs and False not affected OD pair
656         od_new (DataFrame) : the new car trip matrix (371 x 371) which must be updated
657         in the RODY model
658         zone_id (array) : the Paramics IDs for all the RODY zones
659         model_path_intervention : path to location where model is stored
660
661     """
662     # Step 1: Change the format of the OD matrix to fit the SQLITE format
663     # Set an empty list for the values which need to be updated
664     updated_values = []
665
666     # Convert the boolean matrix to a numpy array for easier indexing
667     od_affected_array = np.array(od_affected)
668
669     # Iterate through the boolean matrix
670     for i in range(od_affected_array.shape[0]): # Loop over rows (origin zones)
671         for j in range(od_affected_array.shape[1]): # Loop over columns (destination zones)
672             if od_affected_array[i, j]: # Check if the value is True
673                 origin_zone_id = int(zone_id[i]) # Get the corresponding origin zone ID
674                 dest_zone_id = int(zone_id[j]) # Get the corresponding destination zone ID
675
676                 # Use .iloc to get the value from a DataFrame
677                 demand_value = od_new.iloc[i, j] # Get the new demand value
678
679                 # Append to the list in the required format
680                 updated_values.append((origin_zone_id, dest_zone_id, round(demand_value, 3)))
681
682     # Step 2: Update the updated_values in the .paramics file
683     # Connect to your database
684     conn = sqlite3.connect(model_path_intervention)
685     cursor = conn.cursor()
686
687     # SQL query template to update demand
688     update_query = """
689     UPDATE demandZones
690     SET demand = ?
691     WHERE originZoneId = ? AND destZoneId = ? AND demandId = 4 AND matrixId = 0;
692     """
693
694     # Execute the update for each row in the list
695     for origin, dest, demand in updated_values:
696         cursor.execute(update_query, (demand, origin, dest))
697     conn.commit() # Commit the changes to the database
698
699     conn.close() # Close the connection
700
701 def load_coppling_extern_intern():
702     """
703     Loading information about the external and internal RODY zones and coppling with VMRDH
704     zones
705
706     """
707     # Laad de CSV in en zorg dat de AREANR-kolom als string wordt ingeladen
708     copple_list_extern_zones = pd.read_csv('Data/Coppling_external_(V-MRDH)_to_(RODY)
709     )/tabel_arenrs.csv', delimiter=',', index_col=0, dtype={'AREANR': str})
710     copple_list_extern_zones['AREANR'] = copple_list_extern_zones['AREANR'].str.replace(' ',
711     '') # Remove strings
712
713     # Group the zones to get a list of VMRDH groups per external zone
714     zones_grouped = copple_list_extern_zones.groupby('Bestandsnaam')['AREANR'].apply(list).
715     reset_index()

```



```

711 # Set the grouped zones in different columns into a DataFrame
712 max_zones = zones_grouped['AREANR'].apply(len).max() # Determine the maximum number of
713 VMRDH zones per external RODY zone
714 copple_extern = pd.DataFrame(zones_grouped['AREANR'].tolist(), index=zones_grouped['
Bestandsnaam'], columns=[f'Zone_{i+1}' for i in range(max_zones)])
715 copple_extern = copple_extern.rename_axis('RODY_ex_zone') # Rename axis
716 copple_extern.index = copple_extern.index.astype(str) # Set index as string
717
718 # Maak een lijst om de nieuwe rijen in op te slaan
719 new_rows = []
720
721 for idx, row in copple_extern.iterrows():
722     # Split index to check the number of zones
723     zones = idx.split()
724
725     # if case of more than one zone, split rows and append to new_rows
726     if len(zones) > 1:
727         for zone in zones:
728             new_rows.append([zone] + row.tolist())
729     # if case of 1 zone, add original row
730     else:
731         new_rows.append([idx] + row.tolist())
732
733 # Make a new dataframe of the splitted rows
734 copple_extern = pd.DataFrame(new_rows, columns=['RODY_zone'] + copple_extern.columns.
tolist())
735 copple_extern.set_index('RODY_zone', inplace=True) # RODY zone as index
736 copple_extern = copple_extern.apply(pd.to_numeric, errors='coerce') # Change None to NaN
and convert strings to floats
737 copple_extern.dropna(how='all', inplace=True) # Remove rows with only NaN values and
738 copple_extern.iloc[:,0] = copple_extern.iloc[:,0].astype('float') # Change everything to
float
739
740 # Load the coupling table
741 coppletable = pd.read_csv('Data/Coupling_external(V-MRDH)to_internal(RODY)/
zones_RODY_to_VMRDH.csv', delimiter=';', index_col = 0)
742 # Only select the internal zones
743 copple_intern = coppletable[coppletable['Type'] == 'I']
744 # Transform the VMRDH zones from format 'CXXXX' to XXXX (float)
745 for col in copple_intern.columns:
746     if col.startswith('Omni_'):
747         copple_intern[col] = copple_intern[col].str.replace('C', '', regex=False).astype(
float) # Use float to handle NaN
748 # Drop unnecessary columns
749 copple_intern = copple_intern.drop(columns=['Type', 'Highway', 'Copple_E', 'Center'])
750
751 # Definition of internal and external zones
752 internal_zones = copple_intern.index
753 external_zones = copple_extern.index
754 external_zones = external_zones.astype('int')
755
756 return internal_zones, external_zones, copple_extern
757
758 def reducing_od_matrix_start(od_car_original, reduction_directly_affected,
od_affected_directly):
759     # Select the affected OD pairs
760     affected_pairs = od_affected_directly.stack()[od_affected_directly.stack() == True]
761     od_car_reduced = od_car_original.copy(deep=True)
762     # Loop over the affected OD pairs
763     for (rody_origin, rody_destination) in affected_pairs.index:
764         od_car_reduced.loc[rody_origin, rody_destination] = od_car_original.loc[rody_origin,
rody_destination] * ((100 - reduction_directly_affected) / 100)
765     return od_car_reduced
766
767
768 def change_PT_traveltime(od_time_pt_vmrhd, od_affected_directly, copple_extern,
internal_zones, external_zones, ASC, beta, TT_PT_increase):
769
770     od_time_pt_vmrhd_adjusted = od_time_pt_vmrhd.copy(deep=True)
771

```

```

772     affected_pairs = od_affected_directly.stack()[od_affected_directly.stack() == True]
773
774     # Update the od_time_difference_affected_pairs (371x371 matrix) in the
       od_car_iterative_with_vmrhdh (6101x6101 matrix)
775     # Loop over the affected OD pairs
776     for (rody_origin, rody_destination) in affected_pairs.index:
777         # Select the internal to internal trips (1st quadrant)
778         if rody_origin in internal_zones and rody_destination in internal_zones:
779             od_time_pt_vmrhdh_adjusted.loc[rody_origin, rody_destination] = od_time_pt_vmrhdh.
               loc[rody_origin, rody_destination] + TT_PT_increase
780
781         # Select the internal to external trips (2nd quadrant)
782         if rody_origin in internal_zones and rody_destination in external_zones:
783             # Select the VMRDH zones corresponding to the RODY destination (external zone)
784             vmrdh_destinations = copple_extern.loc[str(rody_destination)].dropna().astype(int)
               .values
785             od_time_pt_vmrhdh_adjusted.loc[rody_origin, vmrdh_destinations + 1000000] =
               od_time_pt_vmrhdh.loc[rody_origin, vmrdh_destinations + 1000000] +
               TT_PT_increase
786
787         # Select the external to internal trips (3rd quadrant)
788         if rody_origin in external_zones and rody_destination in internal_zones:
789             # Select the VMRDH zones corresponding to the RODY destination (external zone)
790             vmrdh_origins = copple_extern.loc[str(rody_origin)].dropna().astype(int).values
791             od_time_pt_vmrhdh_adjusted.loc[vmrdh_origins.transpose() + 1000000,
               rody_destination] = od_time_pt_vmrhdh.loc[vmrdh_origins.transpose() + 1000000,
               rody_destination] + TT_PT_increase
792
793     # Recalculate utility
794     od_utility_pt = ASC['PT'] + beta['PT'] * od_time_pt_vmrhdh_adjusted
795
796     return od_utility_pt

```

# B

## Determination threshold KS-value

This appendix describes the determination of the threshold value to stop the iterative process, which entails that there is reached a new balance between car usage and traffic congestion. The threshold value is determined by looking at the standard deviation of six parallel runs. The travel time CDFs of the individual runs of directly affected OD pairs are shown in Figure B.1.

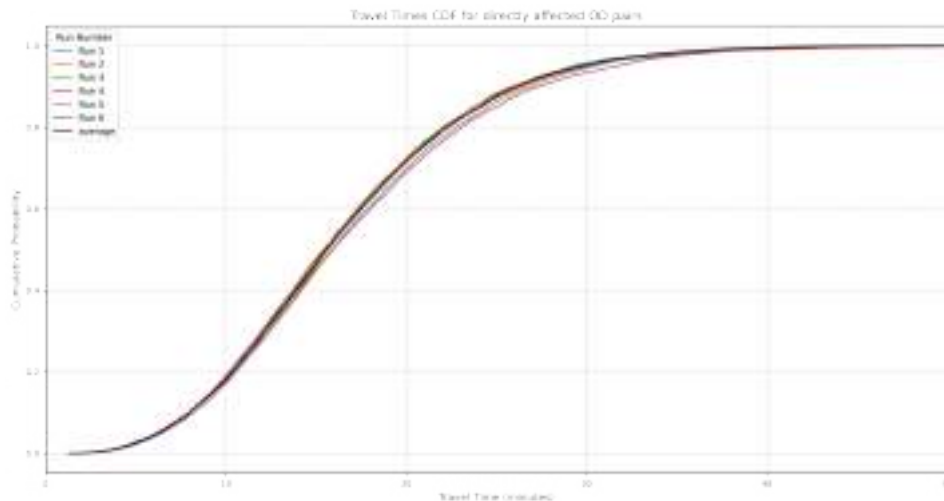


**Figure B.1:** Cumulative distribution functions for travel times of directly affected OD pairs for each individual model run with equal input.

Based on the individual runs, the average travel time CDF is calculated. The standard deviation between iterations is  $\sigma = 0.0084$ . This is the lower bound for the threshold, as this is the variation of model outcome for the same OD matrix.

It is also important to preserve convergence speed of the model, since one iteration will take about five hours to complete. To examine the convergence speed, the DiTra model is applied to the Roseknoop phase 1, without optimising the convergence process. This results in the iteration outcomes in Figure B.2.

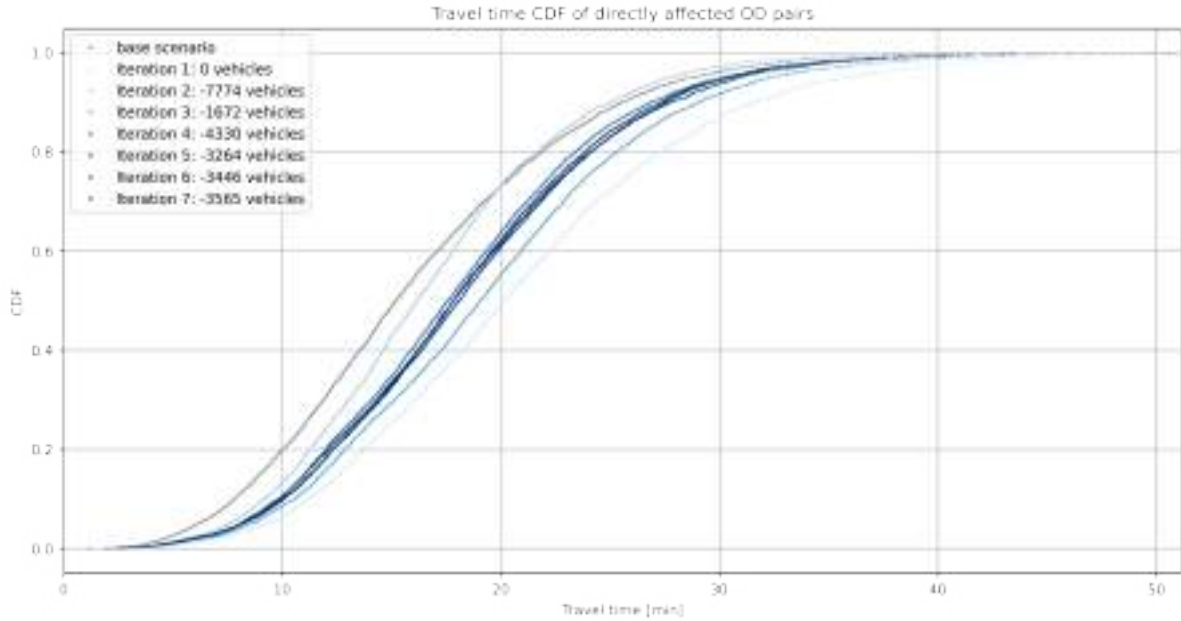


**Figure B.2:** CDFs of different iterations for DiTra model for directly affected OD pairs.

An overview of the iteration outputs is shown in Table B.1. The  $\Delta_{\text{cartrips}}$  show the change in car trips applied in the corresponding iteration.  $\Delta T_{\text{directly}}$  shows the resulting additional travel time for directly affected OD pairs.

Iteration	$\Delta_{\text{cartrips}}$	$\Delta T_{\text{directly}}$	KS value
1	0	+ 4.791 min	-
2	- 7775	+ 0.713 min	0.256
3	- 1672	+ 3.327 min	0.197
4	- 4330	+ 2.046 min	0.090
5	- 3264	+ 2.434 min	0.034
6	- 3446	+ 2.433 min	0.017
7	- 3565	+ 2.246 min	0.014

**Table B.1:** Model results for the different iterations for phase 1 (the values in  $\Delta_{\text{cartrips}}$  and  $\Delta T_{\text{directly}}$  are compared to the base scenario, the KS value is between last iterations)

In Figure B.3, the KS values for directly affected OD pairs is shown. This figure shows the convergence of the model and indicates that from iteration 5, the KS value compared to base stabilises, indicating the model has found a new equilibrium.

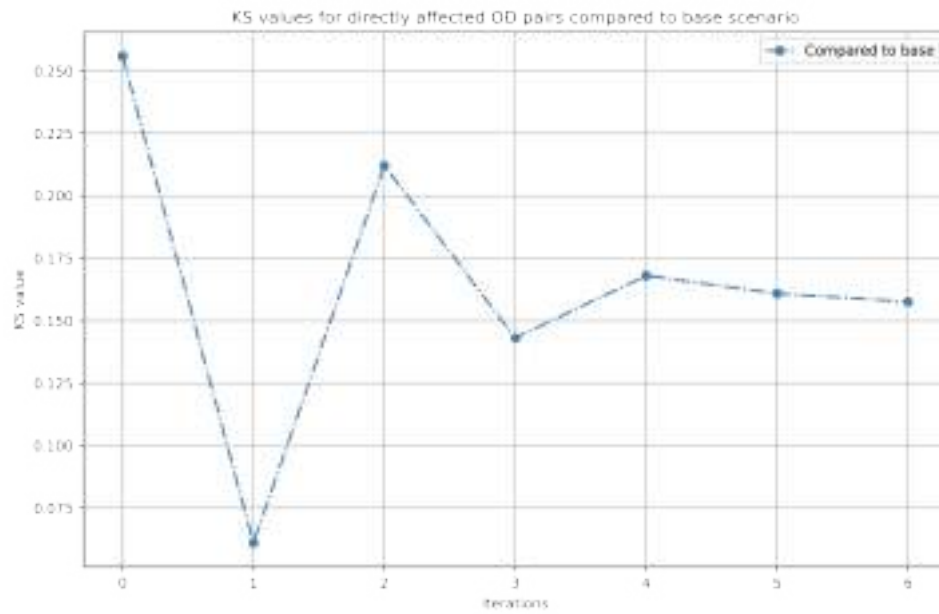


**Figure B.3:** KS value of the iterations of Roseknoop phase 1 compared to the base scenario

Figure B.4 describes the course of the KS values between iterations. This shows a large decent in the beginning, and a slower decent at the end, with the last KS values being almost similar with 0.017 and 0.014, where the equilibrium is reached.

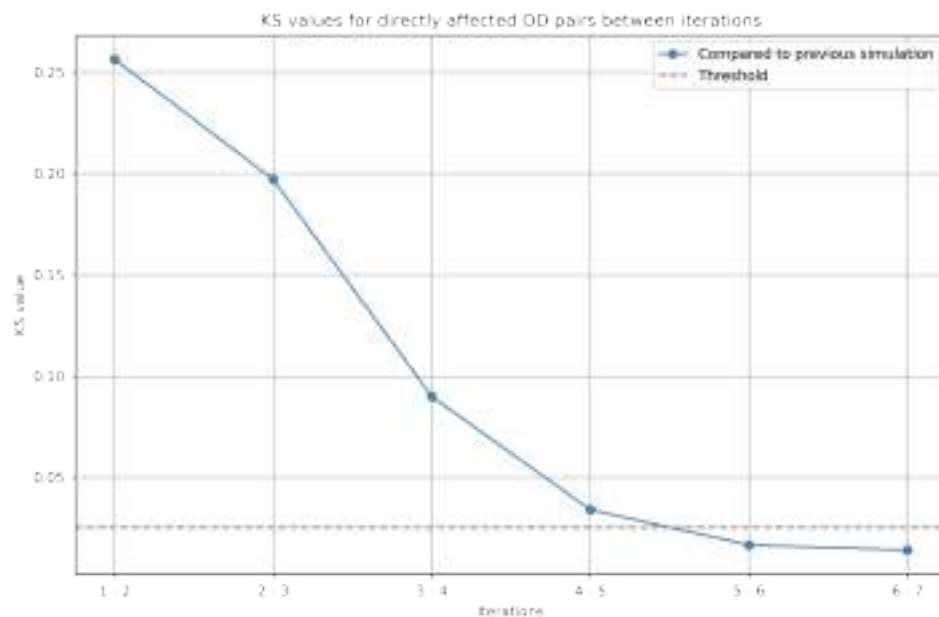


**Figure B.4:** KS value of the iterations of Roseknoop phase 1 compared to the previous iteration

---

Based on these results, the threshold value is set at  $KS_{\text{threshold}} = 3\sigma = 0.0252$ . This value is slightly higher than the KS values observed during equilibrium iterations (0.017 and 0.014), ensuring a reasonable balance between convergence speed and stability. A stricter threshold could unnecessarily extend the iterative process, while a more relaxed one might reduce the accuracy of the final equilibrium state.

Moreover, the chosen threshold remains lower than the KS value observed in iteration 5 (0.034), which is desirable, as this iteration still exhibited significant fluctuations in the number of car trips (ranging from -4330 to -3264). This suggests that setting a higher threshold could result in stopping the iterative process before achieving sufficient stability.

# C

## Reference locations data analysis

The locations of the reference data points are shown in Figure C.1.



**Figure C.1:** Locations of reference point traffic volume

The traffic volume for these data points is plotted in Figure C.2.



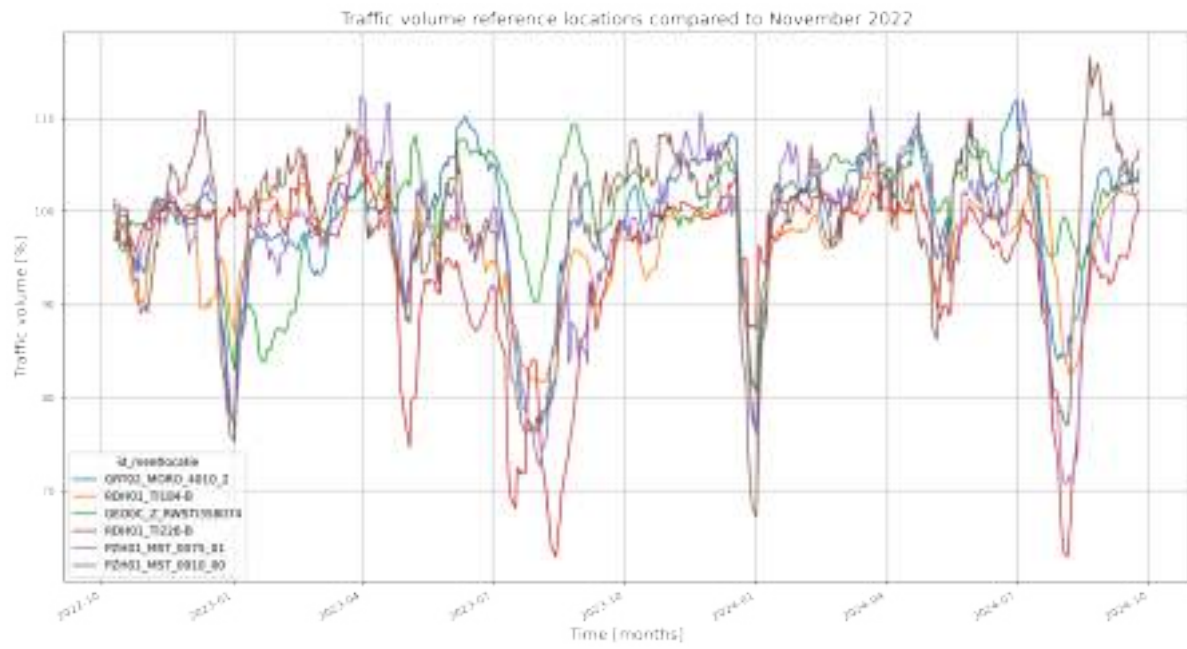


**Figure C.2:** Traffic volume reference traffic data

The average of the relative traffic volume compared to November 2022 is used as overall reference data.

# D

## Mathematical functions change in mobility distribution

In this appendix, the mathematical functions are provided which are obtained as a result of the calibration of the model. For the most frequent trip types, the function for the probability of choosing an alternative is shown.  $P_{\text{alternative}}$  is the probability of choosing the alternative.  $\Delta T$  is the increase in travel time in minutes. It should be noted that these functions are simplified. Based on the utility functions, all lines are non linear, however, practically, they are very close to linear. Therefore, these functions are a way to easily see the effect. For the original non linear functions, use the utility functions and apply the logit model.

For short inner city trips:

$$P_{\text{car}} = 0.53 - 0.014 \cdot \Delta T \quad (\text{D.1})$$

$$P_{\text{PT}} = 0.18 + 0.00233 \cdot \Delta T \quad (\text{D.2})$$

$$P_{\text{bike}} = 0.30 + 0.00667 \cdot \Delta T \quad (\text{D.3})$$

$$P_{\text{notrip}} = 0.004 \cdot \Delta T \quad (\text{D.4})$$

For a trip from the suburb to the city centre:

$$P_{\text{car}} = 0.56 - 0.0153 \cdot \Delta T \quad (\text{D.5})$$

$$P_{\text{PT}} = 0.21 + 0.00467 \cdot \Delta T \quad (\text{D.6})$$

$$P_{\text{bike}} = 0.25 + 0.0067 \cdot \Delta T \quad (\text{D.7})$$

$$P_{\text{notrip}} = 0.007 \cdot \Delta T \quad (\text{D.8})$$

For trips from an adjacent city to Rotterdam:

$$P_{\text{car}} = 0.63 - 0.018 \cdot \Delta T \quad (\text{D.9})$$

$$P_{\text{PT}} = 0.295 + 0.00433 \cdot \Delta T \quad (\text{D.10})$$

$$P_{\text{bike}} = 0.08 + 0.00067 \cdot \Delta T \quad (\text{D.11})$$

$$P_{\text{notrip}} = 0.014 \cdot \Delta T \quad (\text{D.12})$$

For trips from a distant city to Rotterdam:

$$P_{\text{car}} = 0.00115 \cdot \Delta T^2 - 0.04856 \cdot \Delta T + 0.74 \quad (\text{D.13})$$

$$P_{\text{PT}} = 0.27 \quad (\text{D.14})$$

$$P_{\text{bike}} = 0 \quad (\text{D.15})$$

$$P_{\text{notrip}} = -0.00137 \cdot \Delta T^2 + 0.05322 \cdot \Delta T \quad (\text{D.16})$$

# E

## Congestion heat maps of phase 1 (outcome DiTra model)

Below the congestion heat maps of all the different runs from the final RODY simulation, the new equilibrium, are shown.



**Figure E.1:** Congestion heat map of equilibrium phase 1 run 1

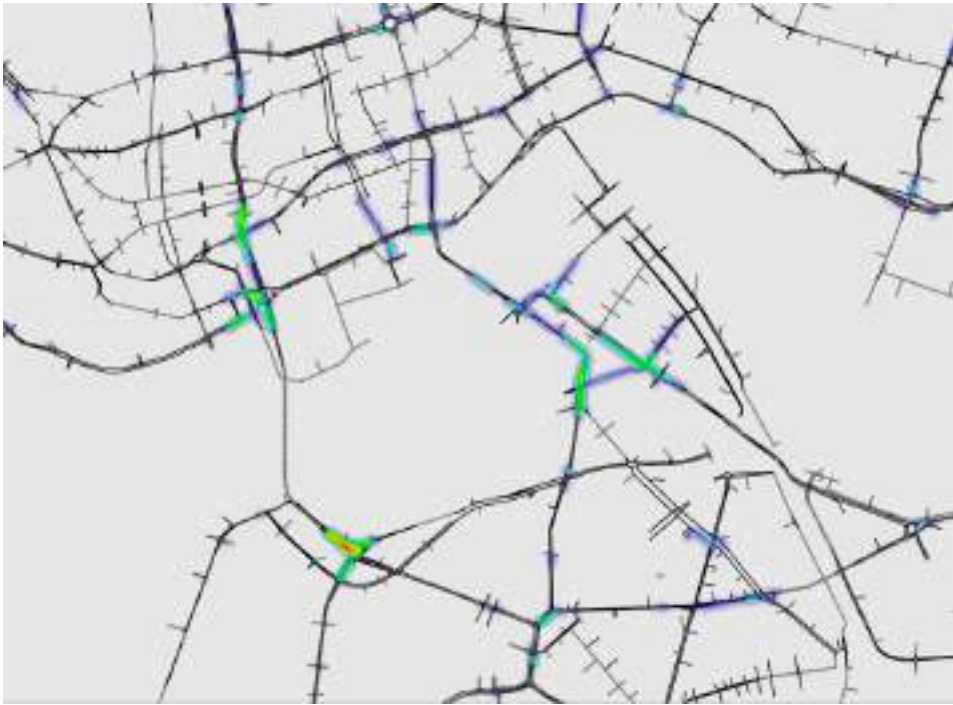


**Figure E.2:** Congestion heat map of equilibrium phase 1 run 2

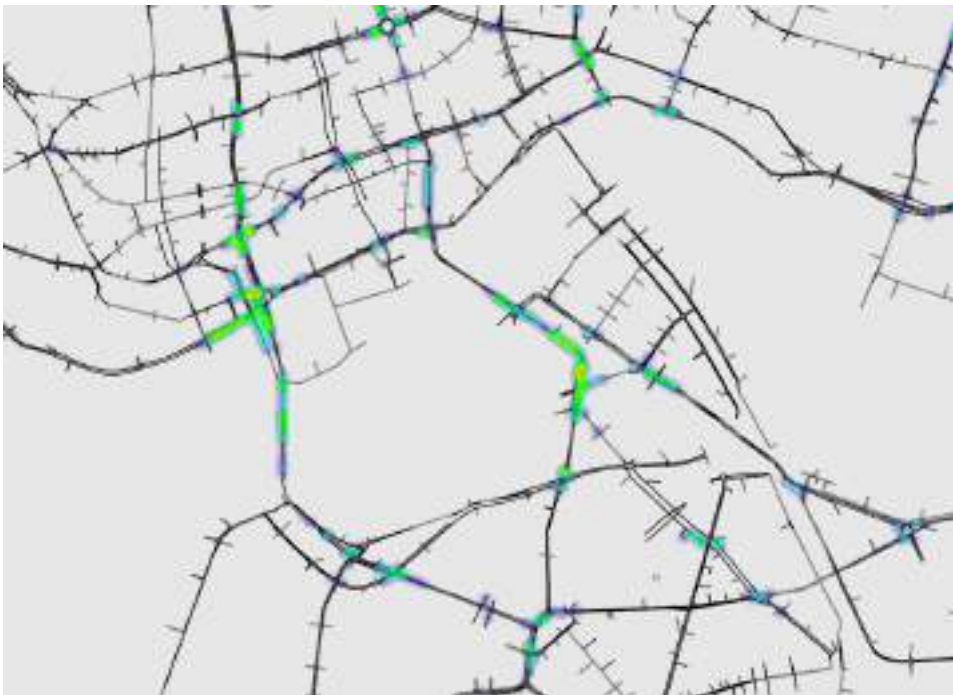


**Figure E.3:** Congestion heat map of equilibrium phase 1 run 3



**Figure E.4:** Congestion heat map of equilibrium phase 1 run 4

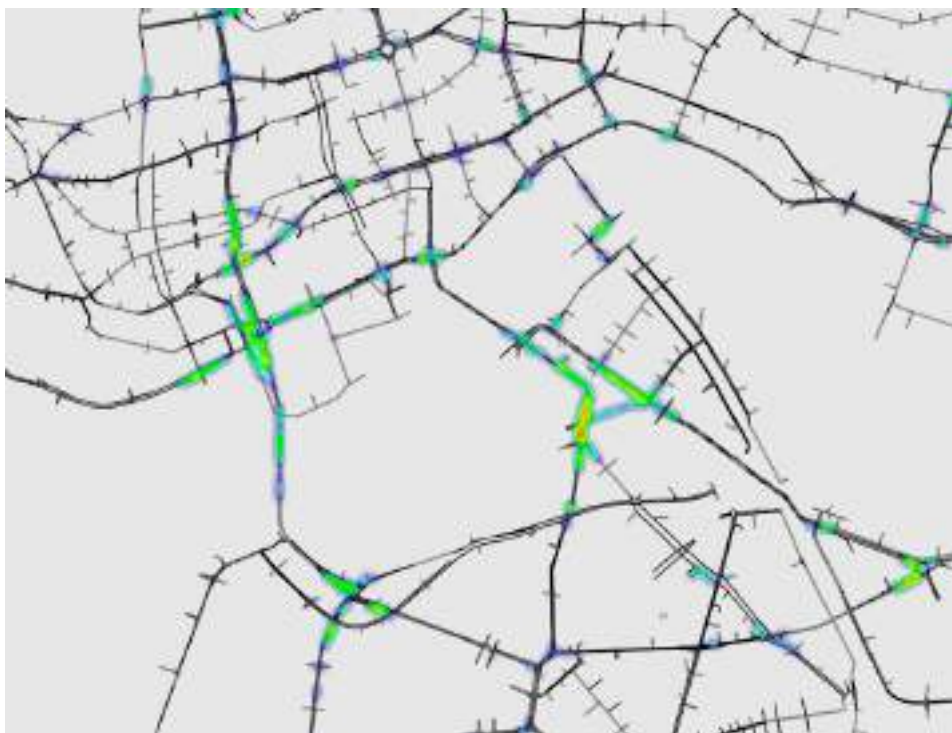


**Figure E.5:** Congestion heat map of equilibrium phase 1 run 5



**Figure E.6:** Congestion heat map of equilibrium phase 1 run 6